

THESIS
H5890
1976
c.2

ORIGINS OF ORE-CONTROLLING FOLDS IN THE TODILTO LIMESTONE
GRANTS MINING DISTRICT, NEW MEXICO

by

Stephen Anthony Hines

11/11/76

RECEIVED
LIBRARY
11/11/76

Submitted in Partial Fulfillment of the
Requirements for the Degree of
Master of Science in Geology

NEW MEXICO INSTITUTE OF MINING AND TECHNOLOGY

Socorro, New Mexico

August, 1976

ACKNOWLEDGMENTS

I am greatly indebted to my advisor, Dr. John Macmillan, and to my committee members, Dr. Antonius J. Budding and Dr. Robert H. Weber, for their guidance, encouragement and patience. I also wish to thank the New Mexico State Bureau of Mines and Mineral Resources for a research assistantship which enabled me to pursue my thesis. Special thanks to my wife, Dale, and fellow students and friends who aided in many ways during the preparation of this thesis.

TABLE OF CONTENTS

	Page
Introduction	1
Objectives	1
Location and accessibility	1
Geologic setting and topography	3
Previous investigations	5
Regional stratigraphy	5
Environment of deposition of the Todilto Limestone	13
Regional tectonic history	16
Local structural geology	19
Intraformational folds in the Todilto Limestone ..	21
Local Stratigraphy	25
Entrada Sandstone	25
Todilto Limestone	27
Summerville Formation	34
Petrology	37
Laminated micrites	37
Gypsiferous micrites	40
Crenulated micrites	41
Pseudosparites	50
Intraclastic pseudosparites	57
Terrigenous arenites and wackes	60
Depositional Environment of The Todilto Limestone	65
Intraformational Folding In The Todilto Limestone	70
Physical description of intraformational folds	70
Areal distribution and stereographic analysis	
of the intraformational folds	72
Interpretation of structural contour map	91
Relationship between intraformational folds and	
the basin and dome system	94

	Page
Genetic Models Of The Intraformational Folds In The Todilto Limestone	98
Soft sediment slumping down the slope of the depositional basin	98
Differential loading and compaction in proximity to bioherms	100
Volumetric changes due to diagenesis	106
Parasitic folding on tectonic features	109
Soft sediment slump off tectonic features	113
Summary And Conclusions	116
Appendices	121
Appendix I: Classification systems	122
Appendix II: Structural data	129
Appendix III: Symbols for stratigraphic sections .	134
Bibliography	136

LIST OF ILLUSTRATIONS

Figure	Page
1. Index map showing location of the Grants mining district	2
2. Generalized map of geology of the western Grants area	4
3. Generalized cross section of the western Grants area	4
4. Lithofacies of the Todilto Limestone	8
5. Diagrammatic Section showing the relationship of stratigraphic units	11
6. Summary of stratigraphic interpretations suggested for the Jurassic in northern New Mexico	12
7. Tectonic map of San Juan Basin and adjacent areas	18
8. The transition zone overlying the upper sandy member of the Entrada Sandstone in the Zia Pit	28
9. The laminated micrite, crenulated micrite and pseudosparite zones exposed in the Zia Pit	30
10. The contact between the Todilto Limestone and the Summerville Formation is defined as the uppermost continuous limestone bed	32
11. Photomicrograph of a laminated micrite with very fine sand and silt grains defining lamination boundaries	39
12. Photomicrograph of a gypsiferous micrite showing the relationship between the microspar and fibrous gypsum	42
13. Photomicrograph showing subequant to equant crystals of spar near the center of a nodule indicating that the sparry nodules are solution-cavity fill	45

Figure	Page
14. Photomicrograph of fractures oriented with a radial pattern around a filled solution-cavity	47
15. Photomicrograph of a highly deformed lamination of pseudospar exhibiting the knotted and twisted form which is characteristic of enterolithic folding	48
16. Photomicrograph of pseudospar bodies which have displaced the laminations above and laterally	49
17. Photomicrograph of silty pseudosparite	52
18. Photomicrograph showing replacement of silty pseudosparite by euhedral purple fluorite	54
19. Photomicrograph of gangue mineralization occurring as fracture filling in silty pseudosparites	55
20. Photomicrograph of an intraclastic pseudosparite with matrix of quartz-silt arenite	59
21. Photomicrograph of a quartz arenite, the cement and matrix are calcite	62
22. Photomicrograph of quartz-silt arenite, the matrix is neomorphosed micrite while the cement is epitaxial calcite overgrowths	64
23. Conjugate fold occurring in Section 9, T12N, R9W, this example exhibits both parallel and similar folding	71
24. Stereographic projection of fold axes in Sections 9 and 15, T12N, R9W	73
25. Stereographic projection of poles to axial planes of folds in Sections 9 and 15, T12N, R9W	74
26. Stereographic projection of fold axes in Section 9, T12N, R9W	76
27. Stereographic projection of poles to axial planes of folds in Section 9, T12N, R9W	77

Figure	Page
28. Stereographic projection of fold axes in Section 15, T12N, R9W	78
29. Stereographic projection of poles to axial planes of folds in Section 15, T12N, R9W	79
30. Stereographic projection of fold axes from geologic station 9M, Section 9, T12N, R9W	81
31. Stereographic projection of poles to axial planes of folds at geologic station 9M, Section 9, T12N, R9W	82
32. Stereographic projection of fold axes of all gentle folds in Section 9, T12N, R9W	83
33. Stereographic projection of poles to axial planes of all gentle folds in Section 9, T12N, R9W	84
34. Stereographic projection of fold axes of all open folds in Section 9, T12N, R9W	85
35. Stereographic projection of poles to axial planes of all open folds in Section 9, T12N, R9W	86
36. Stereographic projection of fold axes of all closed folds in Section 9, T12N, R9W	87
37. Stereographic projection of poles to axial planes of closed folds in Section 9, T12N, R9W	88
38. Stereographic projection of fold axes of all folds having axial planes dipping from 0° to 40° in Section 9, T12N, R9W	89
39. Stereographic projection of poles to all axial planes of folds dipping 0° to 40° in Section 9, T12N, R9W	90
40. Correlation of ore bodies with structural contour map on the surface of the Entrada Sandstone	92

Figure	Page
41. Structural contour map on surface of Entrada Sandstone with axial planes of intraformational folds, Station 9D, Section 9, T12N, R9W	95
41A. Structural section drawn from X to X' in Figure 41.....	95
42. Stages in the growth of the bioherms or "reefs" and development of the intraformational folds	102
43. Section showing a typical "reef" edge and intraformational fold	102
44. Plan of reef edge around an inter-reef lagoon	103
45. Block diagram showing inter-relationship of tepee structures	108
46. Superposed simple tepees separated by erosion surfaces	108
47. Structural section of symmetrical folds showing relation of drag folds and direction of shearing	111
48. Structural section of asymmetrical inclined folds showing relation of drag folds and direction of shearing	111

LIST OF PLATES

Plate	Pocket
I. Base Map: Station 15A	
II. Cross Section of North Wall of Station 15A	
III. Cross Section of South Wall of Station 15A	
IV. Base Map: Section 15, T12N, R9W	
V. Base Map: Section 9, T12N, R9W	
VI. Structure Contour Map: Section 9, T12N, R9W	

INTRODUCTION

The Todilto Limestone contains primary uranium deposits which represent the only important uranium production from limestone in the United States (McLaughlin, 1963). The ore is associated with intraformational folds which are of undetermined origin. The origin of the intraformational folding should be determined as a necessary step for outlining future exploration or development programs.

Objectives

The purposes of this thesis are threefold: (1) to determine the local depositional environment of the Todilto Limestone, (2) to determine the origin of the ore-controlling intraformational folds and (3) to examine possible relationships between the depositional environment and origins of intraformational folding.

Location and Accessibility

The Grants mining district is located about 8 miles north of Grants in west central New Mexico (see Figure 1). The area studied is comprised of Section 15 and the northern portion of Section 9 in T.12N., R.9W. in the Dos Lomas 7 $\frac{1}{2}$ ' U.S.G.S. quadrangle, Valencia County, New Mexico.

The study area can be reached by traveling north from Grants on N.M. 53 to U.S.F.S. Access Road #450 about 1 mile north of the Homestake Partners-United Nuclear mill. Turn east on U.S.F.S. 450 and proceed 4 miles to the cattle guard at the Cibola National Forest boundary. Again turn north

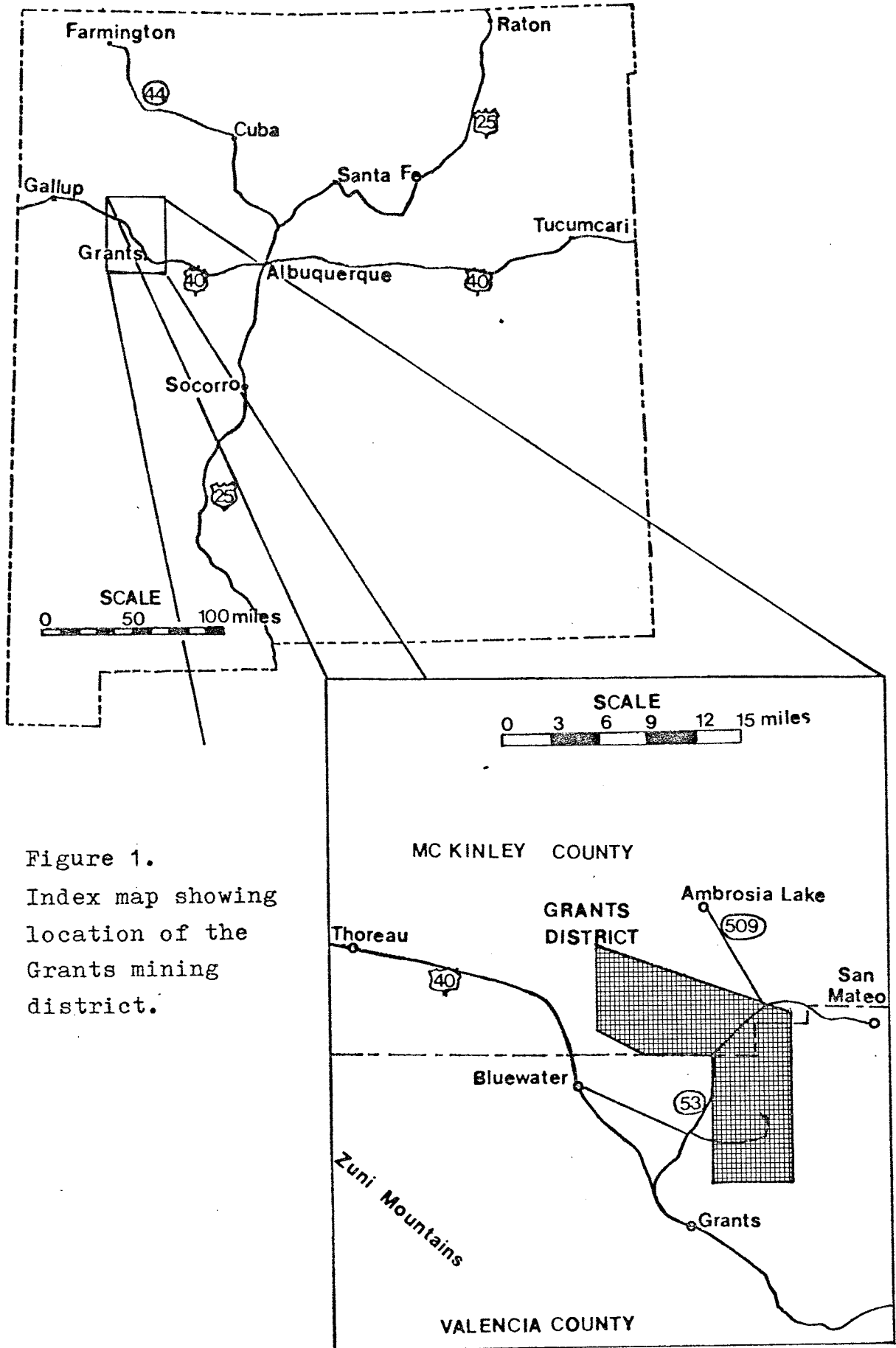


Figure 1.
Index map showing
location of the
Grants mining
district.

just inside the forest boundary. From this point, access roads are not maintained and a four-wheel drive vehicle may be necessary in some seasons.

Geologic Setting and Topography

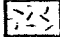
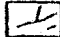

The geologic setting and topography are represented in the generalized geologic map and cross section of Figures 2 and 3.

The Grants mining district is located in what is known as the Grants uranium belt which extends west north west in a band 15 to 20 miles wide and over 90 miles long. It extends from the Rio Grande Trough to the Gallup Sag (see Figure 7). The belt crosses the northwestern end of the Zuni Uplift and follows its northern flank in the area between the Chaco Slope and the uplift (Kelly, 1963).

A topographically lower set of gently dipping questas (7000 feet) is formed by the Wingate and Entrada Formations capped by the Todilto Limestone. Higher mesas are capped by the Dakota Sandstone (7500-7800 feet) or the Mount Taylor volcanics (8000 feet), with the Morrison Formation forming the underlying slopes. Between the two sets of mesas a broad apron (6900-7100 feet) is formed by the weathering of the Summerville Formation and cover of alluvium and blow sand. Small stabilized dunes are a common feature on the western margins of the Entrada-Todilto questas.

Facing Page 4

Figures 2 and 3

Qal	Quaternary alluvial deposits
Qb	Quaternary basalt
Tb	Tertiary basalt
Ks	Cretaceous sediments
Js	Jurassic sediments
Trs	Triassic sediments
Ps	Pennsylvanian - Permian sediments
	Precambrian Complex
	Faults
	Study Area

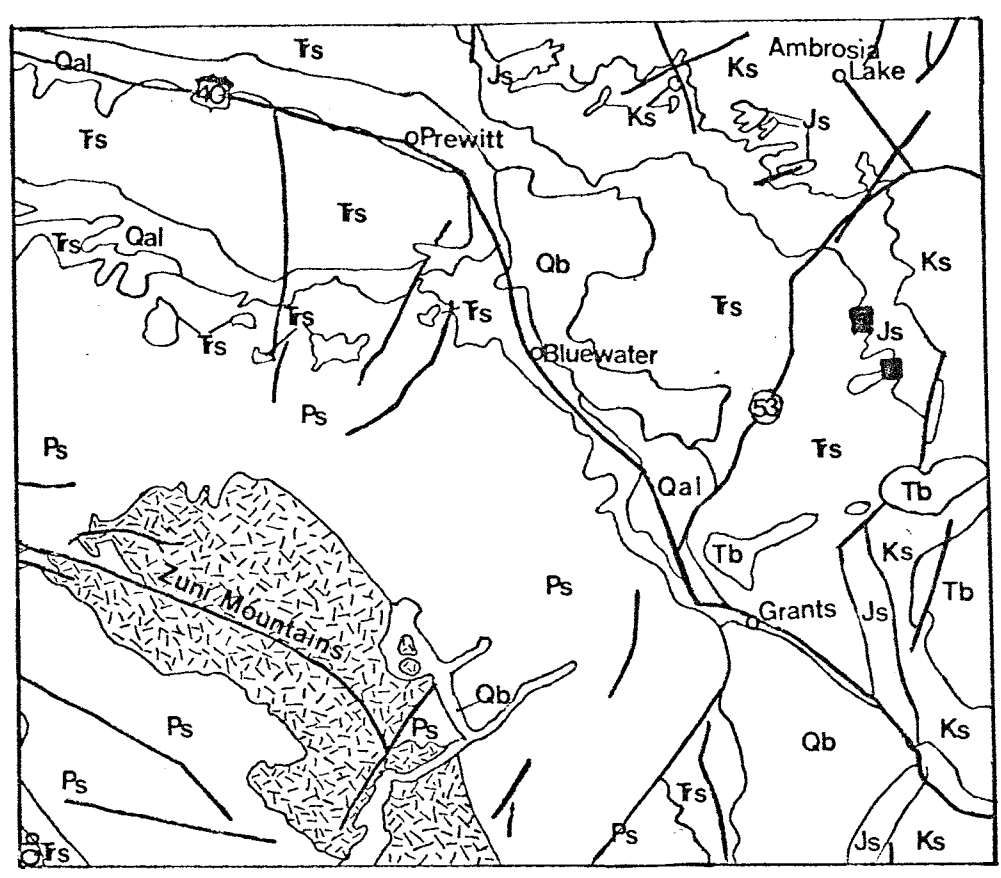
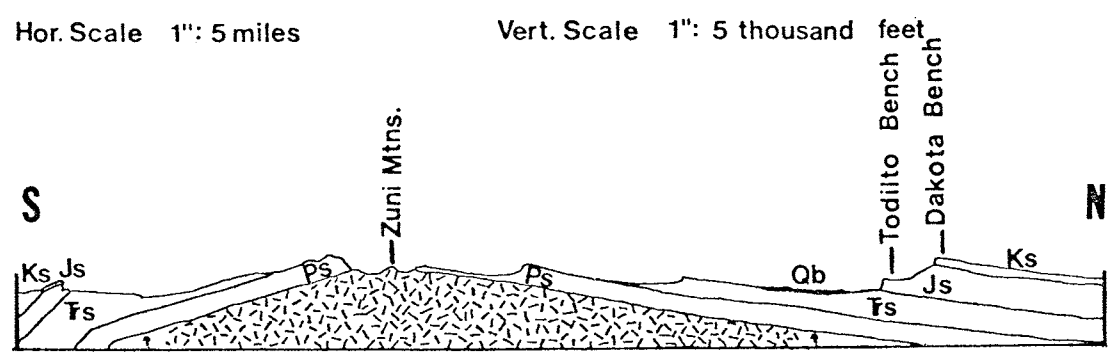


Figure 2. Generalized map of geology of the western Grants area. (After Dane and Bachman, 1957).

Hor. Scale 1": 5 miles Vert. Scale 1": 5 thousand feet

Figure 3. Generalized cross section of the western Grants area. (After Darton, 1928, and Rapaport et al, 1952).



Hor. Scale 1": 5 miles

Vert. Scale 1": 5 thousand feet

Previous Investigations

Regional Stratigraphy

The sedimentary rocks exposed on the northern flank of the Zuni Uplift range in age from Pennsylvanian to Cretaceous and lie on the Precambrian core of the Zuni Uplift. The Todilto Limestone and Morrison Formation of Jurassic age have yielded most of the uranium ore mined in the region, but this study encompasses only the Entrada Sandstone, the Todilto Limestone, and the Summerville Formation of the San Rafael Group.

The Entrada Sandstone was first described at its type locality in the northern end of the San Rafael Swell, Utah (Gilluly and Reeside, 1928). The name Entrada Sandstone was extended by the U.S. Geological Survey to include the upper thick sandstone at the type locality of the Wingate Sandstone (Dutton, 1885), which led to the abandonment of the type locality at Fort Wingate, New Mexico (Baker, et al, 1947). The Entrada is the most extensive unit of the San Rafael Group and ranges from a feather edge in central Colorado to 2000 feet in thickness in central Utah. The Entrada Sandstone generally includes two major lithofacies across the Colorado Plateau. A reddish orange to light grey, well-sorted, arenite with large scale crossbeds is the predominant lithology on the east side of the plateau. This lithofacies interfingers to the west, with a red, earthy siltstone, which comprises the entire section near the western edge of the San Rafael Swell (Wright and Dickey, 1958).

In southern Utah, northeastern Arizona, and northwestern New Mexico, three members of the Entrada Sandstone are recognized: a lower sandy member, present only in Utah and Arizona, a medial silty member, and an upper sandy member (Harshbarger, et al, 1957, pp. 35-38). In northwestern New Mexico, the Entrada rests on the Upper Triassic Wingate Sandstone (Harshbarger, et al, 1957, p. 8) except in the eastern part of the Grants Mining District where it rests on the Chinle Formation as a result of overlap (Silver, 1948).

Several depositional environments have been proposed for the Entrada Sandstone across the Colorado Plateau. The Entrada is predominantly marine in Utah and Arizona but in northeastern Arizona and northwestern New Mexico varies from marine to fluvial and eolian (Hilpert, 1963). The upper sandy member is characterized by large scale, high angle crossbedding, believed to be eolian, and thin, evenly bedded sequences indicative of fluvial deposition (Hilpert, 1963).

The Todilto Limestone, which overlies the Entrada Sandstone in northwestern New Mexico, was first described from an exposure in Todilto Park, New Mexico (Gregory, 1917, p. 55). The first formal usage of the name, Todilto Formation, was by Baker, et al (1927, p. 802) for 250 feet of sand, sandy shale and limestone beds between the associated cliff forming sandstones in Utah, in spite of the fact that they doubted the equivalence of this unit to the typical Todilto Limestone of New Mexico and Arizona. In

1936 (Baker, et al, p. 8) the Todilto was assigned as a member of the Morrison Formation and again in 1947 (Baker, et al, p. 1668) as a member of the Wanakah Formation in the San Rafael Group of Utah and western Colorado. Northrop (1950, p. 36) and Wright and Becker (1951) reassigned it to formation status in the San Rafael Group because of its uniform lithology and wide extent across southern Colorado and New Mexico. Harshbarger, et al, (1957, p. 38) included in the Todilto Limestone a lower mudstone unit, the middle limestone unit and an upper mudstone unit with a total thickness of 25 feet at Todilto Park, New Mexico. The inclusion of the lower and upper mudstone units has not been used in later studies (Ash, 1958, and Hilpert, 1963).

The Todilto may be divided into two distinct members in northwestern New Mexico: a basal limestone member and an upper, geographically restricted, gypsum-anhydrite member (see Figure 4). The basal member consists of thin bedded and laminated, grey, fine-grained limestone with some thin siltstones and seams of gypsum (Hilpert, 1963). The gypsum-anhydrite member is conformable with the basal member and occupies the central area of the depositional basin of the Todilto (Anderson and Kirkland, 1960, p. 44).

In the Laguna district both the limestone and gypsum-anhydrite members are exposed. The limestone member is as much as 35 feet thick at the Sandy Mine but thins rapidly to the northern portion of the Laguna district where it averages 10 feet. It consists of two units which are of nearly equal thickness: a lower, laminated to medium bedded

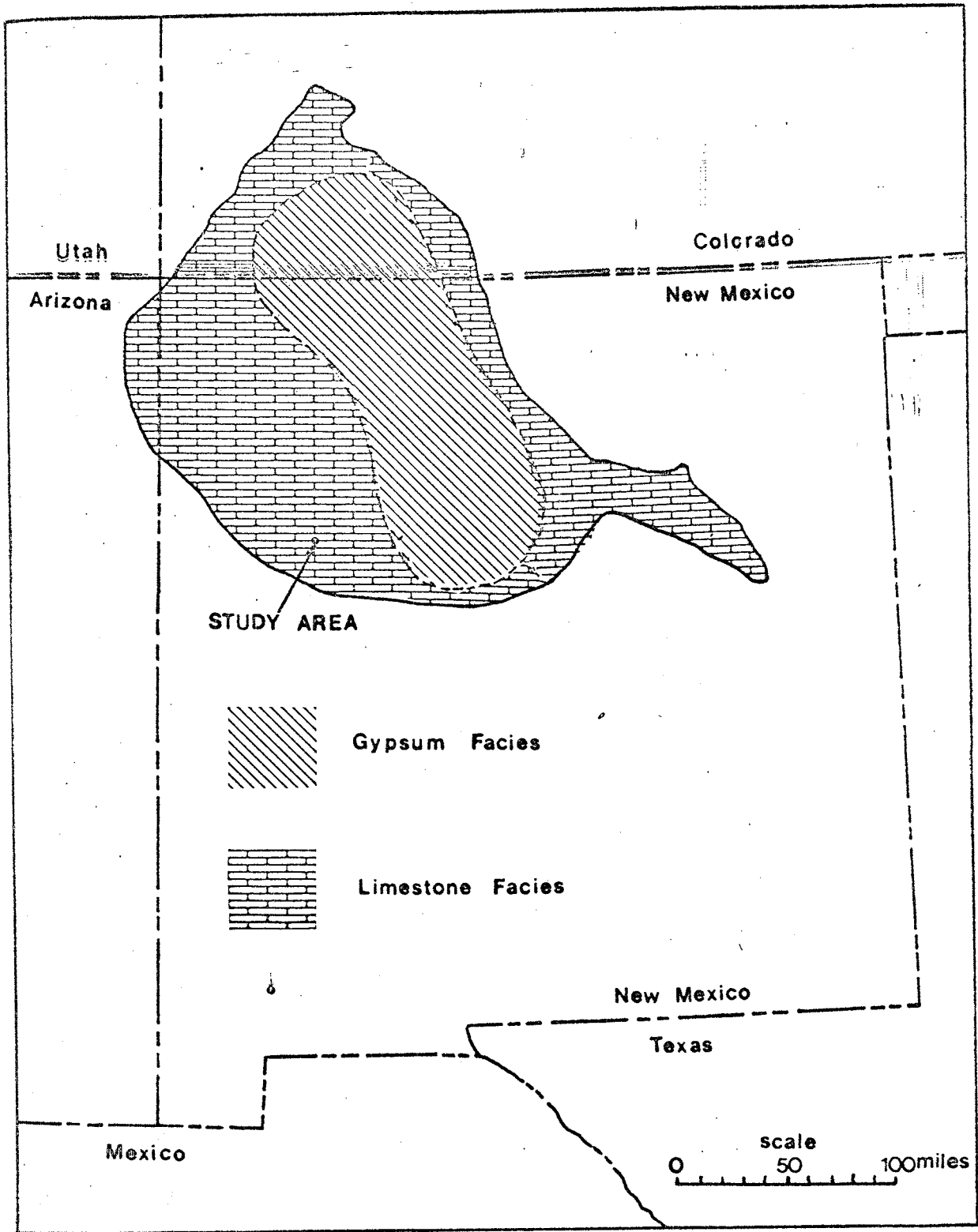


Figure 4. Lithofacies of the Todilto Limestone
(After Kirkland, 1958, p.51)

unit and an upper massive unit which is discontinuous and highly variable in thickness (Hilpert, 1963, p. 11).

In the Grants district only the limestone member is present in outcrop, but the gypsum-anhydrite member has been penetrated by drill holes about 8 miles to the north (Hilpert, 1969, p. 95). The limestone unit is as much as 30 feet thick, but averages about 15 feet. Three units are recognizable and are known as the platy (laminated) zone, the crinkly (crenulated) zone, and the massive upper zone which is locally absent (McLaughlin, 1963).

Kirkland (1958, p. 13) suggested that the repeating cycle of limestone lamina, organic lamina and clastic lamina represents an annual cycle of sedimentation or a varve. Kirkland believes that the limestone laminae represent a seasonal precipitation of limestone from the waters of Lake Todilto. The organic laminae represent a death assemblage after a seasonal planktonic bloom. The clastic laminae are the result of fall and winter run-off carrying clastic sediments into the evaporite basin.

Anderson and Kirkland (1960) proposed that the duration of the deposition of limestone was 15,000 years. The transition of predominant limestone deposition to the deposition of a predominantly gypsum lithology lasted another 3000 years in the San Ysidro, New Mexico area. In thin section, the transition zone shows lenticular gypsum nodules; Kirkland did not suggest an origin of these features.

The nature of contact between the Todilto Limestone and Summerville Formation is not uniform across the Todilto basin

(see Figure 5). An erosional surface occurs at the top of the Todilto gypsum in the Chama Basin (Lookingbill, 1953, p. 53). Ash, (1958, p. 27) cites other localities where deposition of the gypsum member and the overlying Summerville Formation appears to be continuous. Ash also cites (1958, p. 19) some pitting and solution cavities which are present short distances down in the limestone. In many places towards the center of the basin the Todilto Limestone is topped with a breccia unit of limestone embedded in the sand and silt of the overlying Summerville Formation (see Figure 5). The upper portion of the Todilto Limestone also contains lenses of siltstone, indicating a gradational contact with the Summerville Formation (Hilpert, p. 12). About twenty miles south of Grants, the Summerville Formation rests on the Entrada Sandstone with a 15 foot thick quartzite-pebble conglomerate as a basal unit (Hilpert, 1963).

The Summerville Formation was named from exposures in the northern end of the San Rafael Swell, Utah (Gilluly and Reeside, 1928, p. 80). Rapaport, et al, (1952, pp. 27-29) extended the Summerville nomenclature to the Laguna area. Smith (1954) reinterpreted the section north of Thoreau, N.M. and proposed the name Thoreau Formation. Smith correlated the lower even-bedded member of this unit with the Summerville. For the sake of uniformity in nomenclature, this investigator will continue the usage of the name Summerville Formation (see Figure 6).

Regionally, the Summerville ranges in thickness from

Horizontal Scale 1":20 miles

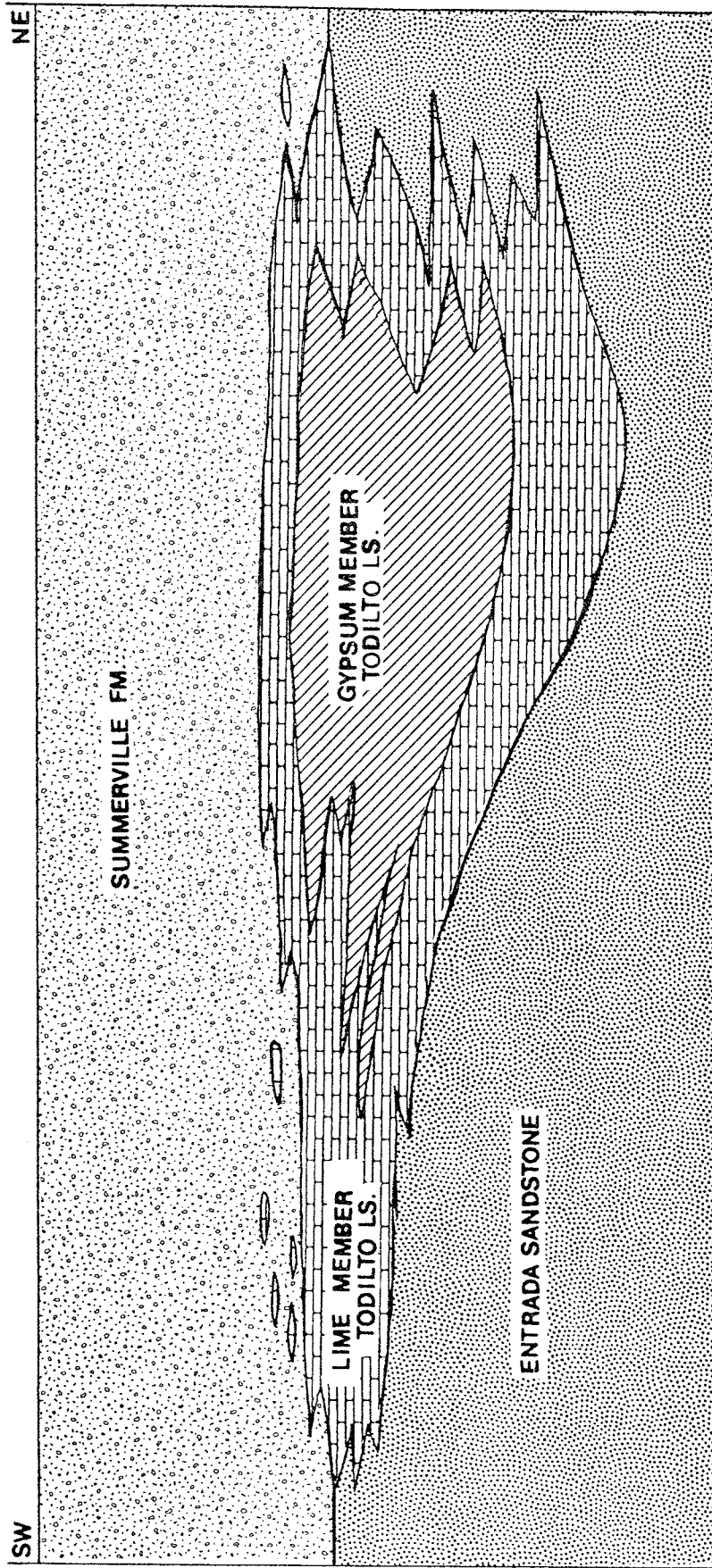


Figure 5. Diagrammatic Section Showing the Relationship of the Stratigraphic Units.
(After Ash, 1958, and Hilpert, 1963).

Figure 6. Summary of stratigraphic interpretations suggested for the Jurassic in northern New Mexico, since 1950.

Harshbarger, Repenning, and Irwin, 1957		Smith, 1954		Rapaport, Hadfield, and Olson, 1952	
Morrison Formation	Bushy Basin Member	Morrison Formation	Bushy Basin shale member	Morrison Formation	Bushy Basin member
	Westwater Canyon Member		Prewitt sandstone member		Westwater Canyon member
	Recapture Member		Chavez member		Recapture member
Cow Springs Sandstone					
San Rafael Group	Summerville Formation	Thoreau Formation	Upper member	San Rafael Group	Bluff sandstone
	Todilto Limestone		Lower member		Summerville formation
	Entrada Sandstone	Todilto Limestone	Entrada Sandstone		Todilto limestone
					Entrada sandstone

50 to 330 feet. The basal silty member overlies the Curtis Formation in the San Rafael area but is considered to be roughly contemporaneous with the Curtis deposition (Harshbarger et al, p. 42). It is a sequence of intercalated, soft, reddish brown mudstone and thin-bedded, silty sandstone units with some gypsum. Subaqueous slump structures are present in many places (Harshbarger, 1957). The basal silty member grades into the upper sandy member which is mostly reddish brown and pale brown, fine-grained, even-bedded sandstone and interbedded siltstones.

The Summerville Formation is considered to represent a transgressive-regressive phase of the Carmel-Summerville Sea (Harshbarger et al, 1957). In the Todilto basin the sediments are probably fluvial and lacustrine in origin (Ash, 1958, p. 29).

Environment of Deposition of the Todilto Limestone

The Todilto Limestone is generally considered to be an evaporite, but the actual environment of deposition is uncertain; published evidence for deposition in a marine embayment versus a lacustrine basin is controversial (Ash, 1958).

Fossil evidence is restricted to two genera of fish, two representatives of two families of Hemiptera (Water Bugs) and a single genus of ostracod. Prior to 1968, North American literature reported no occurrence of the two genera of fish in association with invertebrate fossils.

Swain (1946, p. 553) describes the species of ostracod, Metacypris todiltensis, from the Entrada-Todilto transition

zone. The genus is a nonmarine type and is reported by Swain to be similar to M.whitei Jones, of the Morrison Formation.

The two fish are Pholidophorus americanus, Eastman, identified by Koerner (1930) and Leptolepis schowei, described by Dunkle (1942). Leptolepis belongs to the Isospondyli which include modern trout and salmon and contain both marine and nonmarine types (Ash, 1958, p. 35).

The two types of Hemiptera were reported by Bradbury and Kirkland (1968) from the Entrada-Todilto transition zone at a site near San Ysidro, New Mexico. Giant water bugs or Belostomatidae and backswimmers or Notonectidae are found in apparent death assemblages with both genera of fish.

A possible algal spore and algae that have not been described are reported from Todilto Park, New Mexico (Ash, 1958, pp. 36-40). Ash also identified a highly corroded conifer pollen grain from the limestone at Todadlena, New Mexico.

A reasonable connection with known marine strata of the same age should be shown to support the theory of a marine origin for the Todilto Limestone. A channel or strait was first proposed by Imlay (1952, p. 961) who believed that the Carmel-Summerville Sea was connected to the Todilto basin, because the Todilto Limestone outcrops parallel those of the normal marine limestones of the Curtis Formation in Utah. McKee, et al (1956, p. 3) suggested that several marine connections may have existed,

but evidence is lacking. Harshbarger et al (1957, p. 46) suggested a northwest-trending strait in the Four Corners area across a broad submerged ridge. The pinch out of the Todilto in this direction is well known as is the thinning of the Entrada Sandstone. This is inconclusive evidence for a marine origin, because the thinning of the units might be due to either tidal scouring of the strait or the subaerial erosion in a nonmarine environment (Kirkland, 1958, p. 48).

Anderson and Kirkland (1960, p. 44) suggest that streams which flowed into the Todilto basin probably derived many of their salts from the Permian and Triassic strata. They noted that modern stream waters of southern New Mexico and normal sea water have about the same concentration of calcium carbonate and calcium sulfate, suggesting that either source had the potential of contributing the salts to the evaporite basin.

Anderson and Kirkland (1960) base their interpretation of the lacustrine environment of deposition of the Todilto Limestone on the absence of any marine organism.

Ash (1958, p. 31) believes that a thin marine limestone would indeed seem anomalous included between two thick, pure, coarse clastics with no related shales. The lower unit (the Entrada Sandstone) is believed to be eolian with local playa (inland sabkha) deposits, and the upper unit (the Summerville Formation) is apparently fluvial. No connection with marine strata of the same age has been recognized to substantiate a marine origin for the Todilto Limestone.

Ash (1958) presented much of the evidence cited in this discussion and concluded that the deposition of the Todilto Limestone occurred in a lacustrine environment.

Tanner (1965, p. 564) suggested that late in the history of the Todilto Lake, large quantities of gypsum began to accumulate in a "white sand" dune field across much of the northwest quarter of New Mexico. He goes on to state (Tanner, p. 568) that bands of dunes are oriented at right angles to the prevailing Jurassic wind and cites gypsum surface slopes of 40° , but it is not clear if this value is assumed to be the angle of repose for crossbedded laminations. Smith, Budding and Pitrat (1961) had previously interpreted this paleotopography to be a result of water cut channels on the upper surface of the Todilto Gypsum.

Regional Tectonic History

The Grants uranium belt is located in a region with a complex tectonic history. Hilpert and Moench (1960) believe that the area has been subjected to several minor and one major episode of deformation from the Late Jurassic to the present.

The post-Todilto - pre-Dakota period of deformation produced two distinct sets of folds. In the Laguna mining district, one set consists of broad, gentle folds with sinuous but generally east-trending crestlines. The largest have wavelengths of several miles and an amplitude of a few hundred feet. This set of folds probably also exists in the Ambrosia Lake area (Hilpert and Moench, 1960, p. 438). The second set of folds is well developed in the Laguna

area. Most folds have wavelengths of about a half mile with amplitudes of up to 100 feet, and persistently trend $N10^{\circ}-30^{\circ}W$.

Hilpert and Moench (1960, p. 441), believe that, at least in the Laguna mining district, the intraformational folds of the Todilto Limestone are localized mainly along the flanks and troughs of these two sets of Late Jurassic folds, and that the Todilto is somewhat thicker in the troughs than on the crests of the folds.

The second and major episode of deformation probably occurred in Laramide (Late Cretaceous to Early Tertiary) time. Uplift occurred in the Zuni Mountains area and was accompanied by the subsidence of the San Juan Basin (Hilpert and Moench, 1960). (See Figure 7.) The strata are tilted northerly to northeasterly on the west side of the Mount Taylor area and northerly to northwesterly on the east side. The McCarty's syncline, which is located 8 miles east of Grants and trends north-northeast, developed near the eastern end of the Zuni Uplift. The Ambrosia Dome, which is located in Sections 14 and 15, T14N, R10W, probably started to form during Morrison time and became well defined in this period (Hilpert and Moench, 1960, p. 443).

The third episode of deformation was from Middle to Late Tertiary time, with minor continuation into the Quaternary, when the Colorado Plateau was regionally uplifted and the Rio Grande Trough subsided. In the Grants uranium belt this deformation was characterized by fracturing which trends both north and east as well as paralleling the faults

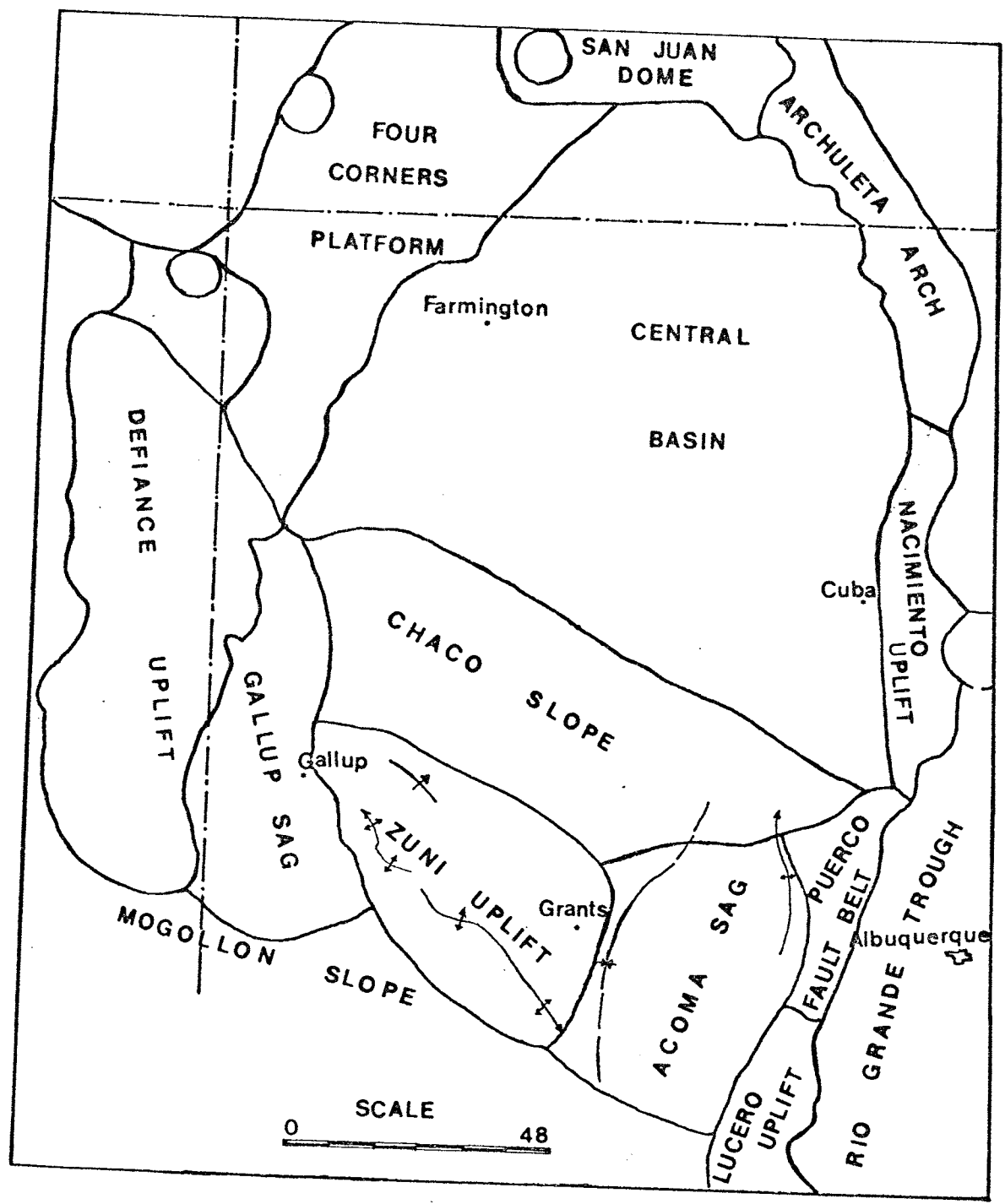


Figure 7. Tectonic map of San Juan Basin and adjacent areas. (After V.C. Kelly, 1963).

from the Laramide deformation (Kelly, 1963, p. 20).

Mount Taylor volcano developed in late Pliocene time and concurrently, headward erosion began cutting into the Mount Taylor Field. Some of the later eruptions flowed into the lower topographic surfaces such as the Grants Mesa surface. Continued erosion brought this geomorphology to its recent aspect while minor faulting cut several late Pliocene basalt flows of the Mount Taylor volcanic field. Recent basalt flows, such as the McCarty's basalt flow, flowed over 30 miles (Nichols, 1946). These flows are dated at about 1000 A.D. and are faulted by renewed movement along older faults.

Local Structural Geology

Thaden, et al (1967a, 1967b) mapped the geology of the Bluewater and Dos Lomas Quadrangles, encompassing the area of the Grants mining district. Their maps include structural contours drawn on the base of the Dakota Sandstone which illustrate the parallel to sub-parallel relationship between the folding and faulting in the area.

The faults displacing the strata in the northeastern part of the Zuni Uplift display two general trends. One set of faults is approximately parallel to the axis of maximum flexure of the Zuni Uplift (N40-60°W), and the other is normal to the axis (N5°W to N35°E) (Rapaport, et al, 1952, p. 42, and Gableman, 1956, p. 392). Vertical displacement ranges from 5 to 570 feet, and most faults are high-angle normal faults. Faults in the eastern portion of the Grants district tend to be downthrown toward the McCarty's

syncline to the east. The contemporaneity of faulting and folding is suggested by the close alignment and by the fact that faults pass upward into folds (Rapaport, et al, 1952, p. 43).

McLaughlin (1963) makes the following observations:

- 1.) No primary ore has been found in these faults, although small ore bodies occur within approximately 150 feet of major faults.
- 2.) Ore bodies in the Todilto Limestone occur within the outcrop belt at considerable distances from known faults.
- 3.) Faults displace ore bodies in at least two cases.

Large scale folding occurs at about right angles to the axis of the Zuni Uplift as a series of plunging anticlines and synclines with wavelengths of 2 to 4 miles (Gableman, 1956, p. 391). The axes of these folds are approximately parallel to the major fault trends, that is N5°W to N35°E, and Hilpert (1969, p. 103) suggests that the folds are probably related to the subparallel faults and are probably of the same age. Thus the data of Rapaport et al, 1952, Gableman, 1956, and McLaughlin, 1963, would place the age of the major faults and associated folds as Laramide or younger, which is younger than the uranium deposits.

Although eastward trending pre-Dakota folds are observed in the sediments overlying the Todilto Limestone (Hilpert, 1969), little descriptive data has been published. Ellsworth and Mirsky (1952, p. 14) were the first to publish a structural contour map drawn on the top of the Entrada

Sandstone. They attempted to correlate the mineralized zones to the minor interformational folding in Section 9, T12N, R9W. They did not differentiate between intraformational or interformational folds in their discussion of age and orientations of the folds. Although several interpretations are possible, two sets of folds are present with trends of N25°W and N80°E respectively (see Plate VI).

Ellsworth and Mirsky (1952, p. 5) make the following observations:

- 1.) All of the large ore bodies and most of the small ore bodies lie on anticlinal "nosés".
- 2.) The shapes and directions of elongation of the large ore bodies suggest control by a conjugate joint system.
- 3.) The trends of all large ore bodies examined are generally parallel to the strike of the structural contours on the Entrada Sandstone-Todilto Limestone contact which would not be expected if they were independent of structure.

Intraformational Folds in the Todilto Limestone

Rapaport, et al (1952) first described the intraformational folds and dated their development as shortly after deposition of the Todilto sediments. They proposed that the intraformational folds were due to creep of the unlithified Todilto Limestone down a gentle slope toward the basin under the weight of the overlying Summerville silts and sands.

Later the same year, Rapaport (1952) suggested that

the intraformational folds are a result of slippage between the competent Entrada Sandstone and the equally competent upper member of the Summerville Formation. The intermediate, incompetent, thinly bedded sediments of the Todilto Limestone and the basal sediments of the Summerville Formation responded by flowage under differential stress during the creation of the Zuni Uplift in Laramide time.

Gableman (1956) described some of the intraformational folds in detail and drew conclusions similar to those of Rapaport et al regarding the age of their formation. Gableman (1956, p. 389), believes that the deformation was due to compression related to diagenesis including dehydration of the sediments and recrystallization of the upper units of the Todilto Limestone.

Hilpert and Moench (1960) described the association and probable contemporaneity of the intraformational folds with the large pre-Dakota folds. They suggest that the origin of the intraformational folding is soft sediment slumping off the large anticlines.

Perry (1963) introduced a reef model of deposition for some of the recrystallized masses in the upper Todilto Limestone. He suggests that the intraformational folds are a result of differential compaction and loading associated with subsidence of the reef masses into the underlying units of the Todilto Limestone.

Bell (1963) suggested that the intraformational folds were a result of stress provided by the hydration of anhydrite and solution of the resulting gypsum early in the

diagenetic history of the Todilto Limestone.

Paragenesis of Uranium Ores in the Todilto Limestone

Truesdell and Weeks (1960) described three distinct types of ore: uranium ore, uranium-fluorine ore, and uranium-vanadium ore.

The uranium ore contains no appreciable amount of vanadium or fluorine. This occurs partly in separate deposits and partly within deposits containing irregularly distributed vanadium minerals. Some pyrite formed before colloform uraninite replaced the limestone, starting along grain boundaries and finally replacing the grains themselves. Detrital grains commonly served as nucleating centers, as did boundaries between coarsely crystallized, light colored calcite and the finer grained matrix; ore formed on these boundaries commonly extends into and replaces the limestone. The last deposited uranium was in a fine grained intergrowth of calcite and uraninite (Truesdell and Weeks, 1960, p. 52).

The fluorite-bearing uranium ore is more scarce than the other types of ore. The limestone has been recrystallized and partly replaced by purple fluorite. The fluorite seems to have been introduced after partial recrystallization of the rock but before uranium mineralization. Coarse calcite cut the fluorite which often enclosed ostracod shells without filling them. Both the calcite and the fluorite were replaced with dendritic uraninite and pyrite. Most of the uraninite is in interstitial replacements of the fine grained matrix adjacent to the fluorite. No evidence of

uraninite-fluorite intergrowth occurs, nor any genetic connection between these minerals in time or space (Truesdell and Weeks, 1960, p. 53).

The average vanadium ratio of the Todilto ores is in general less than 1:1, the vanadium is spottily distributed areally and in detail. The minerals in relatively unoxidized uranium-vanadium ore are uraninite, coffinite, haggite, paramontroseite, vanadium clay, barite, pyrite, galena, specular hematite and calcite. Recrystallization of calcite preceded, and in some cases, accompanied the deposition of the ore minerals. Precipitation of ore minerals generally began along grain boundaries and then gradually replaced the grains themselves. Some solution cavities became lined with ore minerals and were later filled with coarse calcite. Where solution cavities were absent, late pyrite or marcasite appears to have replaced uraninite-ringed quartz without replacing the uraninite (Truesdell and Weeks, 1960, p. 54).

Oxidized minerals are the dominant minerals found in many of the near-surface deposits as well as the deep areas exposed by mining excavations. Most of the oxidized minerals fill or coat the walls of fractures and bedding plane joints, and occupy solution cavities associated with coarse grained calcite (Granger, 1963, p. 35).

LOCAL STRATIGRAPHY

Entrada Sandstone

In the Grants mining district, both the medial silty member and upper sandy member of the Entrada Sandstone are present. The Entrada Sandstone is roughly 180 feet thick in the study area. The lower silty member crops out poorly due to a talus and alluvium cover and is not examined in this study. The upper sandy member, however, is well-exposed as a rounded cliff-forming unit.

The quartz arenites of the upper sandy member make up about 110 feet or 60 percent of the total Entrada thickness. Colors of the quartz arenites range from moderate reddish brown to pale reddish orange, and where the upper portion of the member has been bleached, possibly by ore bearing fluids, it is greyish orange pink to yellowish grey. The clastic material is usually rounded, moderately to well-sorted, coarse silt to medium sand size, quartz. Plagioclase feldspar and opaque contents are less than 10 percent. Cement is predominantly calcite spar and locally silica. In the upper portion of the section the bonding agent is a neomorphosed micrite matrix.

The quartz arenites are typically well cross-stratified with simple and planar cross-stratification prevalent. The sets of cross strata are lenticular to tabular, generally with symmetric nonplunging axes according to the classification scheme of McKee and Weir (1953). The high angle cross-strata are straight to concave with an average dip of 27

degrees. The individual strata vary from thin to thick laminations and are medium to large scale in length; individual sets are as much as 20 feet thick.

No fossils occur in the upper sandy member of the Entrada Sandstone within the study area. An eolian environment of deposition is generally accepted throughout the literature and is supported by the findings of this study.

A transition zone is recognized in the upper sandy member of the Entrada Sandstone separating the high angle cross-bedded arenites below from the laminated micrites of the Todilto Limestone.

The transition zone ranges from 1 to 15 feet thick; the thinnest exposure measured was at the Zia Mine in Section 15 and seems to thicken both to the north and south. The transition zone is well exposed throughout the study area except where covered by alluvium or talus, and often weathers more rapidly than the quartz arenites or laminated silty microspars.

Quartz-silt arenites constitute the entire transition zone. They range in color from very pale orange to yellowish grey. The clastic material is subrounded to rounded, poorly to moderately sorted, medium silt to very fine sand-size quartz. Plagioclase feldspar and opaque minerals occur in trace amounts. The micrite matrix is incompletely neomorphosed to a pseudospar.

The transition zone is characterized by near horizontal, thin and laterally continuous bedding, and low angle, small scale, tabular to wedge-shaped sets of planar and trough

cross-strata. The sets of cross-strata are often asymmetric and have both plunging and non-plunging axes. No other current structures or fossils occur in the transition zone in the study area (see Figure 8).

The transition zone and the top 15 to 40 feet of the upper sandy member of the Entrada Sandstone show reduction of the hematite stain. Locally this causes a variegated coloration, but the resulting yellowish grey color is common across most of the area. In the southern portion of Section 4, the reduction follows a few major joints an additional 15 feet down into the red quartz arenites of the Entrada Sandstone.

Smith (1954, p. 14) does not recognize a transition zone and reports that beds of the Todilto Limestone truncate cross-laminations of the Entrada Sandstone with sharp angular unconformity approximately 12 miles northwest of the study area in the Thoreau Quadrangle.

Todilto Limestone

The Entrada-Todilto contact is conformable and varies from an intertonguing to gradational nature. In one or two localities a true intercalated relationship occurs between the clastic beds of the Entrada and the carbonate beds of the Todilto. A mixed gradational contact is most common so that the lowest limestone bed is very silty and each higher bed of limestone gradually becomes purer, with only thin partings of silt or sand separating laminations of limestone.

In the Grants district, the Todilto Limestone ranges from 15 to 28 feet in thickness. Although the lower units

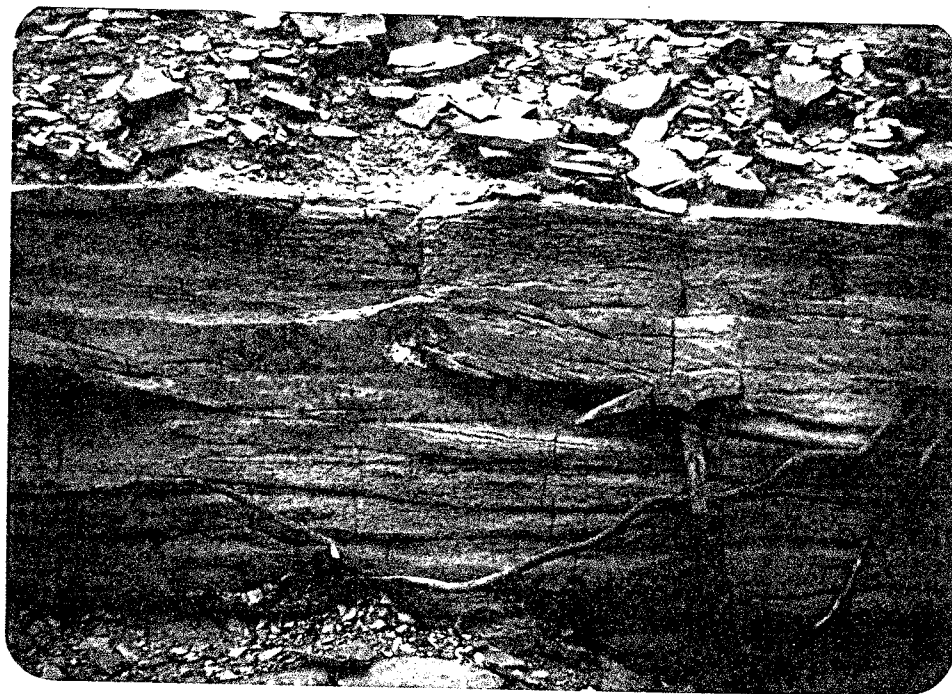


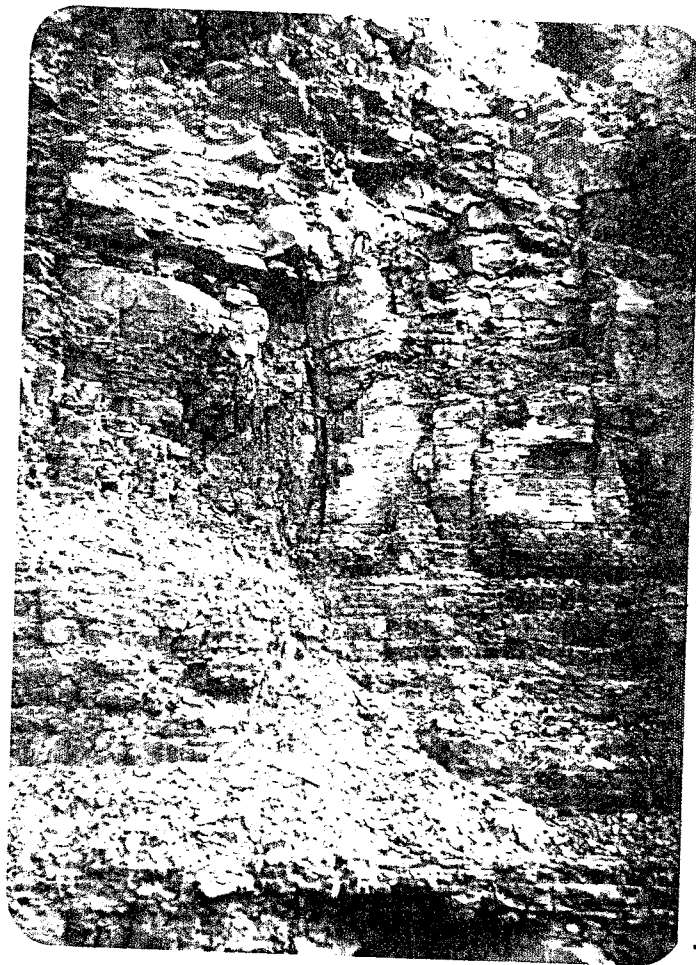
Figure 8. The transition zone overlying the upper sandy member of the Entrada Sandstone in the Zia Pit.

of the limestone are widely exposed, exposure of the complete Todilto section occurs only locally in mining excavations.

The Todilto Limestone has been divided into three separate lithologic zones by previous authors (McLaughlin, 1963, p. 136, and Gableman, 1956, p. 389). The three lithologic zones were briefly summarized earlier in this investigation. A more descriptive terminology is suggested so that the relationship between lithologies and lithologic zones is clear. The three zones will be referred to as the laminated micrite (platy) zone, the crenulated micrite (crinkly) zone and the pseudosparite (massive or recrystallized) zone (see Figure 9).

The laminated micrites and rarely, intercalated gypsiferous micrites occur in a zone at the base of the Todilto Limestone. This zone is 7 to 13 feet thick. At Station 9D (see Plate V) a thinly laminated unit is truncated by a planar erosion surface that is covered by an overlying thinly bedded unit resulting in a slight angular unconformity of less than 8 degrees. Quartz-silt arenite and wacke parting occur in the lower half of the laminated to thinly bedded zone. The gypsiferous micrites have been used on a local basis as marker horizons by previous investigators.

Slight undulation of laminations and thin beds, to extreme contortion of bedding, occurs at several locations in the study area (see Plate II, column 3). These disturbed beds always lie on the same horizon as, or just above, the



Pseudosparite Zone

Crenulated Micrite
Zone

Laminated Micrite
Zone

Figure 9. The laminated micrite, crenulated micrite and pseudosparite zones exposed in the Zia Pit.

gypsiferous micrites, but never in direct contact with these gypsiferous sediments. Interpretation of the origin of these features yields two possibilities: 1) the contortions are a result of foundering of the lime sediments as a result of dissolution of underlying gypsiferous units; 2) the contorted bedding is a result of swelling and heaving caused by the hydration of anhydrite to gypsum.

The laminated micrite zone grades rapidly upward into the crenulated micrite. The crenulated micrites occupy a zone that is generally 1 to 5 feet thick and is well exposed in both outcrop and mining excavation. The abundance of the crenulations, as well as the sparry nodules, shows a definite gradational increase from the base of the crenulated micrite zone to the pseudosparite zone.

Pseudosparites and some of the intraclastic pseudosparites occur in a zone at the top of the Todilto Limestone. This zone is from 2 to 13 feet thick and is best exposed in mining excavations.

The contact between the Todilto Limestone and the Summerville Formation is arbitrarily chosen as the upper surface of the topmost continuous bed of limestone. This arbitrary definition commonly includes several feet of thinly interbedded, very silty pseudosparites and quartz-silt arenites and wackes within the upper zone because of the local intertonguing of the Todilto carbonate beds with the overlying Summerville terrigenous beds (see Figure 10).

The terrigenous clastics are predominantly calcareous quartz-silt arenites and wackes, and less commonly very

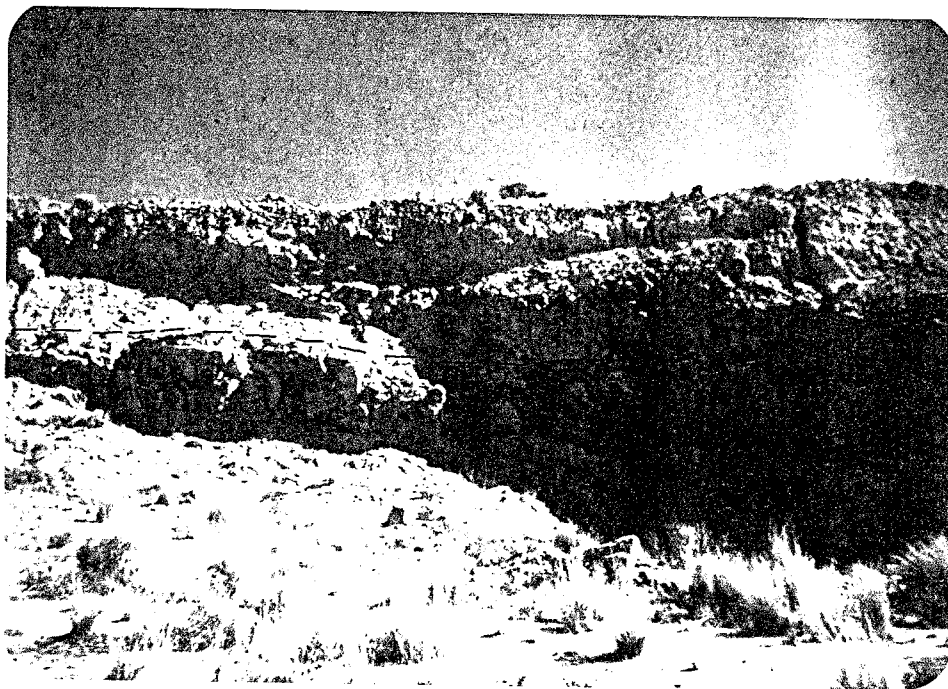


Figure 10. The contact between the Todilto Limestone and the Summerville Formation is defined as the uppermost continuous limestone bed because of the local intertonguing of the Todilto carbonate beds with the Summerville terrigenous beds.

fine-grained quartz arenite. In extreme cases, the terrigenous clastics constitute a maximum of 12 feet or 43 percent of the total thickness of the Todilto Limestone. They range in color from white to light brownish grey. The clastic material is poorly to well sorted, fine silt to fine sand-size quartz, and rarely fragments of limestone, siltstone or claystone. The bedding of the terrigenous clastics is usually indistinct to faint, but may be inferred by the long orientation of concretions, and carbonate or claystone pebbles parallel to bedding.

No channels on the upper surface of the upper zone have been identified in the study area, however, Rapaport (in McLaughlin, 1963, p. 139) has cited such channels in Sec. 30, T13N, R9W. At that locality, considerable portions of the Todilto were eroded, and erosional patterns on the Todilto surface trend northeastward.

In the study area, the upper surface of the pseudo-sparite zone exhibits up to 5 feet of relief over about 50 feet of lateral distance (see Plates II and III), but this relief can be in part erosional and in part depositional. Intraclasts present within the pseudosparites are also indications of local erosion and deposition.

The transition from Todilto to Summerville deposition indicates an influx of terrigenous clastics of fluvial origin, with steadily decreasing amounts of carbonate matrix. Lime intraclasts are present both in the pseudosparites within the Todilto Limestone and as granule to cobble sized clasts in the basal units of the Summerville Formation.

Summerville Formation

In the Grants mining district, the Summerville Formation overlies the Todilto Limestone. The Summerville Formation is about 215 feet thick, and consists of quartz-silt arenites and wackes which have been divided by previous workers into a lower silty member and an upper sandy member. The silty member locally crops out on the stripped-off Todilto bench as a talus-covered slope, and the sandy member as a horizontally bedded cliff-forming unit. Most of the exposures studied in the area were a result of past mining excavations and the strata above the basal units are not discussed in this study. The basal units consist of an intraformational conglomerate which grades upward into the quartz-silt arenites and wackes, characteristic of the silty member of the Summerville Formation.

The intraformational conglomerate is discontinuous and ranges in thickness from 0 to 8 feet and varies from very pale orange to yellowish grey in color. The clasts are very poorly sorted, granule to cobble size, and subangular to subrounded. Clast lithologies are silty pseudosparite, calcareous quartz-silt arenite and wacke, as well as montmorillonitic claystone. The matrix ranges from calcareous quartz arenites to calcareous quartz-silt wacke, the same composition as the non-conglomeratic sediments above. Stratification within the conglomerate is poorly developed except locally by parallel alignment of clasts. Possible pebble imbrication occurs at only one locality.

Rarely, quartz-silt arenites and wackes and thin,

non-fossiliferous recrystallized limestone lenses less than 1 foot thick occur within the intraformational conglomerates. These limestone lenses may be vertically separated from the Todilto Limestone by as much as 20 feet of clastic sediments.

The sediments directly above the intraformational conglomerate consist of the calcareous quartz-silt arenites and wackes of the lower silty member of the Summerville Formation. Colors of the quartz-silt arenite and wacke units range from dark reddish brown to yellowish grey. The clastic material is poorly to well sorted, medium silt to medium sand-size quartz. Roundness varies from subangular to subrounded in the medium sand sizes. Locally, the matrix of the wackes is neomorphosed micrite. Calcite cement and locally clay minerals are the predominant bonding agents. Bedding is locally well-defined, and ranges from thick laminations to thin beds.

Cross-stratification of the sediments is uncommon, but locally both simple and trough cross-stratification occurs, the latter being the predominant form. The sets of cross-strata are lenticular, plunging to non-plunging, and symmetric. The low-angle cross-strata are straight to concave and are small to medium scale, individual sets are usually less than 6 feet thick.

Limey concretions occur locally in irregular zones in the Summerville sediments.

The basal 5 to 15 feet of the Summerville Formation commonly exhibit reduction of the hematite stain. The hematite stain of the quartz-silt arenites and wackes of the

upper zone of the Todilto Limestone are also reduced. The reduction does not follow any systematic pattern, however, the intraformational folds in the upper zone of the Todilto Limestone commonly act as boundaries between reduced and oxidized units.

PETROLOGY

The Todilto Limestone in the Grants mining district is divisible into easily recognized rock types, based on primary and secondary textures. The rocks examined from the underlying Entrada Sandstone and overlying Summerville Formation are incorporated into this discussion to clarify the nature of the upper and lower contacts of the Todilto Limestone. The rock units within the Todilto Limestone are discussed in the order of ascending stratigraphic position: (1) Laminated Micrites, (2) Gypsiferous Micrites, (3) Crenulated Micrites, (4) Pseudosparites, (5) Intraclastic Pseudosparites, (6) Terrigenous Arenites and Wackes.

Laminated Micrites

Geographically, the most widely distributed lithology is laminated micrite, comprising the lower one-third of the Todilto Limestone.

Macroscopically, the micrites are medium light grey (N6) to light olive grey (5Y7/1) and medium dark grey (N4) to brownish grey (5YR4/1) on fresh surfaces. The thin laminations and thin beds in the micrites are laterally continuous for tens of feet, and the only current structures observed are scour marks. Fossils were not recognized in hand samples of this unit taken from the study area. Very fine sand to coarse silt is sparsely distributed on planes separating laminations or beds. Commonly the micrite is rich in organic material and yields a fetid odor when struck with the hammer.

In thin-section the laminated micrites exhibit limited

variability in the amount of terrigenous debris, and a typical diagenetic history (see Figure 11).

The terrigenous constituents of the laminated micrites constitute 5 to 25 percent of the total rock composition. Quartz is the predominant mineral with less than 2 percent plagioclase feldspar (in the oligoclase-andesine range) and a trace of hematite and other opaques. Grain size ranges from very fine sand to medium silt. The grains are subhedral to anhedral and their shape ranges from elongate to subequant. Roundness varies from subangular to subrounded, and decreases with decreasing grain size. Grain orientation is roughly parallel to lamination and only locally is there enough grain to grain contact to suggest a grain supported texture.

The non-terrigenous material consists of calcite micrite to microspar with a trace of organic debris and an occasional ostracod test. Very rare, medium sand size intraclasts of silty micrite occur. Microspar crystals are equant and vary from 0.01 to 0.05 mm.

Laminations are distinct in the thin section due to horizons of silt, changes in crystal size and changes in color due to organic material. The thinly bedded micrites are internally laminated, but the laminations are less pronounced. The only current structures which occur are scour marks from 2.0 to 7.0 cm long and filled with quartz-silt.

The major diagenetic change in the laminated micrites is the local neomorphism of micrite to microspar. Intraclasts of silty micrite float in the microspar, indicating

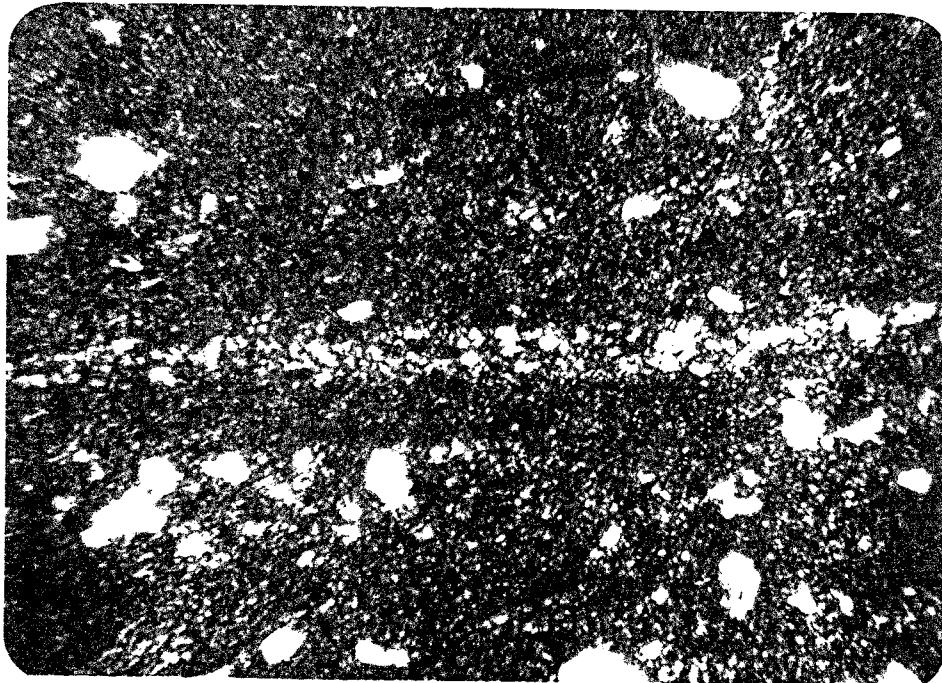


Figure 11. Photomicrograph of a laminated micrite with very fine sand and silt grains defining lamination boundaries.

that the microspar is not a cement. Although locally the microspar has a uniform crystal size, it shows a gradational relationship to micrite, indicating the microspar is a diagenetic alteration of micrite. In a few areas, neomorphism produced equant crystals from 0.025 to 0.15 mm, but these patches make up only a small portion of the rock.

Gypsiferous Micrites

Gypsiferous micrites occur locally within the laminated micrites. This lithology is rare, and does not occur any higher in the stratigraphic section.

Macroscopically the gypsiferous micrites are greyish orange (10YR7/4) to greyish yellow (5Y8/4) and yellowish grey (5Y8/1) to white (N9) on fresh surfaces. The gypsiferous micrites occur as thin beds which are laterally continuous for a hundred feet and more but thicken and thin from 0.5 to 8.0 cm across 50 feet of lateral distance. The gypsum occurs as fibrous selenite or satin spar in thin lenticular bodies, set in a silty micritic matrix.

In thin-section the terrigenous constituents are restricted to very fine sand to medium silt size quartz and a trace of hematite which, together, make up 25 percent of the total rock composition. The grains range from anhedral to subhedral, their shape ranges from elongate to subequant, and rounding from angular to subrounded. Grain orientation is roughly parallel to bedding and only 20 percent or less of the silt grains exhibit grain to grain contacts.

The non-terrigenous material consists of 40 percent

fibrous gypsum, and calcite ranging from microspar, 45 percent, to pseudospar, 15 percent. The gypsum is fibrous to equant in shape and ranges from 0.25 to 1.0mm for the equant grains, to over 4.0 mm for the larger fibers. Most of the fibrous gypsum exhibits multiple polysynthetic twinning oriented to within 30 degrees of perpendicular to bedding. The microspar is equant to bladed and ranges from 0.062 to 0.25 mm in size. (See Figure 12)

Bedding is distinguishable by silty horizons and slight variations in the microspar texture. No fossils are present in this lithology, nor are any current structures identifiable.

The principal diagenetic alteration of the gypsiferous micrite is the neomorphism of micrite to microspar and locally to pseudospar. It is impossible to determine whether the primary CaSO_4 mineral was gypsum or anhydrite, but the polysynthetic twinning of the fibrous gypsum may be a result of hydration of anhydrite or heating of the thin-section (Kerr, 1959, p. 225). There is no evidence of replacement of calcite by gypsum or vice versa, which supports a primary origin for the calcium sulphate.

Crenulated Micrites

Crenulated micrites occur at several horizons near the middle of the stratigraphic section. The crenulated micrites of this zone are geographically widely distributed but vary locally in thickness from 1 to 3.5 feet.

Macroscopically, the crenulated micrites vary from



Figure 12. Photomicrograph of a gypsiferous micrite showing the relationship between the microspar and fibrous gypsum.

yellowish grey (5Y8/1) to brownish grey (5YR4/1) and greyish orange yellow (5YR7/2) to medium dark grey (N4) on fresh surfaces. The crenulated micrites are thinly bedded, but exhibit internal laminations which bend around sparry nodules, producing their distinctive wavy appearance. Some of the larger nodules resemble gypsum nodules in size and shape but are composed of clear to white calcite spar. The abundance of the nodules increases gradationally upward from the laminated micrite unit to the overlying pseudospar unit. No macrofossils occur in hand samples of this unit in the study area. The crenulated micrites yield a fetid odor when struck with the hammer.

Thin-section analysis of crenulated micrites indicates that terrigenous constituents comprise about 10 percent of the total rock. Quartz is the predominant mineral with 1 percent plagioclase feldspar and a trace of hematite and other opaques. Grain size ranges from coarse to medium silt and sorting is moderate. Roundness ranges from sub-angular to rounded, the grains are subhedral to anhedral, and their shape varies from elongate to subequant. Grain orientation is roughly parallel to bedding and because of the concentration of the silt on the interlamination planes there is local grain contact causing an isolated grain supported texture.

The non-terrigenous material consists of 20 to 60 percent micrite, and 30 to 66 percent calcite spar in nodular bodies. The micrite shows a very faint localized mosaic of microspar in the 0.004 to 0.016 mm range. The nodular bodies

have a distinctive internal structure. The edge of the nodule consists of a crust of equant to bladed crystals, ranging in size from 0.016 to 0.062 mm and oriented perpendicular to the surface of the nodule. Toward the center of the nodule, the crystals of spar become equant and increase in size, so that the center of the nodule consists of a near equant mosaic of crystals up to 4.0 mm in size. (See Figure 13.) This fabric indicates that the sparry nodules are a solution-cavity fill.

The laminations become thinner toward the filled solution-cavities and locally only the silty portion of a lamination separates two nodules. No current or other sedimentary structures occur in this lithology. Ostracod tests, floating in the micrite matrix, are common in this lithology.

Diagenesis of the original micrites is not extensive as evidenced by the rarity of localized patches of microspar and by the small crystal size of the microspar. A few samples exhibit neomorphism of the micrite to microspar ranging in size from 0.004 to 0.25 mm, near the margins of the solution-cavity fill.

The texture and composition of the solution-cavity fill has been described above, however the whole-rock texture greatly resemble that of the rocks occurring at the transition from lime to gypsum-anhydrite facies of the Todilto in the Jemez Springs area (Kirkland, 1958, p. 29). Kirkland states that the material in the nodules is gypsum at that location, but in the study area no pseudomorphs

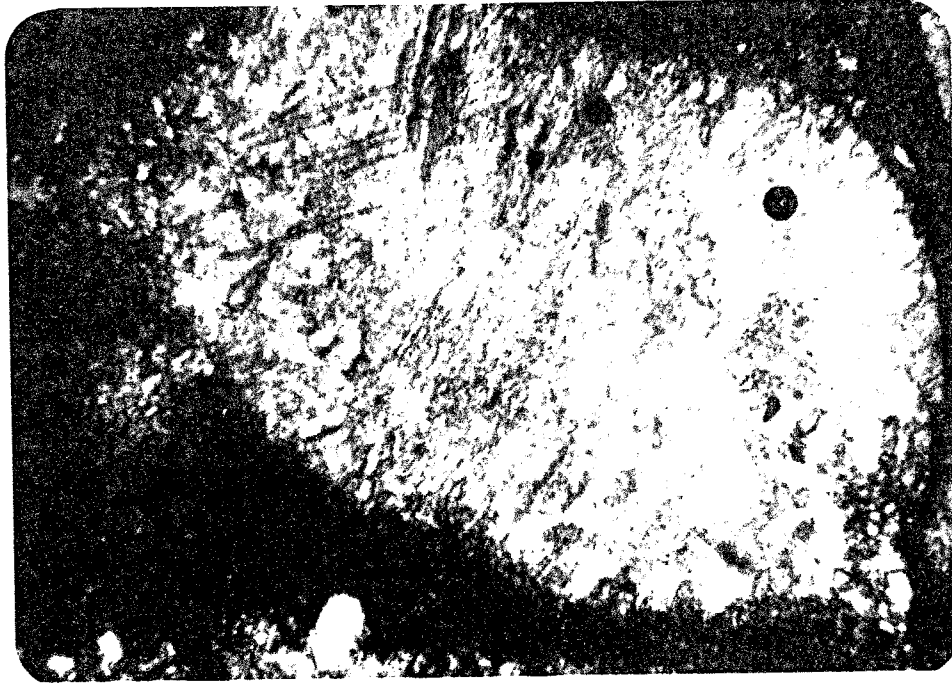


Figure 13. Photomicrograph showing subequant to equant crystals of spar near the center of a nodule indicating that the sparry nodules are solution-cavity fill.

after gypsum or anhydrite occur in the nodules.

It is here assumed that the material in the nodules was a calcium sulphate, which was later dissolved forming a moldic porosity which was subsequently filled by calcite spar. Neomorphism of micrite to microspar occurred after filling of the nodular cavities because the microspar does not alter the crust in the solution-cavity fill.

There are two examples of this lithology which show possible evidence for displacive crystal growth. In the first example fractures are oriented with a radial pattern around a filled solution-cavity (see Figure 14). The fractures are not in contact with the nodule but begin a few millimeters from the edge of the nodule and become progressively larger away from the nodule until they terminate at a lamination plane. The fractures are filled with bladed to fibrous calcite crystals oriented perpendicular to the fracture walls. The suggestion is that, at some time, expansion of the nodule displaced the lamination and the deformation was in the form of fractures. It is not known whether the expansion was due to the hydration of calcium sulfate or by later crystal growth of the calcite spar within the nodule.

A second example exhibits possible enterolithic folding and displacive crystal growth. (See Figures 15 and 16.) A highly deformed lamination of pseudospar in Figure 15 presents the knotted and twisted form which is characteristic of enterolithic folding. The large pseudospar body in Figure 16 may have displaced the laminations above and

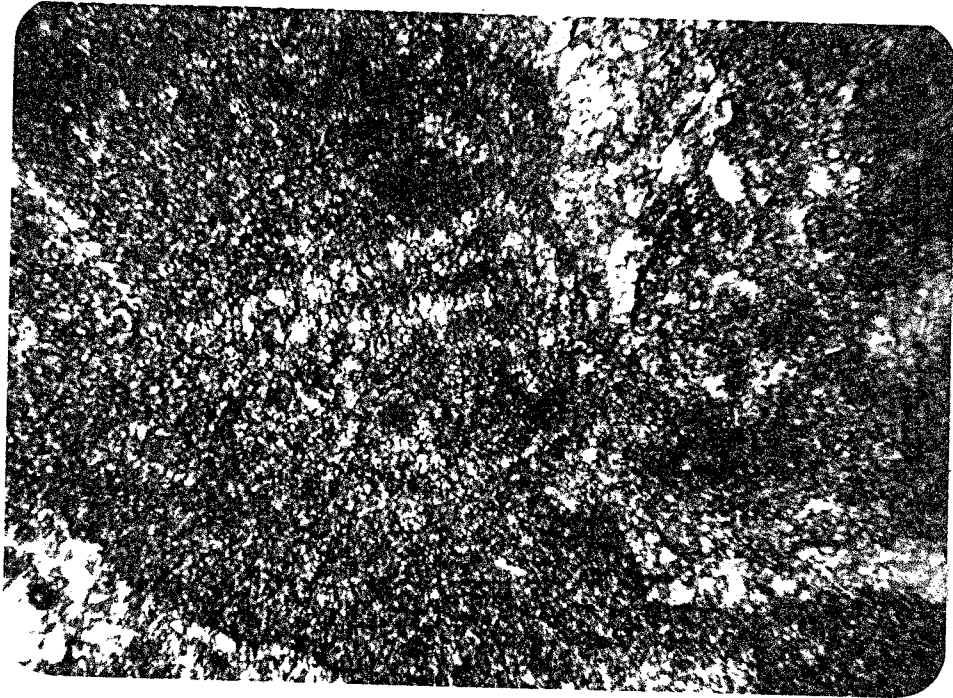


Figure 14. Photomicrograph of fractures oriented with a radial pattern around a filled solution-cavity (without crossed nicols).



Figure 15. Photomicrograph of a highly deformed lamination of pseudospar exhibiting the knotted and twisted form which is characteristic of enterolithic folding.



Figure 16. Photomicrograph of pseudospar bodies which have displaced the laminations above and laterally (without crossed nicols).

laterally, but this body appears to be a thicker portion of a neomorphosed lamination, rather than solution-cavity fill described earlier in the text.

Pseudosparites

In most of the study area, an irregular upper zone of the Todilto Limestone occurs which may actually represent sediments originally similar to the laminated micrites and crenulated micrites, but which are now modified by neomorphism.

Macroscopically, the pseudosparites are very pale orange (10YR8/2) to greyish, orange pink (5YR7/2), and brownish grey (5YR4/1) to light olive grey (5Y6/1) on fresh surfaces. The pseudosparites appear to be moderately to thickly bedded, but on close examination they are irregularly bedded with rapid changes in thickness from 2 to 13 feet over 100 feet of lateral distance. Locally, relict crenulations and laminations occur due to slight variations in color and crystal size. On weathered surfaces fine sand to silt size terrigenous grains are common. No macrofossils occur in hand samples of this lithology. Non-terrigenous material includes finely to coarsely crystalline calcite and fluorite. Box works after an unidentified mineral are filled with zoned calcite and siderite. Along faults and joints, calcite spar and black to brown siderite rhombs are common as replacement and fracture-filling minerals. Minor gangue minerals, as well as secondary uranium minerals, are also common in this zone.

In thin-section the pseudosparites exhibit numerous

localized variations from a standard fine to medium crystalline silty pseudosparite (see Figure 17).

Terrigenous constituents comprise from 3 to 20 percent of the total rock. Quartz is the predominant mineral with less than 1 percent plagioclase feldspar; a trace of hematite and other opaques occur. Grain size ranges from very fine sand to medium silt. The grains are subhedral and their shape varies from subequant to elongate. Roundness varies from angular to subrounded. Grain orientation is random if the silt is uniformly dispersed through the sediment, but local concentrations of silt, indicative of primary lamination, show orientation of the long dimension parallel to bedding and no imbrication. Grain to grain contacts occur in the siltier horizons, resulting in a grain supported texture.

The non-terrigenous material consists of 63 to 95 percent spar and microspar to pseudospar, 3 percent to only a trace organic material, and less than 1 percent randomly distributed ostracod tests. Microspar crystals are equant, subhedral to euhedral, and vary from 0.01 to 0.05 mm. Pseudospar crystals are equant to bladed, subhedral to euhedral, and vary from 0.25 to 4.0 mm with a few crystals over 4.0 mm in size. Bedding in the thin-section ranges from indistinct to distinct, principally in the form of silty laminations and laminations defined by changes in crystal size across possible bedding horizons. No current or biogenic structures occur in this lithology.

Diagenesis of the representative lithology is relatively



Figure 17. Photomicrograph of silty pseudosparite
(with crossed nicols).

simple, but extensive, widespread neomorphism produces the microspar and pseudospar. In some cases this neomorphism results in the total or partial obliteration of the original depositional textures. Fracturing and the subsequent fracture-filling with bladed to equant calcite and siderite post-dates the neomorphism.

Additional diagenetic changes produce the major atypical examples occurring in the field. One of the most interesting types is the replacement of some silty pseudosparites by euhedral, very dusky purple (5P2/2) fluorite (see Figure 18). Fluorite may make up as much as 65 percent of the whole rock composition locally. Because of the small crystal size (0.025 to 0.25 mm), the original microspar and pseudospar textures are preserved.

According to Truesdell and Weeks (1960), fluorite post-dates partial recrystallization of the rock but predates uranium deposition. Some ostracod tests were partly filled with fluorite. Later calcite spar cut the fluorite and then both were replaced with uranium minerals and pyrite. Truesdell and Weeks (1960, p. 53) state that there was no evidence of uranium-fluorite intergrowth in the polished section, nor any genetic connection between these minerals in time and space.

A less common variation in the basic silty pseudosparite is associated with precipitation of primary uranium ore and gangue minerals as a fracture filling (see Figure 19).

The ore-bearing fluids had little effect on the host silty pseudosparite at a distance of more than 5 mm from



Figure 18. Photomicrograph of replacement of silty pseudosparite by euhedral purple fluorite (without crossed nicols).



Figure 19. Photomicrograph of gangue mineralization occurring as fracture filling in silty pseudosparites. Siderite comprises most of the material in this photograph with hematite occurring as thin films between crystal faces of siderite (without crossed nicols).

the fracture boundary. The paragenesis of the fracture-filling gangue minerals is as follows:

- a). Calcite spar comprises about 15 percent of the fracture-fill and occurs on the fracture surfaces as a discontinuous veneer of subhedral to euhedral, equant to fibrous shaped crystals which are oriented perpendicular to the fracture wall and range in size from 0.25 to 4.0 mm.
- b). Siderite comprises about 35 percent of the fracture-fill and occurs as a continuous coating on either the fracture surface or the veneer of calcite spar. The siderite occurs as equant to bladed, subhedral to euhedral crystals which range in size from 0.5 to 4.0 mm.
- c). Hematite comprises from 3 to 8 percent of the fracture-fill and occurs as thin films between crystal faces of siderite and barite, and as poikilitic bodies in larger crystals of barite. The hematite also occurs as euhedral pseudomorphs after pyrite, ranging in size from 0.2 to 2.0 mm.
- d). Barite comprises from 10 to 20 percent of the fracture-fill as a continuous coating over the earlier mineral phases and in some fractures it occurs as a stellated mass. Barite crystals range in size from 0.5 to 3.75 mm, are euhedral, and exhibit bladed to fibrous shapes.
- e). Calcite spar comprises from 10 to 25 percent of the fracture-fill and commonly closes the fracture.

The calcite occurs as subhedral to euhedral, equant to blade shaped crystals which range in size from 0.25 to 4.0 mm. There is a high percentage of enfacial junctions among the triple junctions and crystal size increases away from the fracture walls.

Several variations of the above paragenesis occur that combine the mineral phases in the following suites:

- 1). a-b
- 2). b-e
- 3). a-b-e
- 4). a-c, d-e
- 5). a-c-e

Only secondary uranium minerals occur in the fracture-filling as local intercrystalline films. The data is insufficient to place the uranium in the paragenetic sequence. H.C. Granger (1963, p. 35) suggests that the barite is associated with the unoxidized, or primary uranium minerals, however in the study area most barite samples were taken from exposures of secondary mineralization in mine excavations.

Intraclastic Pseudosparites

Intraclastic pseudosparites are relatively uncommon and occur near the contact between pseudosparites of the Todilto Limestone and the terrigenous deposits of the Summerville Formation.

Macroscopically the intraclastic pseudosparites are greyish, orange pink (5YR7/2) to pinkish grey (5YR8/1) and light grey (N7) to yellowish grey (5Y8/1) on fresh surfaces. Bedding is laterally discontinuous, rapidly thickening and

thinning from 0.3 to 3.5 feet over 10 feet lateral distance, and may occur as isolated masses surrounded by pseudosparites. Orientation of the clasts is roughly parallel to bedding. At one locality, four clasts were imbricated. Clast sizes vary from granule to pebble size. The composition of most clasts is microsparite and silty microsparite, a few clasts are calcareous quartz-silt wackes and an occasional bentonitic claystone pebble occurs. The matrix enveloping the clasts varies from silty pseudosparite to calcareous quartz-silt wacke and calcareous quartz arenites.

In thin-section the intraclastic pseudosparites exhibit a limited range of variations from the typical lithology (see Figure 20).

Intraclasts constitute 10 to 55 percent of the whole rock composition. The lithologies of the intraclasts are microsparite, laminated silty microsparite, and pseudosparite. Clast size ranges from very coarse sand to cobble. Roundness varies from subangular to rounded. Most clasts were semi-lithified before transport and deposition, as evidenced by the rounded clast boundaries and lack of deformation by loading. Clast orientation is parallel to bedding.

The matrix is silty microspar. Quartz-silt comprises 10 to 45 percent of the matrix. There is also a trace of plagioclase feldspar, a trace of opaque minerals and local concentrations of clay minerals. The non-terrigenous constituents are microspar and fine grained pseudospar. There are a few clasts of clayey micrite which are angular

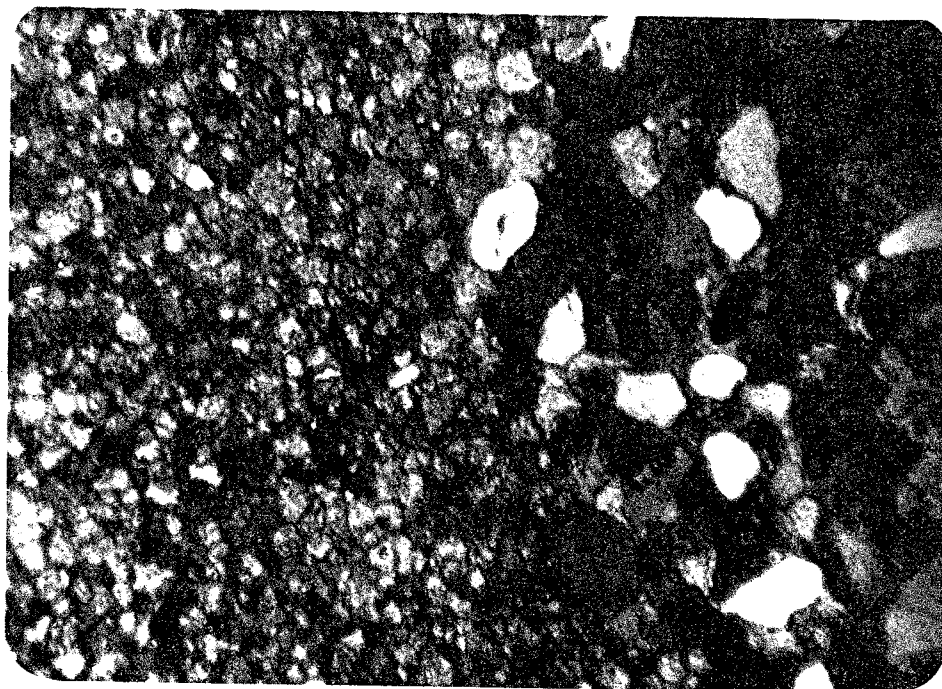


Figure 20. Photomicrograph of an intraclastic pseudosparite, the matrix in this example is a quartz-silt arenite but commonly occurs as a silty microspar (crossed nicols).

to subrounded, and have a very irregular, feathery contact with the silty matrix.

Included with the intraclastic pseudosparites are sedimentary limestone breccias which occur at the top of the pseudosparite wedge (see Plate II, Cross Section of Northwall of Station 15A).

On weathered surfaces the sedimentary limestone breccias are very pale, yellowish brown (10YR7/2) to light olive grey (5Y6/1) and dark grey (N3) to light grey (N7) on fresh surfaces. The sedimentary limestone breccias occupy the upper 0.5 to 1.0 foot of the pseudosparite wedge. Breccia clasts range from granule to cobble size and are very angular. The distance of transport is less than one foot for any individual clast, and clasts can be traced by their shape and surface texture to their original locations. The matrix varies from a very silty pseudosparite to a calcareous quartz-silt wacke. Complete pore-fillings of calcite and siderite crystals are widespread.

In thin-section the angular clasts of the breccias are similar to the standard pseudosparite lithology. The major difference is the relative lack (from 8 percent to only a trace) of terrigenous debris within breccia clasts themselves.

Terrigenous Arenites and Wackes

In the study area, the Upper Jurassic strata are predominantly terrigenous clastics. Although the clastics were not extensively sampled in this study, they are locally interbedded with the limestone and occur directly below it

as the Entrada Sandstone, and directly above it as the Summerville Formation.

Macroscopically the terrigenous clastics are greyish, orange pink (5YR7/2) to pinkish grey (5YR8/1) and very light grey (N8) to yellowish grey (5Y8/1) on fresh surfaces. Bedding thickness varies from thickly laminated to thickly bedded. Locally, bedding is faint to indistinct and internally homogeneous. The quartz arenites of the Entrada Sandstone, and to a lesser extent of the Summerville Formation, exhibit cross-bedding, which is described in the last chapter. Grain size ranges from medium sand to medium silt. Quartz is the predominant mineral, composing 90 percent or more of the terrigenous material. Present in varying amounts are plagioclase feldspar, hematite stain and dark opaque minerals. The matrix is neomorphic pseudospar, and in a few cases, clay minerals. The cement is calcite spar, often occluded with clay minerals or hematite stain.

In thin-section the terrigenous clastics are classified according to texture, and to a lesser extent, according to grain size. The basic criteria for this scheme is as follows:

Arenites - more than 50 percent terrigenous material and less than 25 percent matrix, so that a grain supported texture is maintained.

(See Figure 21.)

Quartz-silt arenites - as above but the terrigenous material falls in the silt size range.



Figure 21. Photomicrograph of a quartz arenite, the cement and matrix are calcite (crossed nicols).

(See Figure 22.)

Wackes - more than 50 percent terrigenous material and more than 25 percent matrix, so that a matrix supported texture is maintained.

The terrigenous material is 75 to 97 percent quartz, 8 percent to a trace feldspar (oligoclase-albite), 7 percent to a trace hematite and other opaques, and a trace of amphibole. Grain size ranges from medium sand to medium silt. Roundness ranges from subangular to rounded, with the larger grains exhibiting better rounding. Sorting is typically moderate but ranges from moderate to poor in rare cases.

The cement and matrix are predominantly calcite. The calcite is fine grained and occurs as epitaxial overgrowths on quartz grains. The matrix is neomorphosed micrite and ranges from equant 0.01 mm microspar to equant 0.25 mm pseudospar. Generally the neomorphic matrix comprises 75 percent or more of the calcite in the rock.

Grain orientation is roughly parallel to bedding or cross-bedding but few grains are sufficiently subspherical to produce this fabric.

Diagenesis seems to be simple cementation coinciding with neomorphism of a micrite matrix.

The stratigraphic occurrence of these rock types is discussed in the preceding chapter.



Figure 22. Photomicrograph of quartz-silt arenite. The matrix is neomorphosed micrite while the cement is epitaxial calcite overgrowths (crossed nichols).

THE DEPOSITIONAL ENVIRONMENT OF THE TODILTO LIMESTONE

The depositional environment of the Todilto Limestone, and the corresponding depositional history, may be interpreted by close examination of the paleontologic, petrologic and stratigraphic evidence.

Fossils found in the study area consist entirely of ostracods. These ostracods closely resemble the species, Metacypris todiltensis, as first described by Swain (1946), but a definite identification was not made. The genus, Metacypris, ranges from fresh to brackish waters in all recent forms. No member of a biota restricted to a marine environment was found in the study area, or by previous investigators. Also present throughout the limestones are organic-rich laminations, which Kirkland (1958) interprets as sapropel, that is, ooze composed of plankton and water at the time of deposition. He also notes that fragments identified as tracheids and fibers from vascular plants occur in most of these laminations. Although such organisms were not identified in this study, the amount of carbonaceous material that is present suggests deposition in anaerobic bottom waters.

The following features occur in the lower zone of the Todilto Limestone: horizontal rhythmic laminations and thin bedding, scour marks, shrinkage cracks, disturbed bedding and clastic lenses. All of these features fit the criteria for the lacustrine environment, summarized by Picard and High (1972).

The terrigenous material shows a rapid decrease in size, roundness and abundance from the eolian quartz arenites of the upper sandy member of the Entrada Sandstone to the silts present in the micrites and pseudosparites. In the laminated and thinly bedded zone, the quartz-silt occurs along the interfaces between the laminations. This is interpreted to be a result of seasonal or periodical influx of the terrigenous material by either ephemeral streams or eolian transport. In the Todilto Limestone, previous reports (Rapaport et al, 1952, and Ash, 1958) do not cite occurrences of silt greater than about 8 percent of the total rock. Analyses of samples from the study area show as much as 25 percent in the upper and lower zones. The terrigenous material of the basal Summerville returns to coarser grain sizes and exhibits a wider range of rounding.

In the crenulated micrite zone, the solution-cavity fillings of calcite spar resemble the lobate outlines of gypsum-anhydrite nodules noted in the sabkha environment (Kendall and Skipwith, 1969, and Lucia, 1972). No gypsum-anhydrite, nor pseudomorphs after these minerals, have been identified in any such nodular bodies in the study area. Kirkland (1958, p. 26) describes lenticular gypsum nodules from the limestone-gypsum transition zone which are identical in outline to the solution-cavity fillings from the study area. Ash (1958, p. 24) reports that these calcite spar bodies occur at Satan Pass and Todilto Park, New Mexico.

There is no conclusive evidence to suggest that the

sediments of the crenulated limestone zone were exposed to subaerial conditions. Evidence of subaerial exposure often includes such sedimentary structures as birdseye structures, mudcracks, raindrop impressions, salt casts, salt polygons, stromatolites, clastic dikes and adhesion ripples. However, if the calcite spar bodies do represent gypsum-anhydrite nodules, then they are indicative of either coastal or inland sabkhas.

Petrographic examination reveals no dolomite rhombohedrons, nor any ghosts of dolomite rhombs indicating dedolomitization. All chemical analyses by previous investigators (Bell, 1968, p. 13, and Allen and Balk, 1954, p. 77) show 2 percent or less $MgCO_3$. In the coastal sabkhas of the Persian Gulf, dolomitization is contemporaneous with the deposition of gypsum (Butler, 1969). The lack of dolomite in the sabkha environment indicates that the chemical composition of the waters present was not comparable to the composition of sea water, suggesting that the coastal sabkha model does not apply to the Todilto Limestone.

Modern inland sabkhas associated with lakes are of two major types: 1) sabkhas with lakes fed by ephemeral flood waters which carry a wide range of clastic material, and 2) sabkhas which are the result of subsiding lake waters and are characterized by horizontal bedding, gypsum nodules, salt crusts, adhesion ripples, and lateral association with bedded evaporites if precipitation of evaporites from the standing water takes place. A rise of the water table

would tend to remove the more soluble salts and might produce casts or collapse features.

Glennie (1972) interpreted the Ten Boer Member of the Rotliegendes of northwestern Europe as an inland sabkha laterally associated with ephemeral lakes. He interprets the sabkha facies of the Ten Boer Member to be the result of flooding and ensuing desiccation. Laterally, this inland sabkha grades into a clayey sequence in which halite is a characteristic component. Eugster and Surdam (1973) proposed that the depositional environment of the Wilkins Peak Member of the Green River Formation was a vast playa fringing a lake. They believe that the interstitial water of the inland sabkha, and the lake water, was highly alkaline but that seasonal fluctuation produced the interlamination of trona, dolomite and chert.

Thus the crenulated limestone zone may represent a period of deposition when receding waters resulted in the development of lake-flats. The lake-flat sabkha surface was probably very close to the level of the water table, because desiccation cracks did not develop or were not preserved. The development of the lake-flat sabkha facies possibly marks the beginning of the deposition of bedded gypsum-anhydrite of the Gypsum Member of the Todilto Limestone.

The relict laminations and relict crenulations of the pseudosparite zone suggest that the original sediments were similar to the laminated micrites and the crenulated micrites. The relict textures suggest that the pseudosparites do not

represent a different primary facies such as a reef. The alteration of the laminated micrites and crenulated micrites suggests that the depositional conditions were intermittently those of a lake and a lake-flat sabkha.

The intraclastic pseudosparites of the upper zone indicate locally higher current velocities and erosion of the sediments. These intraclastic pseudosparites do not exhibit any of the lateral relationships that would indicate that they are reef-front talus deposits such as a rapid increase in thickness and clast size toward associated reefs. The intraclasts are apparently a result of the transition from the lacustrine and lake-flat environments of the Todilto Limestone to the fluvial environment of the Summerville Formation.

Finally, the position of the Todilto Limestone in the vertical succession supports the lacustrine and lake-flat environments of deposition. The Todilto Limestone occurs between two continental (mixed eolian and fluvial) units, the Entrada Sandstone and the Summerville Formation.

INTRAFORMATIONAL FOLDING IN THE TODILTO LIMESTONE

Physical Description of Intraformational Folds

The intraformational folds occurring in the study area are small, ranging in size from three inches to 50 feet in half-wavelength. Most of the intraformational folds have amplitudes which are generally smaller than the half-wavelength. The largest intraformational fold in the study area has an amplitude of about 18 feet and a 50 foot half-wavelength. The axes of the intraformational folds are traceable over a few feet to approximately 250 feet, but a few adjacent folds with small wavelengths and subparallel fold axes can be traced up to 1200 feet laterally (extending from Station 9A, Section T12N, R9W, into Section 4, T12N, R9W).

The intraformational folds occur throughout the Todilto Limestone and extend into the overlying basal units of the Summerville Formation.

The intraformational folds exhibit a wide variety of styles. Most of the anticlinal folds are inclined, asymmetric, gentle and open forms (Fleuty, 1964) with closed and recumbent forms much less common. The synclinal folds are generally inclined, open forms. Often isolated anticlinal forms are separated by extensive intervals (several times the half-wavelength of the anticline) of planar beds. That is, well-defined wave trains of anticlines and synclines are not always developed. Conjugate folds occur at several localities in the study area (see Figure 23).

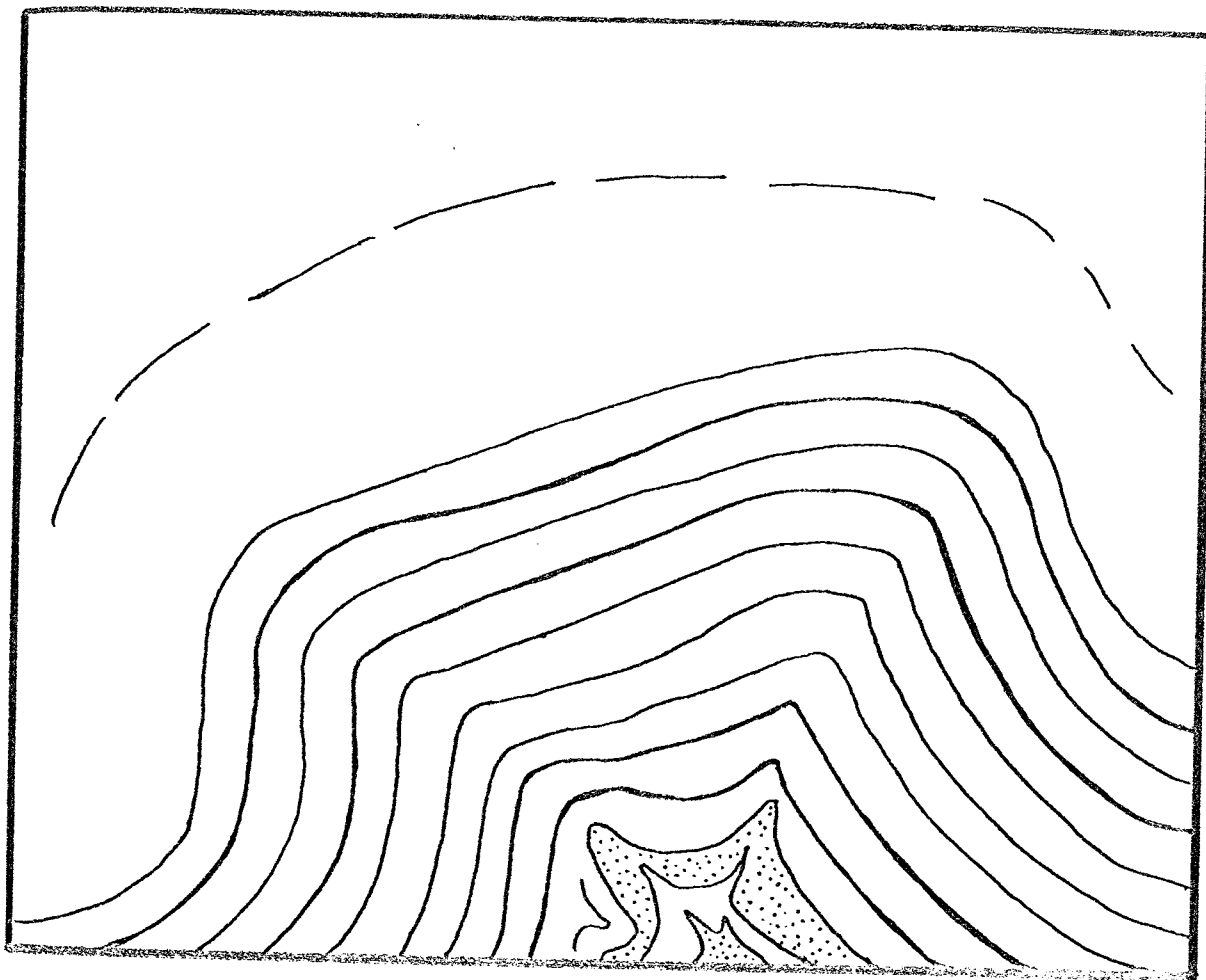


Figure 23. Conjugate fold occurring in Section 9, T12N, R9W, this example exhibits both parallel and similar folding. The silt pod occurring in the core of this fold indicates flowage at the time of folding.

Parallel and similar folds occur in the study area; some individual intraformational folds exhibit both types. Some of the folded units maintain the same thickness throughout all parts of the fold, but others exhibit thinning of the limbs and thickening at the crests and troughs. Some intraformational folds have brecciated cores, indicating that some of the sediments were lithified or semi-lithified at the time of folding, but evidence of flowage, such as silt pods in the cores and on the flanks, is widespread, indicating that other sediments may have been poorly consolidated at the time of folding.

Areal Distribution and Stereographic Analysis of the Intraformational Folds

One hundred and three intraformational folds were measured in this study. These intraformational folds occur in the mining excavations and in outcrop along the Todilto bench. The mining excavations are widely spaced and do not represent a uniform or random sampling of the area, so that data on the spatial density of intraformational folds is not available. The orientation data for all intraformational folds plotted on the base maps (see Plates IV and V) is presented in Table 1 in Appendix II.

Stereographic projections of all fold axes and poles to axial planes of intraformational folds in Sections 9 and 15, T12N, R9W, are presented in Figures 24 and 25. (All stereographic projections are lower hemisphere projections on Schmidt nets.) In an effort to isolate any variation in the orientation of intraformational folds as a function of

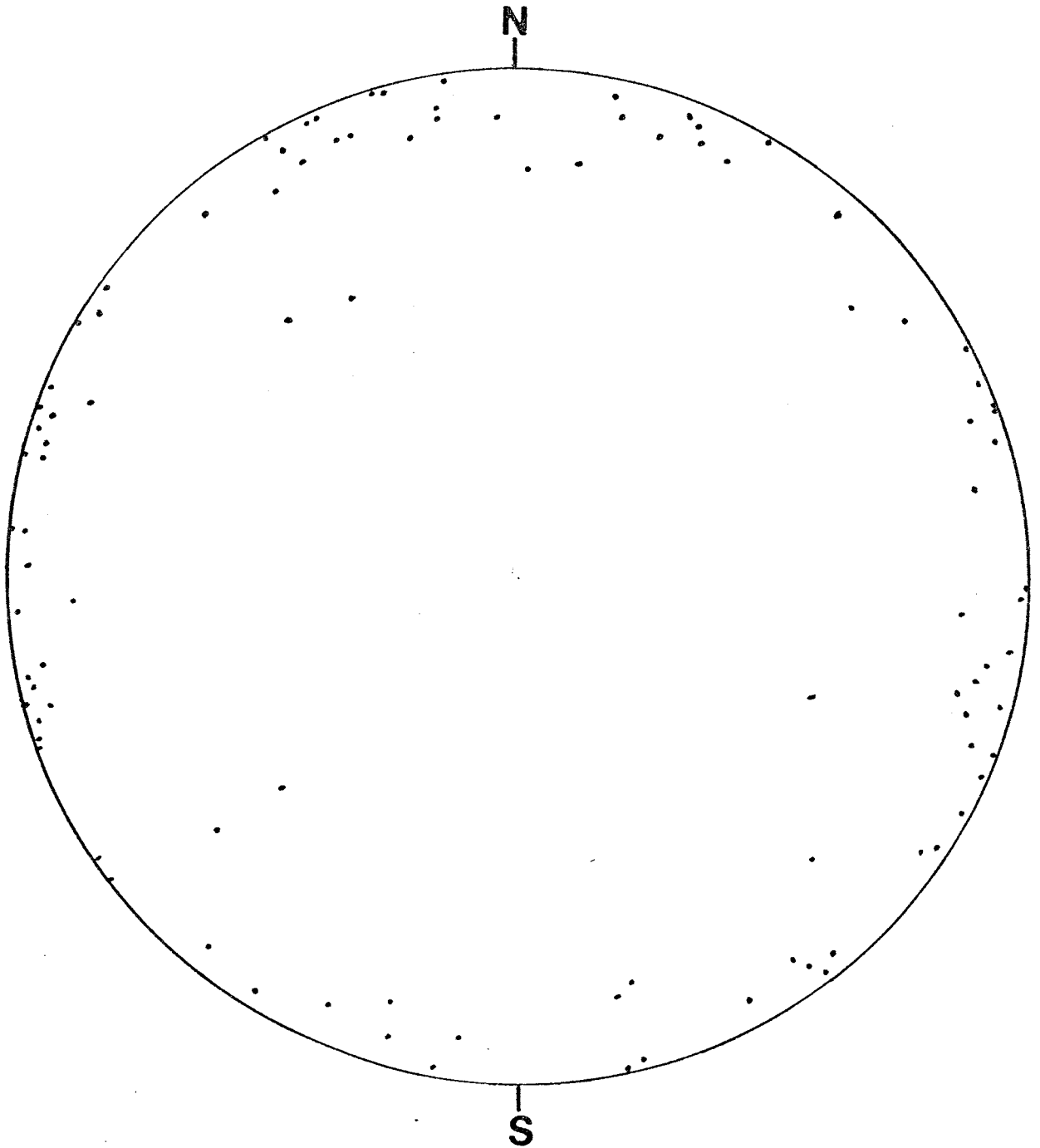


Figure 24. Stereographic projection of fold axes in Sections 9 and 15, T12N, R9W, (103 points).

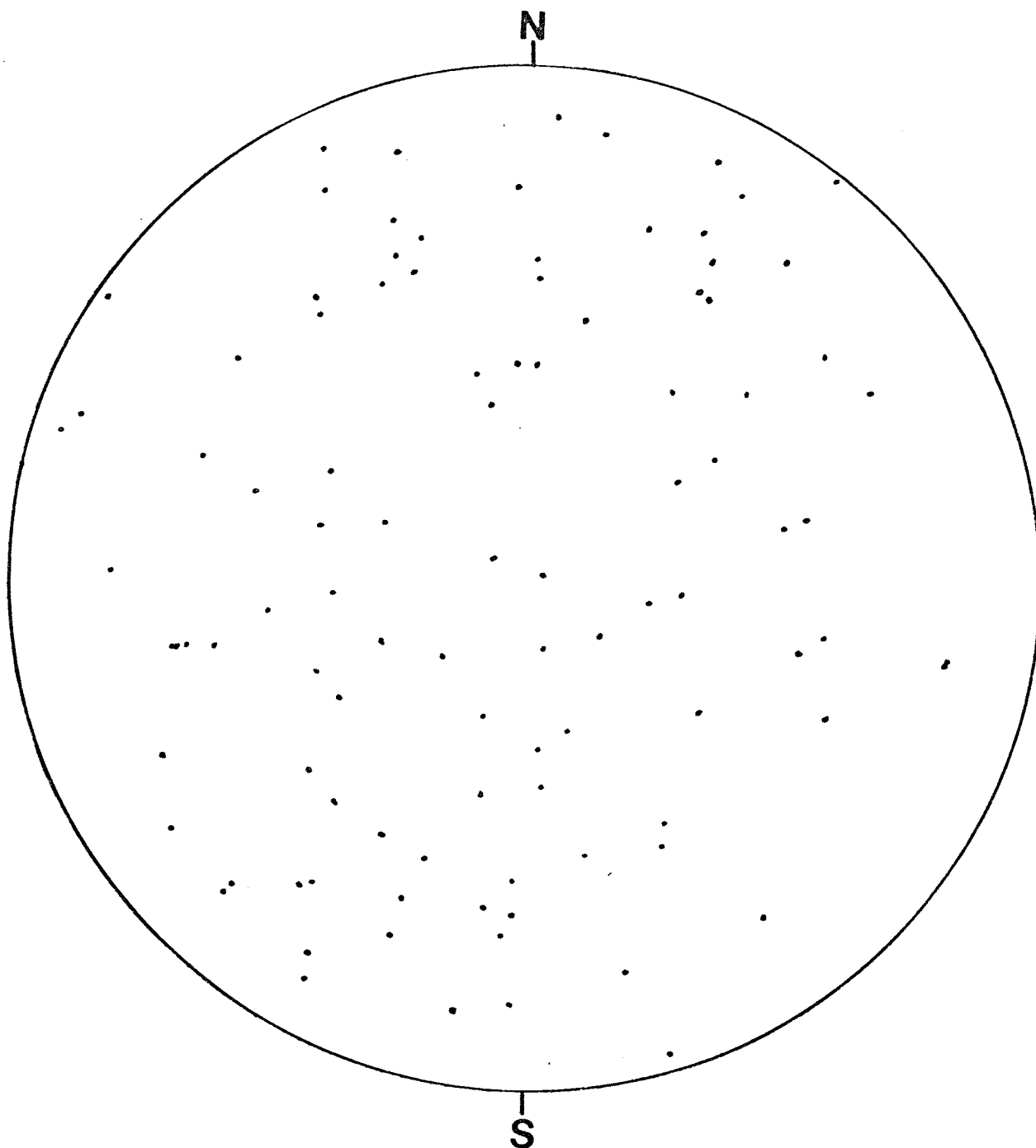


Figure 25. Stereographic projection of poles to axial planes of folds in Sections 9 and 15, T12N, R9W, (103 points).

geographic position, stereographic projections were made of the eighty-seven axes and poles to axial planes of intraformational folds in Section 9 (see Figures 26 and 27), for comparison with the stereographic projections of the sixteen fold axes and poles to axial planes of intraformational folds in Section 15 (see Figures 28 and 29).

The poles to axial planes (Figures 25, 27, 29) occur at all possible orientations without any major concentrations at a point or along great or small circles. The stereographic projections of fold axes (Figures 24, 26, 28) show that they occur at all azimuths, but 85 percent plunge 12° or less. Moreover, the fold axes are parallel to subparallel to the strike of the axial plane regardless of the orientation of the axial plane (see Table 1 in Appendix II).

If sets of superposed folds are present, a point concentration of poles to axial planes could indicate the coplanar orientation of the axial planes of the youngest fold set. The poles to axial planes of the older fold sets would be redistributed along great or small circles. The lack of such concentrations on the stereographic projections indicates that superposed sets cannot be determined for the entire study area at this geographic scale.

Additional geographic subdivisions were used in order to find domains or areas where single fold patterns can be analyzed, but even for very small areas, similar patterns on the stereographic projections result. Such subdivisions included local groups of geologic stations as well as single

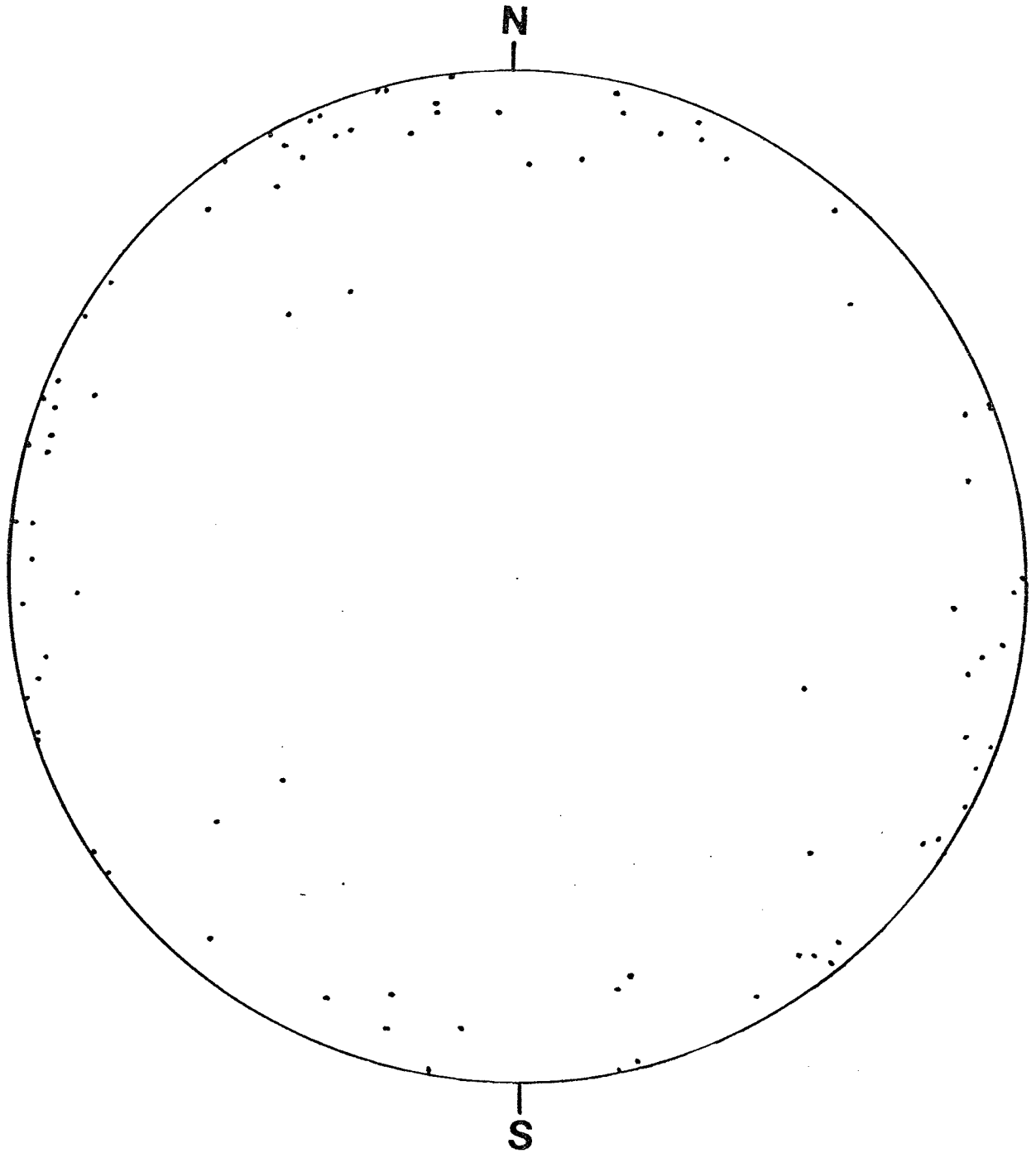


Figure 26. Stereographic projection of fold axes in Section 9, T12N, R9W, (87 points).

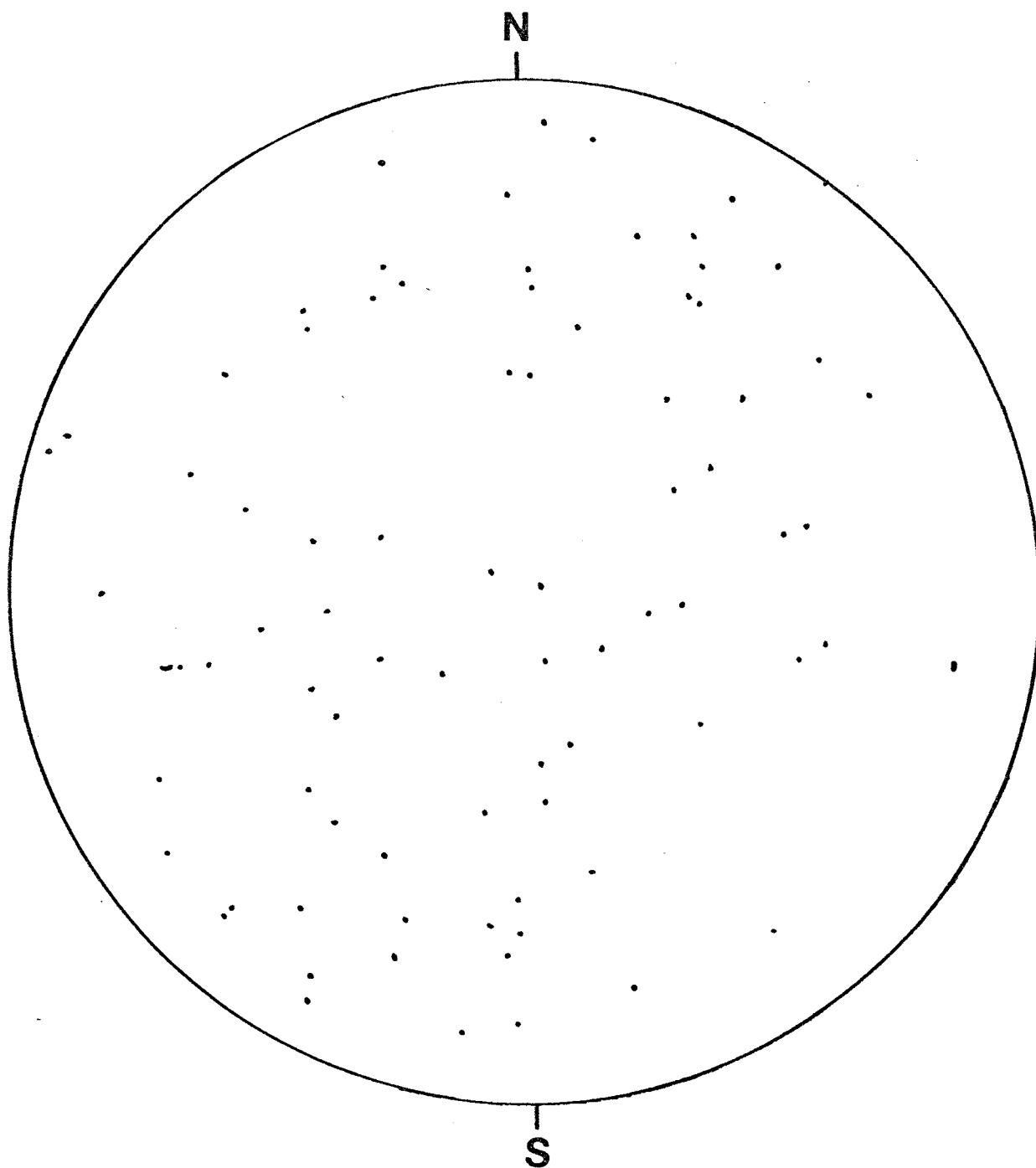


Figure 27. Stereographic projection of poles to axial planes of folds in Section 9, T12N, R9W, (87 points).

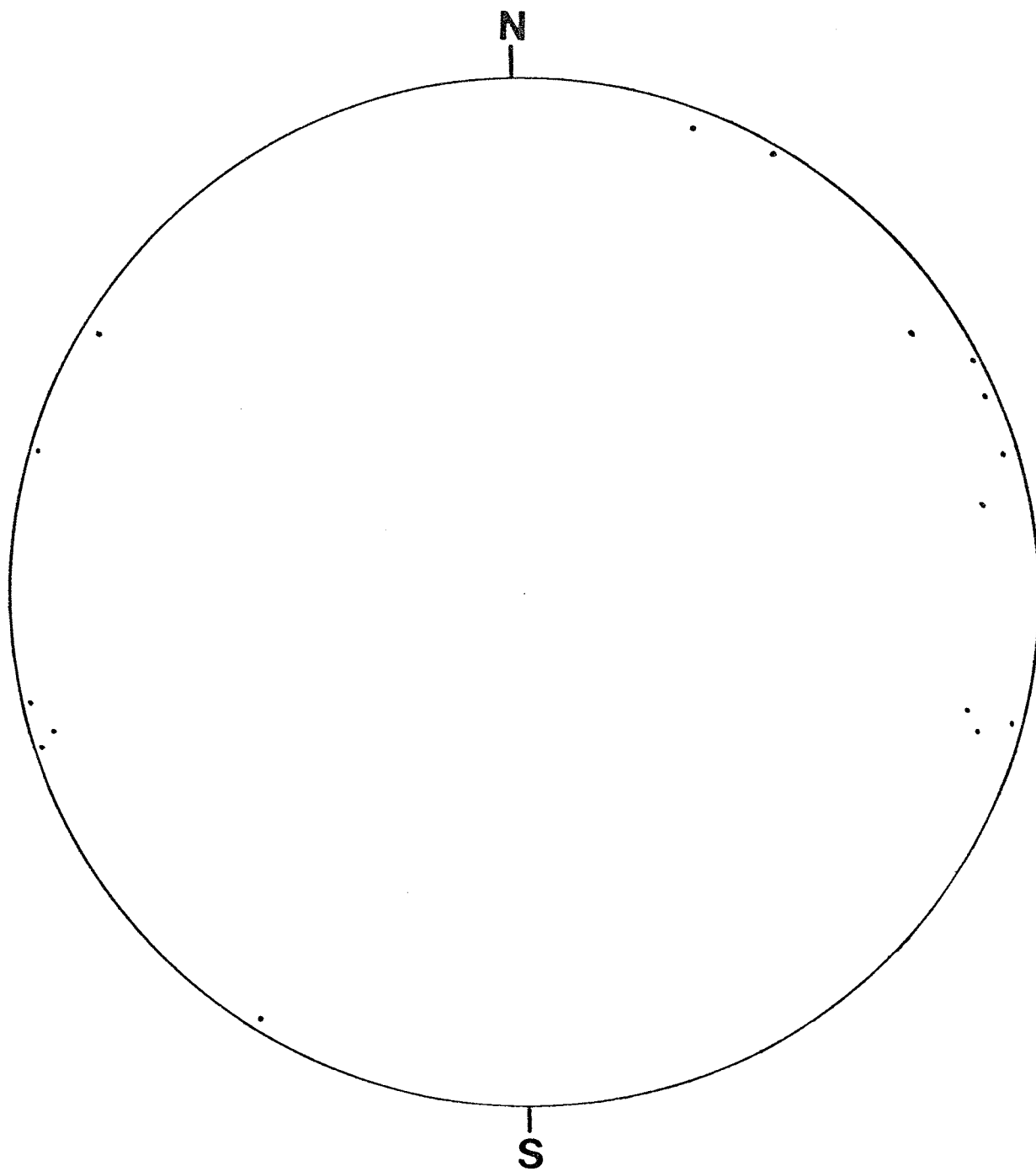


Figure 28. Stereographic projection of fold axes in Section 15, T12N, R9W, (16 points).

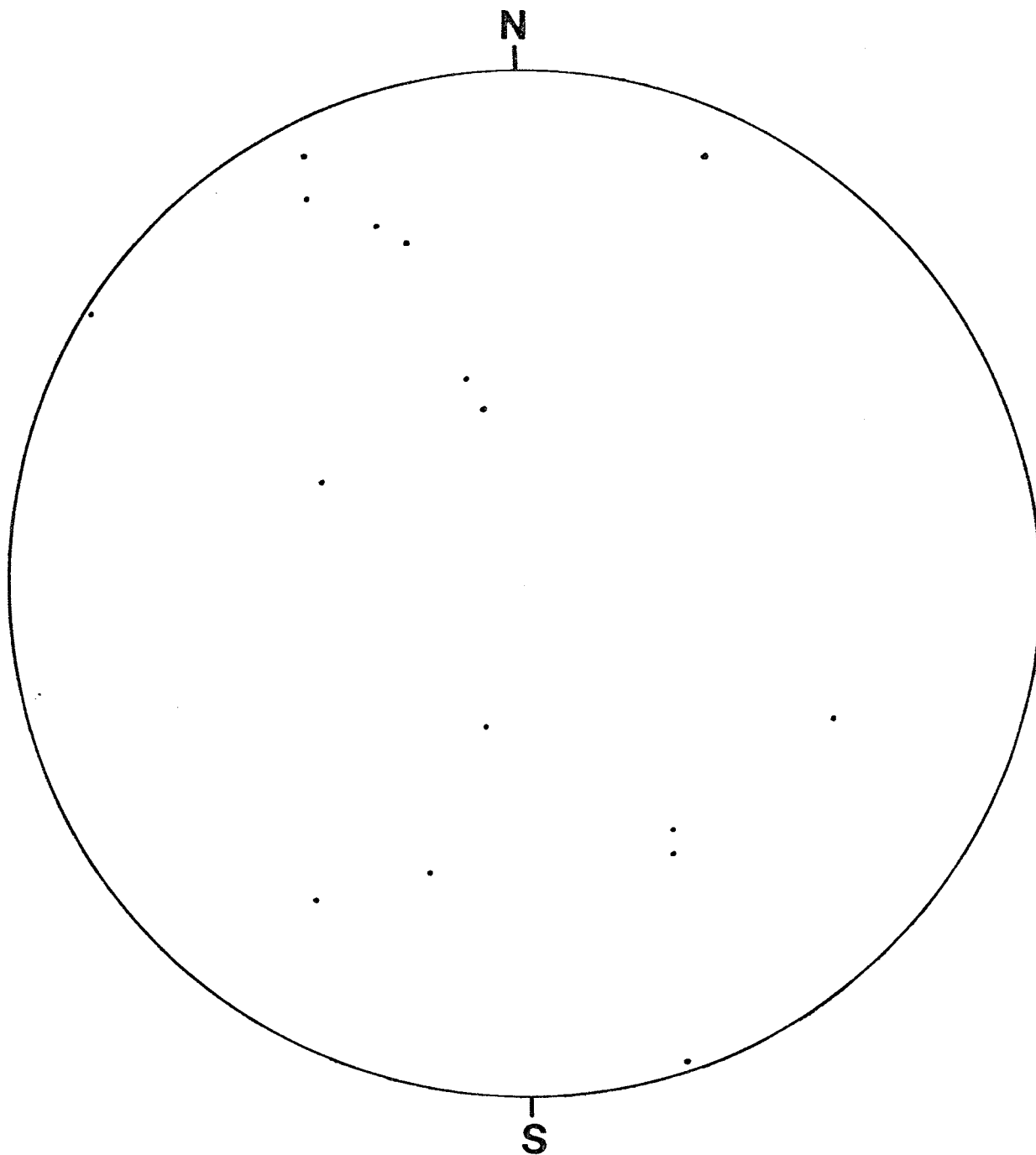


Figure 29. Stereographic projection of poles to axial planes of folds in Section 15, T12N, R9W, (16 points).

geologic stations such as 9M (see Figures 30 and 31) which is a series of trenches occupying an area 450 feet in diameter.

In a further attempt to identify discrete fold sets, the intraformational folds were subdivided according to fold profile by the system proposed by Fleuty (1964, p. 470) which is based on the fold dihedral angle or interlimb angle. The intraformational folds occurred in the following categories:

Gentle folds	interlimb angle from 170° to 120°
Open folds	interlimb angle from 120° to 70°
Close folds	interlimb angle from 70° to 30°

The stereographic projections of the fold axes and poles to axial planes of the gentle folds (see Figures 32 and 33), open folds (see Figures 34 and 35), and close folds (see Figures 36 and 37) do not exhibit any pattern unique to their categories nor are the patterns different from those based on geographic position of the folds.

Stereographic projections of the axes and poles to axial planes of intraformational folds that have axial planes dipping 0° to 40° (recumbent to gently inclined) (see Figures 38 and 39) also do not show any concentrations of poles to axial planes at a point or along great or small circles. Moreover, more detailed analyses do not indicate any systematic orientation, or change in orientation of fold axes as a function of axial plane orientation.

Thus, no discrete fold sets nor sequence of superposed fold sets can be identified on the basis of domain analysis

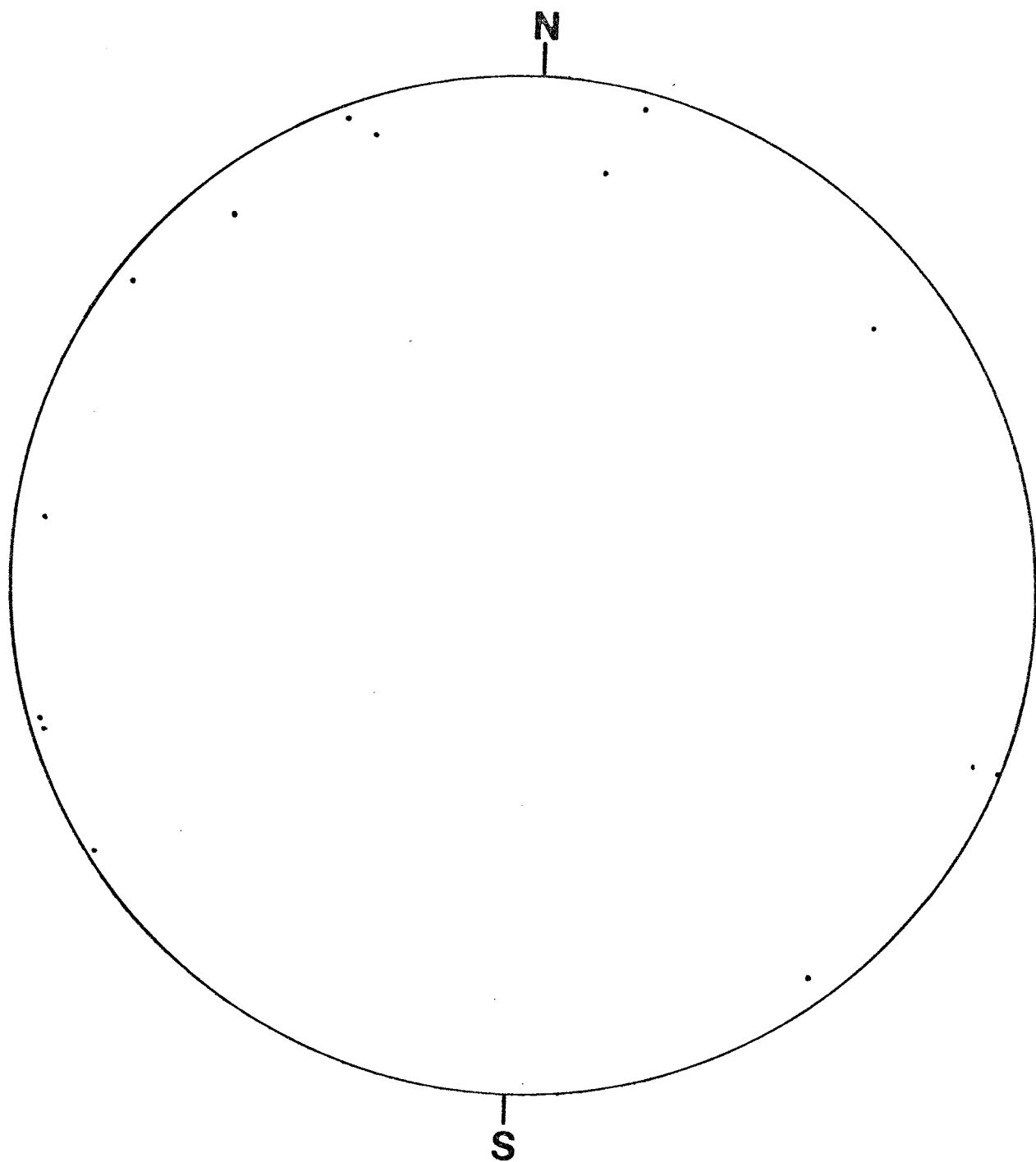


Figure 30. Stereographic projection of fold axes from geologic station 9M, Section 9, T12N, R9W, (14 points).

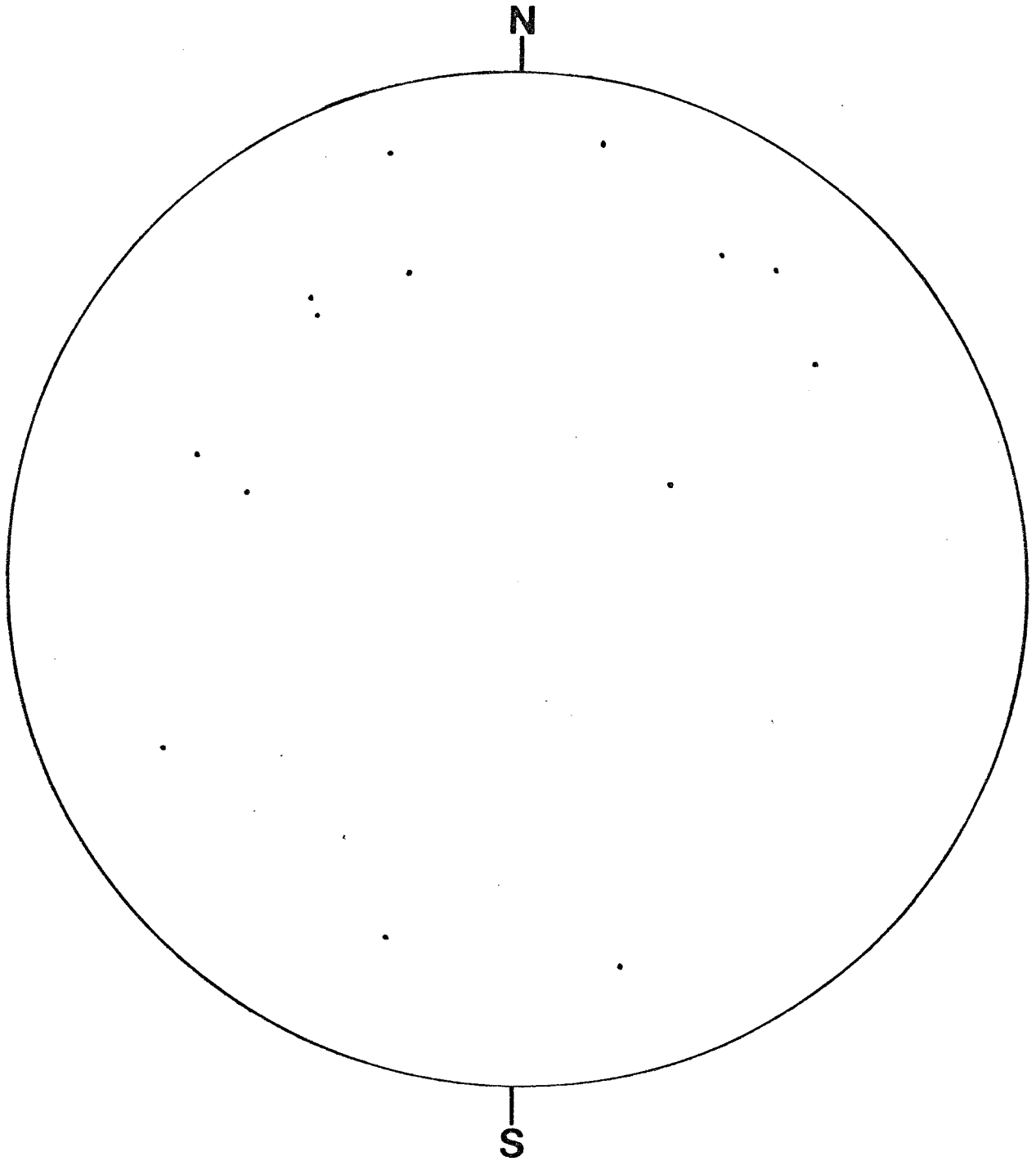


Figure 31. Stereographic projection of poles to axial planes of folds at geologic station 9M, Section 9, T12N, R9W, (14 points).

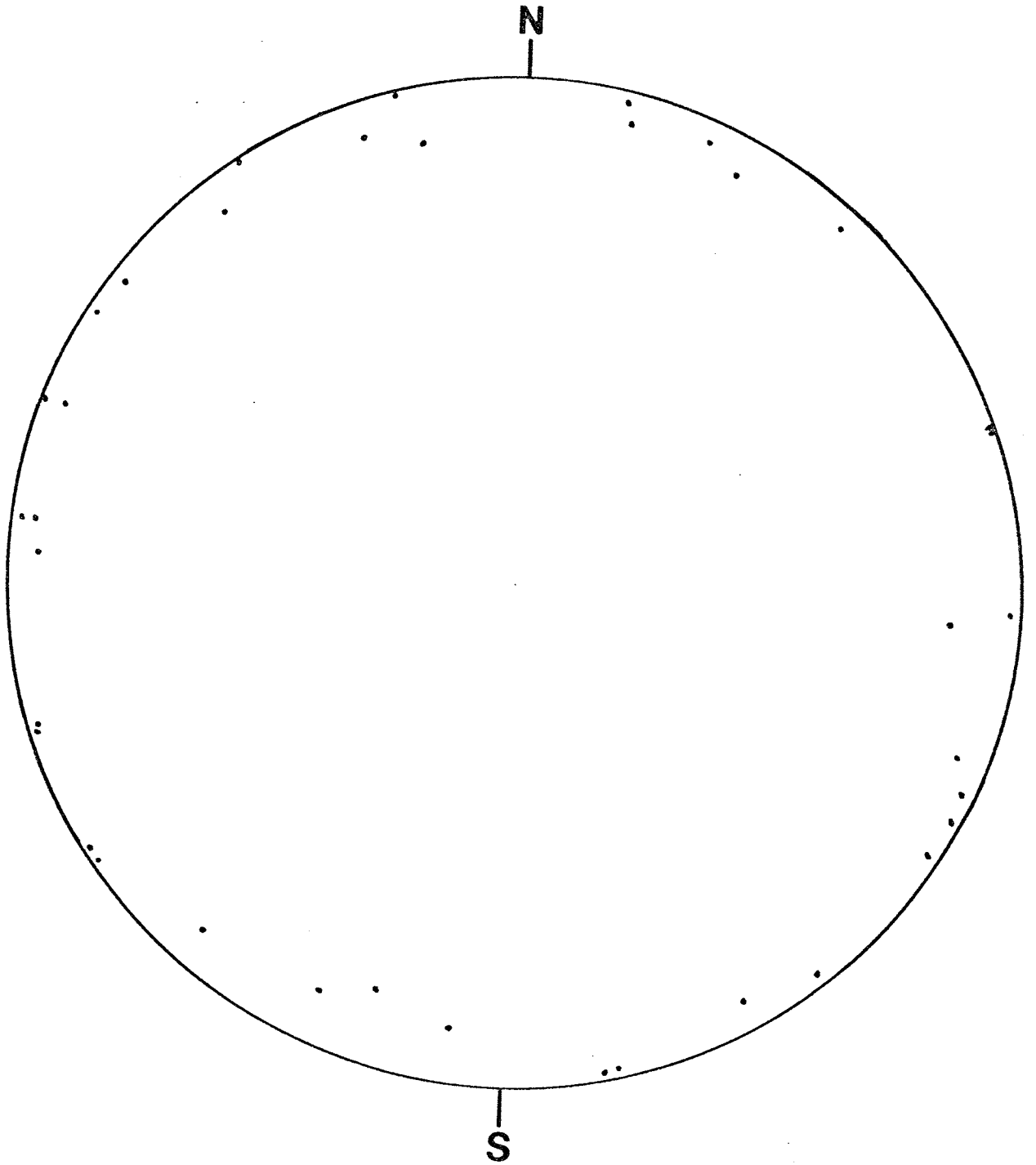


Figure 32. Stereographic projection of fold axes of all gentle folds in Section 9, T12N, R9W, (37 points).

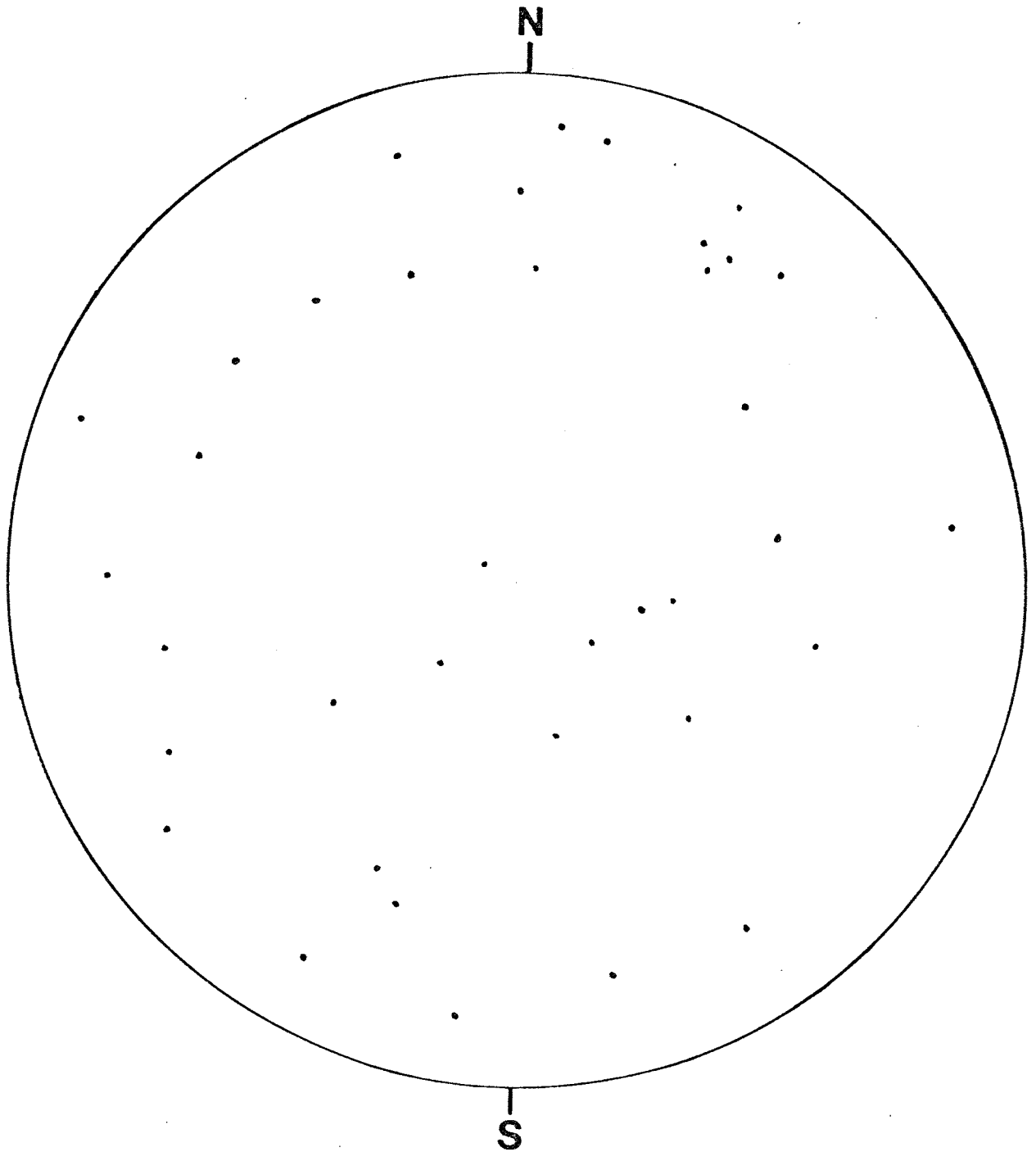


Figure 33. Stereographic projection of poles to axial planes of all gentle folds in Section 9, T12N, R9W, (37 points).

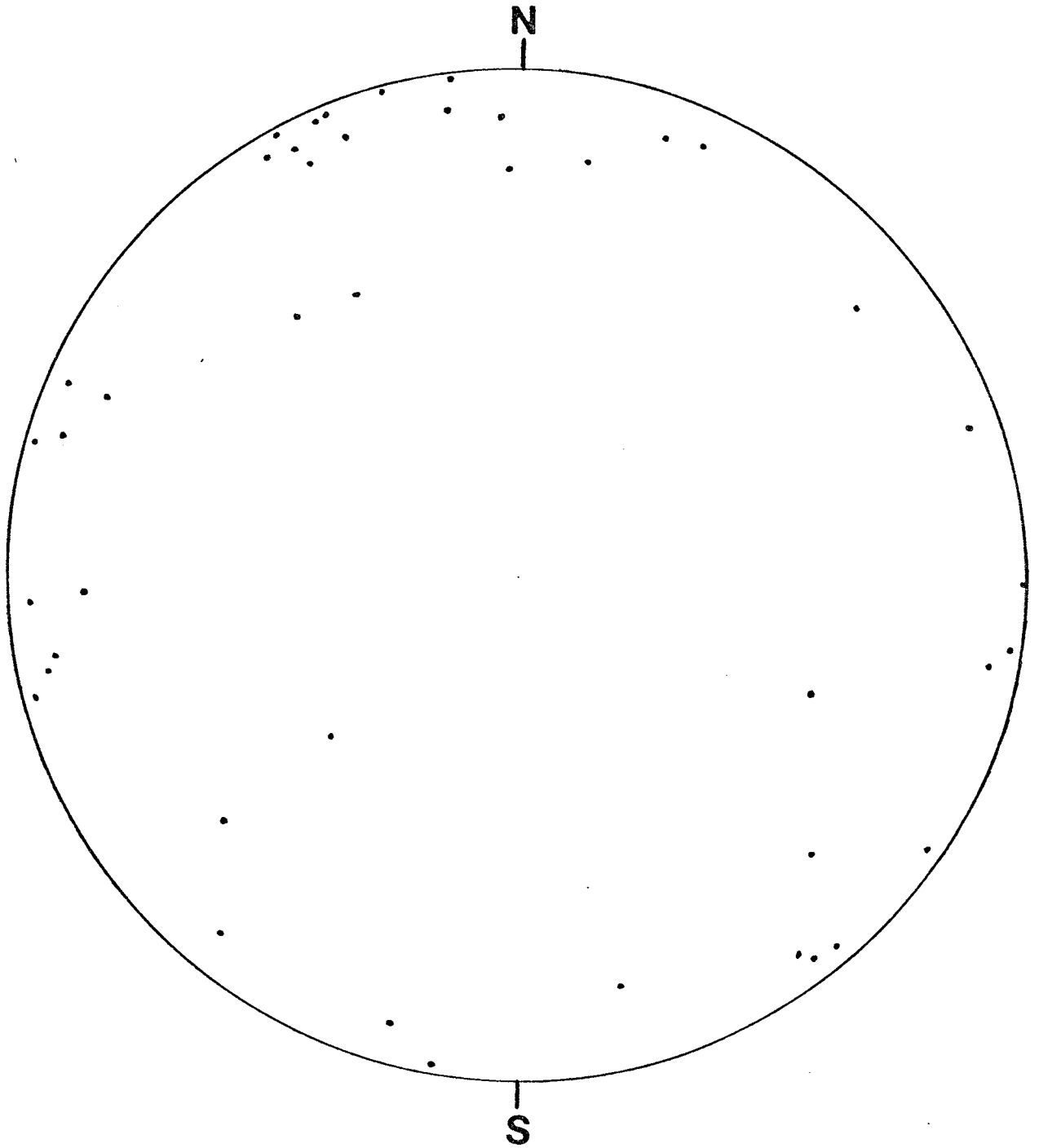


Figure 34. Stereographic projection of fold axes of all open folds in Section 9, T12N, R9W, (43 points).

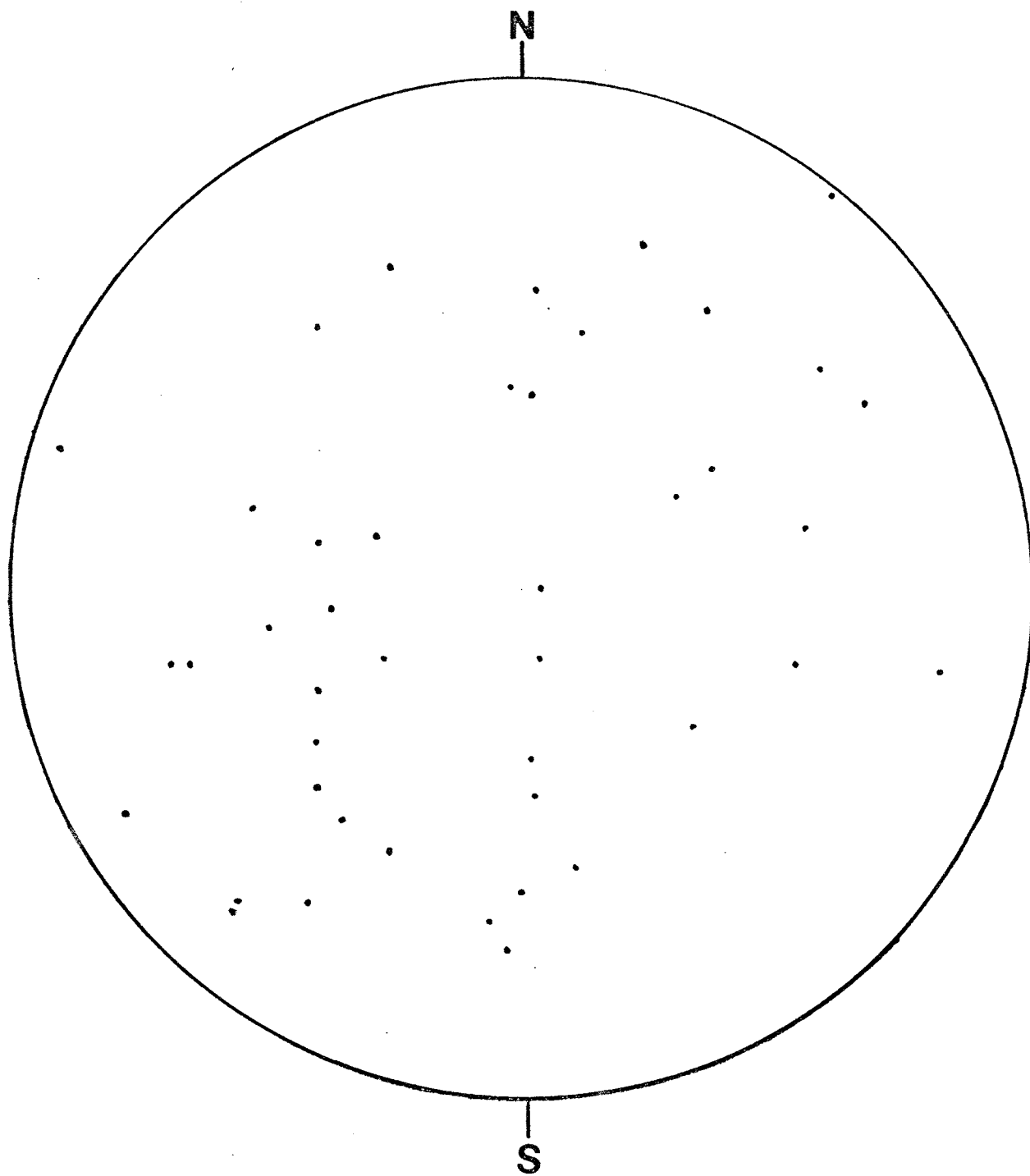


Figure 35. Stereographic projection of poles to axial planes of all open folds in Section 9, T12N, R9W, (43 points).

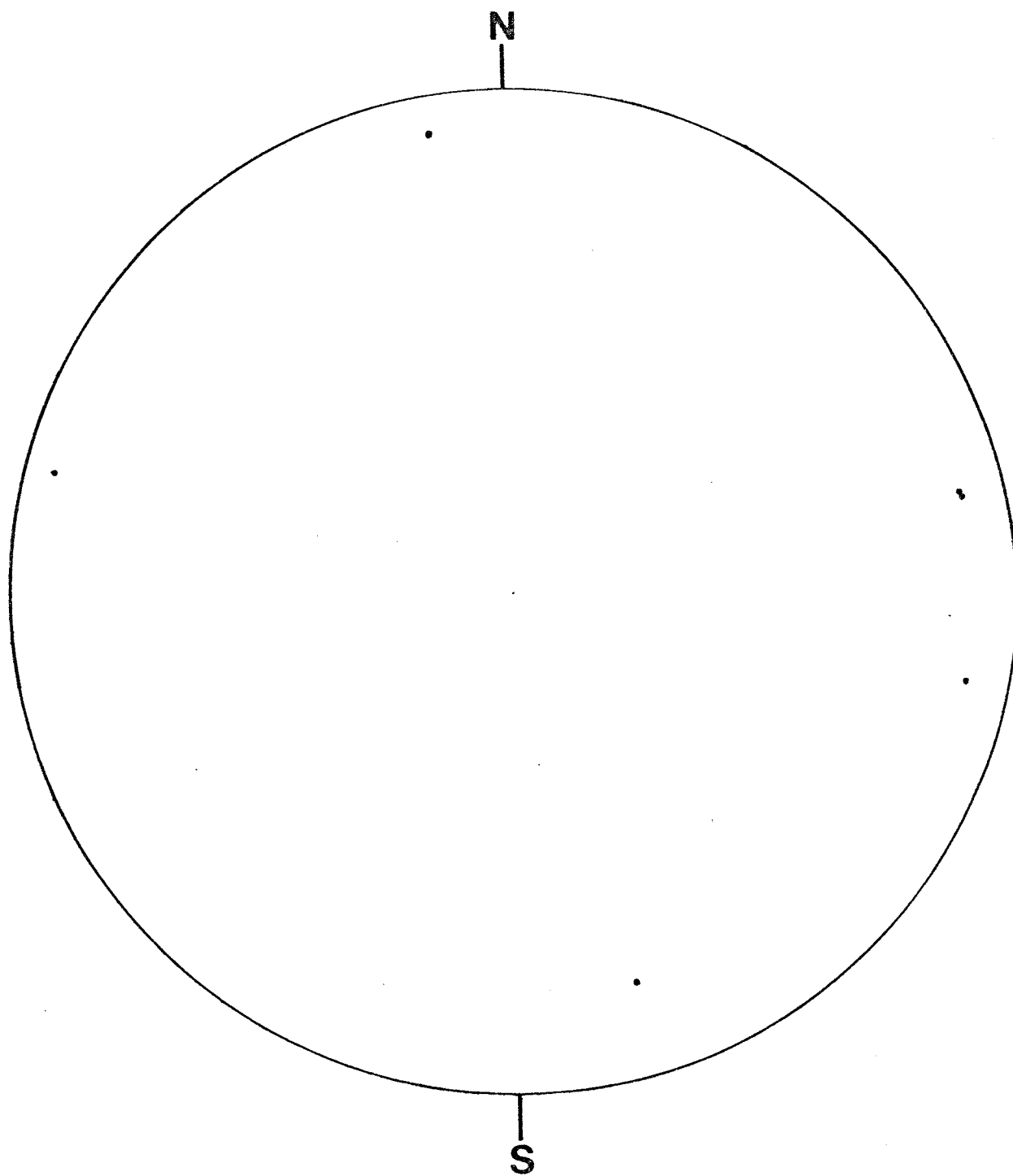


Figure 36. Stereographic projection of fold axes of all closed folds in Section 9, T12N, R9W, (6 points).

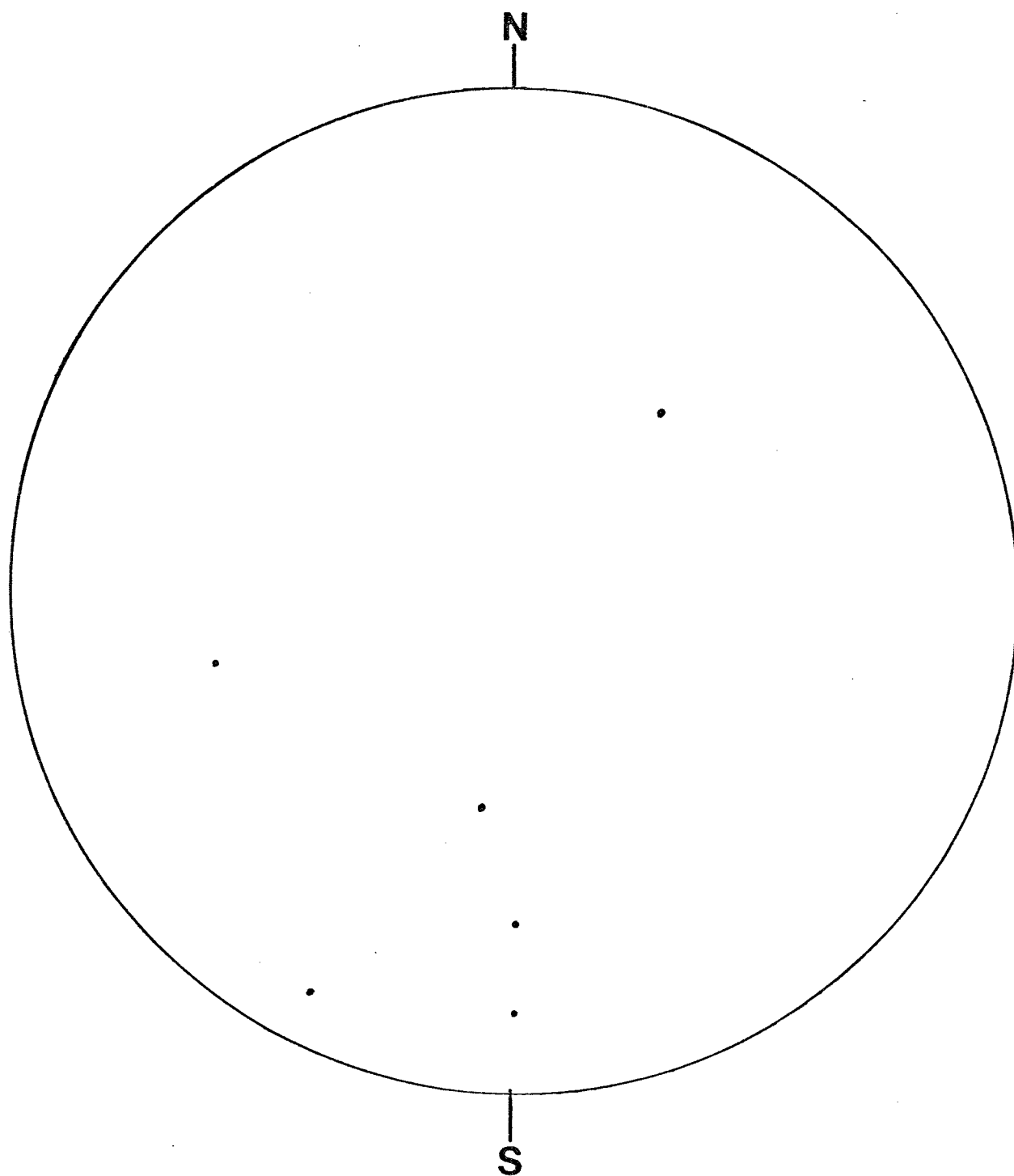


Figure 37. Stereographic projection of poles to axial planes of closed folds in Section 9, T12N, R9W, (6 points).

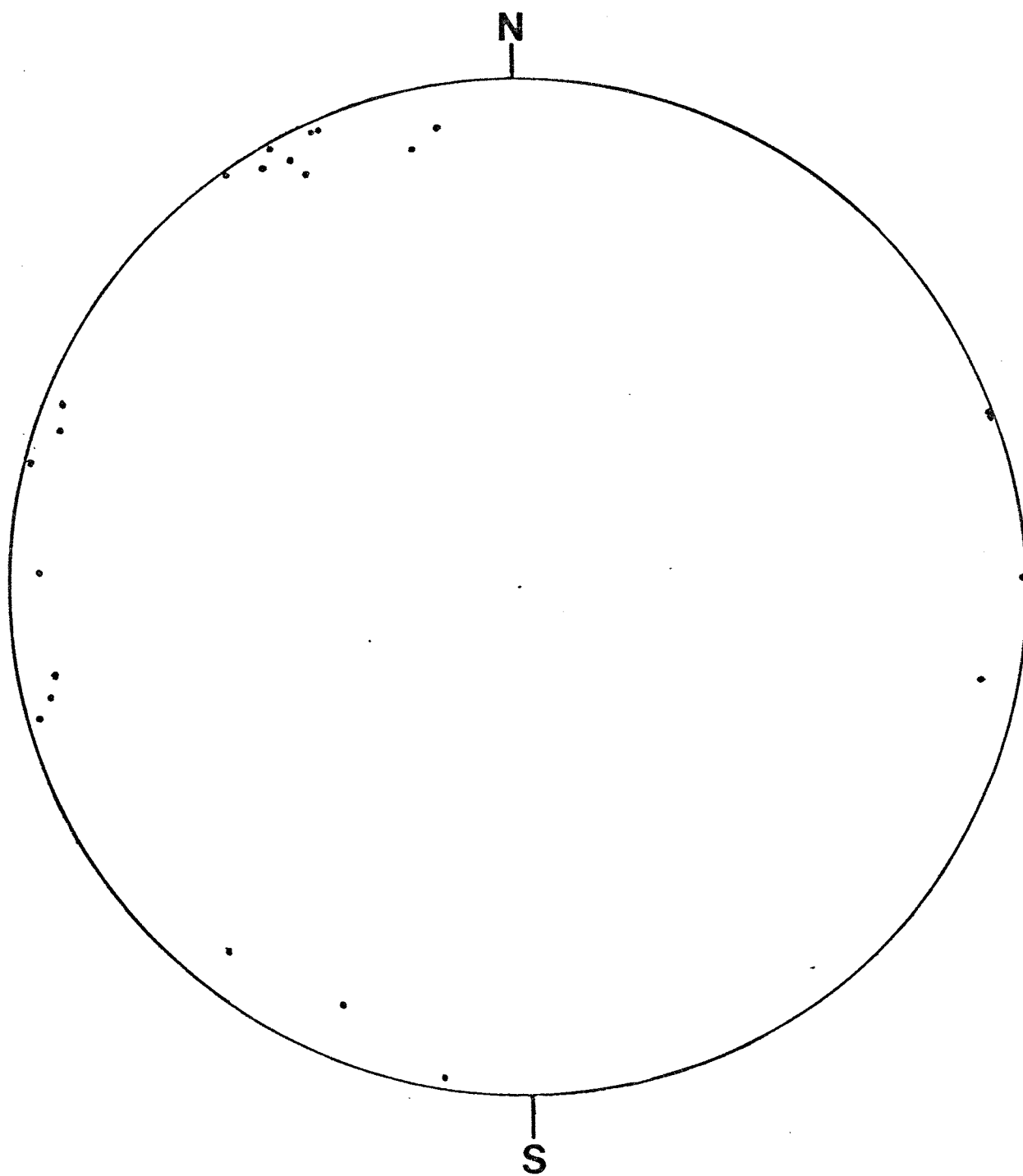


Figure 38. Stereographic projection of fold axes of all folds having axial planes dipping from 0 to 40° in Section 9, T12N, R9W, (23 points).

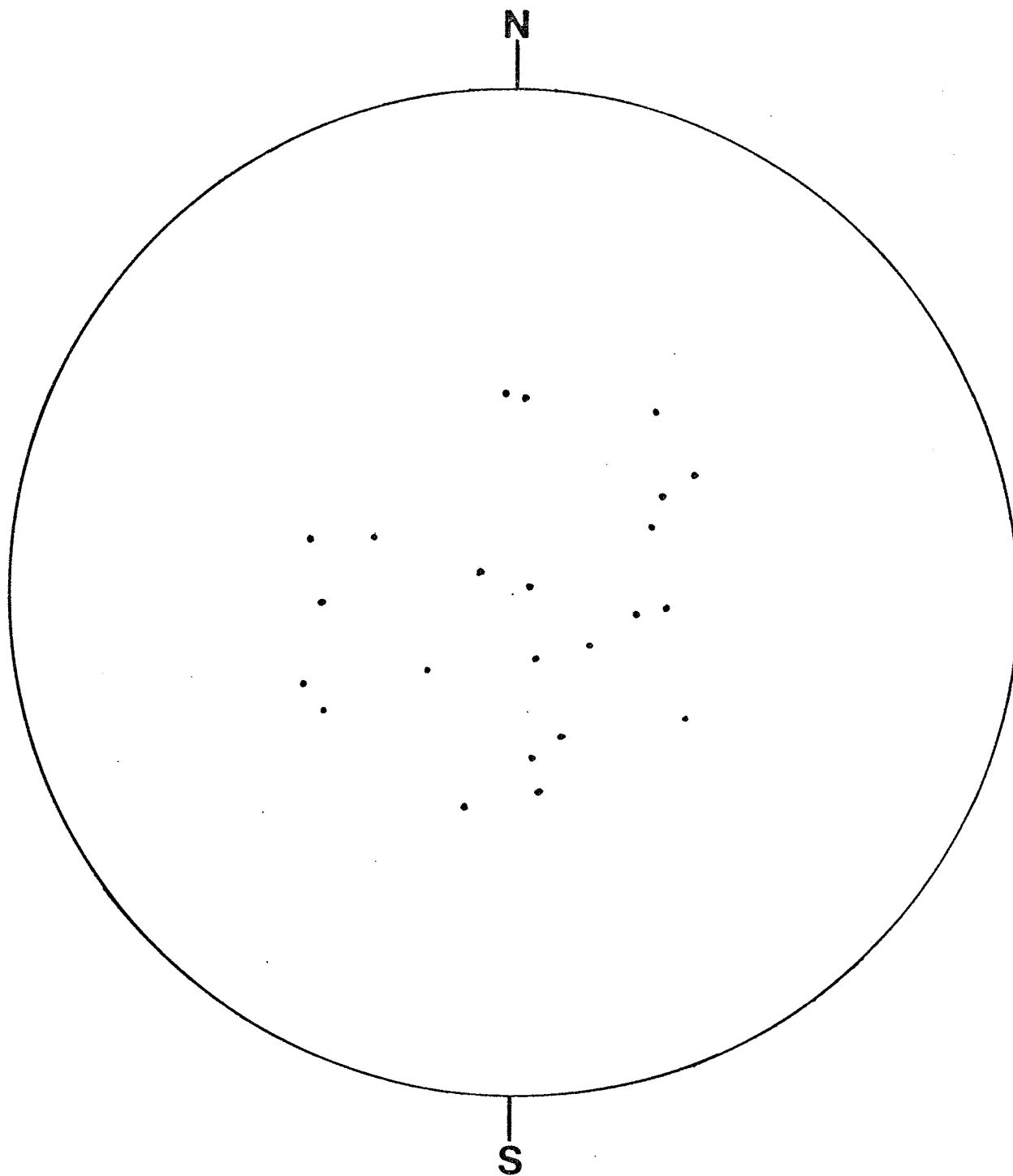


Figure 39. Stereographic projection of poles to all axial planes of folds dipping 0 to 40° in Section 9, T12N, R9W, (23 points).

or fold style. Two explanations are possible. First, a very complex history of folding exists, involving many discrete fold sets, so that the present number of measurements is insufficient to resolve the fold history. This explanation does not appear to be valid on the basis of the regional tectonic history of the study area. The second explanation is that the intraformational folds did not have a characteristic fold style nor a uniform orientation at the time of their formation.

Interpretation of Structural Contour Map

A structural contour map of the contact between the Entrada Sandstone and Todilto Limestone in Section 9 was presented in a report by Ellsworth and Mirsky (1952), who suggested that most of the ore bodies lie on anticlinal "noses" and that the ore trends appear to parallel conjugate joint directions (see Figure 40). Gableman (1956) revised the map and stated that the ore trends that are parallel to the conjugate joint direction are secondary deposits. The structural contour map of Section 9 is reproduced for this investigation without designation of mineralized areas in Plate VI.

The structural contour map reveals an irregular series of domes and basins having less than 30 feet of relief and diameters of about 425 feet. The flanks of the domes generally dip from 2° to 17° , however a few surfaces occur with dips of 23° to 30° over very short distances.

The contoured surface may represent either a tectonically deformed surface, paleotopography or possibly tectonic

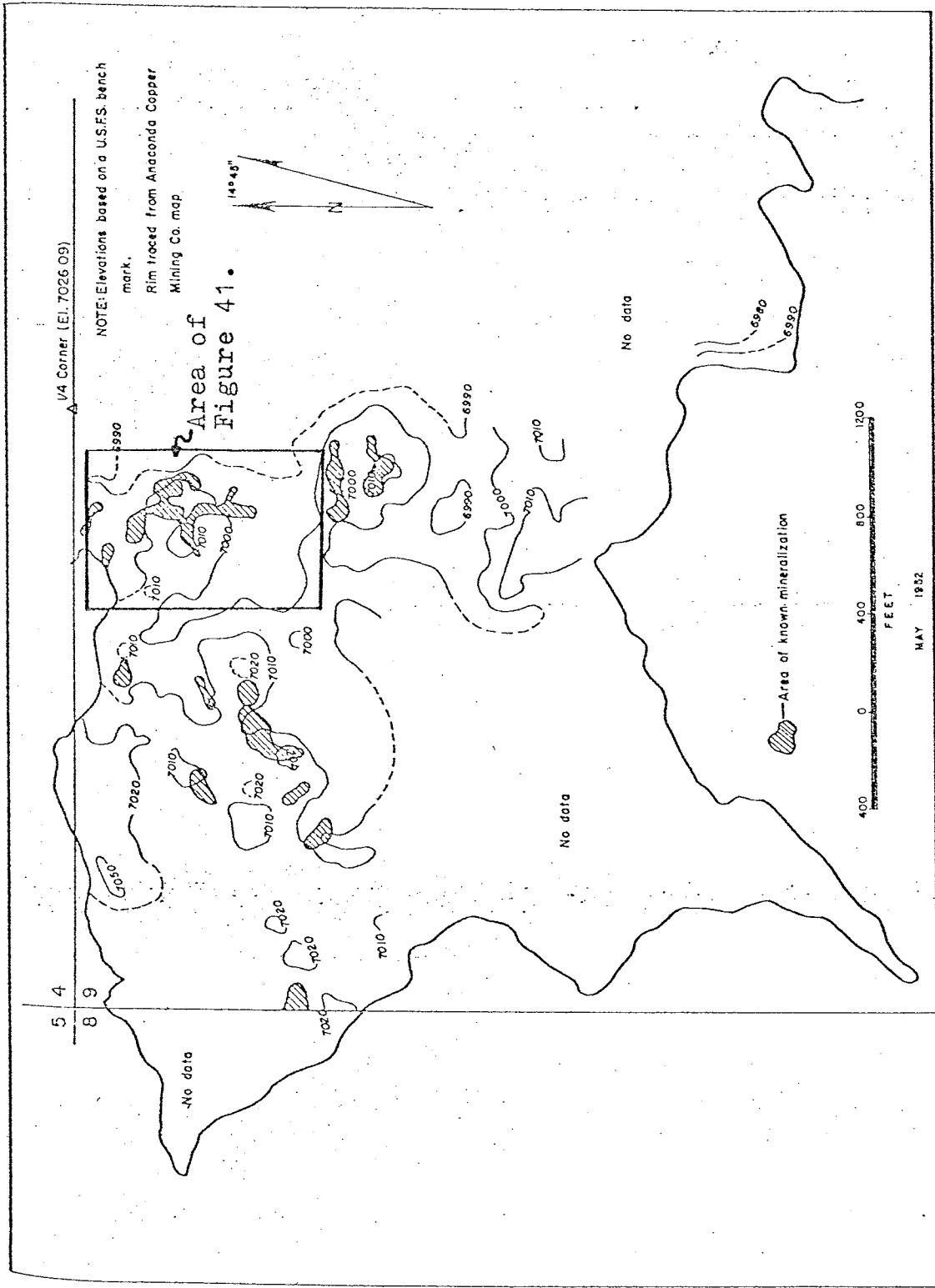


Figure 40. Correlation of ore bodies with structural contour map on the surface of the Entrada Sandstone (from Ellsworth and Mirsky, 1952, p.15).

deformation superposed on paleotopography. Dip and strike data on undisturbed beds in the Todilto Limestone (not spatially associated with intraformational folds) closely follows the apparent dips and strikes of the contoured surface of the Entrada Sandstone. This correlation of dip and strike data supports the tectonic origin of the contoured surface.

There are two major fold trends evident in the structural contour map of Section 9 (Plate VI). A set of folds trends $N25^{\circ}W$ with sinuous crestlines and wavelengths of 400 to 575 feet. The second set of folds trends $N85^{\circ}E$ with sinuous crestlines and wavelengths of 675 to 800 feet.

The trends of the two sets of folds correspond to the trends of the two sets of pre-Dakota folds occurring in the Laguna mining district as described earlier in this study. The set which trends $N10^{\circ}$ to $30^{\circ}W$ in the Laguna area has wavelengths of about a half mile and amplitudes of up to 100 feet. A larger set in the Laguna area is sinuous but generally trends $N70^{\circ}$ to $90^{\circ}E$ and has wavelengths of several miles and an amplitude of a few hundred feet (Hilpert and Moench, 1960, p. 438). If the large-scale folding in the Laguna mining district is continuous into the study area, the smaller folds in the study area may be second order folding on the larger folds. Further investigations outside the study area is necessary to interpret their relationships.

The intersection of anticlinal folds of the two fold sets causes the dome-like features and the intersection of

synclinal folds of the two fold sets tends to cause the basin-like features. Intersection of anticlinal folds of one fold set with synclinal folds of the other fold set results in intermediate or subdued high areas.

The surface trace of the axial plane of a large syncline lies 500 to 1500 feet east of the map area shown in Plate VI and trends N35°E. The fold is of the set of Laramide structures described earlier in this investigation (Gableman, 1956, p. 392). The Laramide structures appear to have a much larger wavelength (2 to 4 miles) than the basin and dome system and may account for the lower elevations of the contact to the southeast of the map shown in Figure 41 and Plate VI but not for any smaller scale structure.

Relationship Between Intraformational Folds and Basin and Dome System

The relationship between the axial planes of the intraformational folds and the dome and basin system is illustrated in the map of station 9D (see Figure 41). Mining excavation provides exposure of intraformational folds over 70 percent of the circumference of a large dome. The mining excavation closely follows the axes and strikes of the axial planes of the intraformational folds rather than the mineralized areas outlined in Figure 40 which were determined by drill hole analysis prior to excavation. This indicates that the intraformational folds are a more consistent site of uranium deposition than the conjugate joint sets cited by Gableman (1956).

Figure 41. Structural contour map on surface of Entrada Sandstone with axial planes of intraformational folds, Station 9D, Section 9, T12N, R9W. (contour map after Ellsworth and Mirsky, 1952) Horizontal scale 1": 100'.

Figure 41A. Structural section drawn from X to X' in Figure 41. Vertical scale 1": 50'. Horizontal scale 1": 50'.

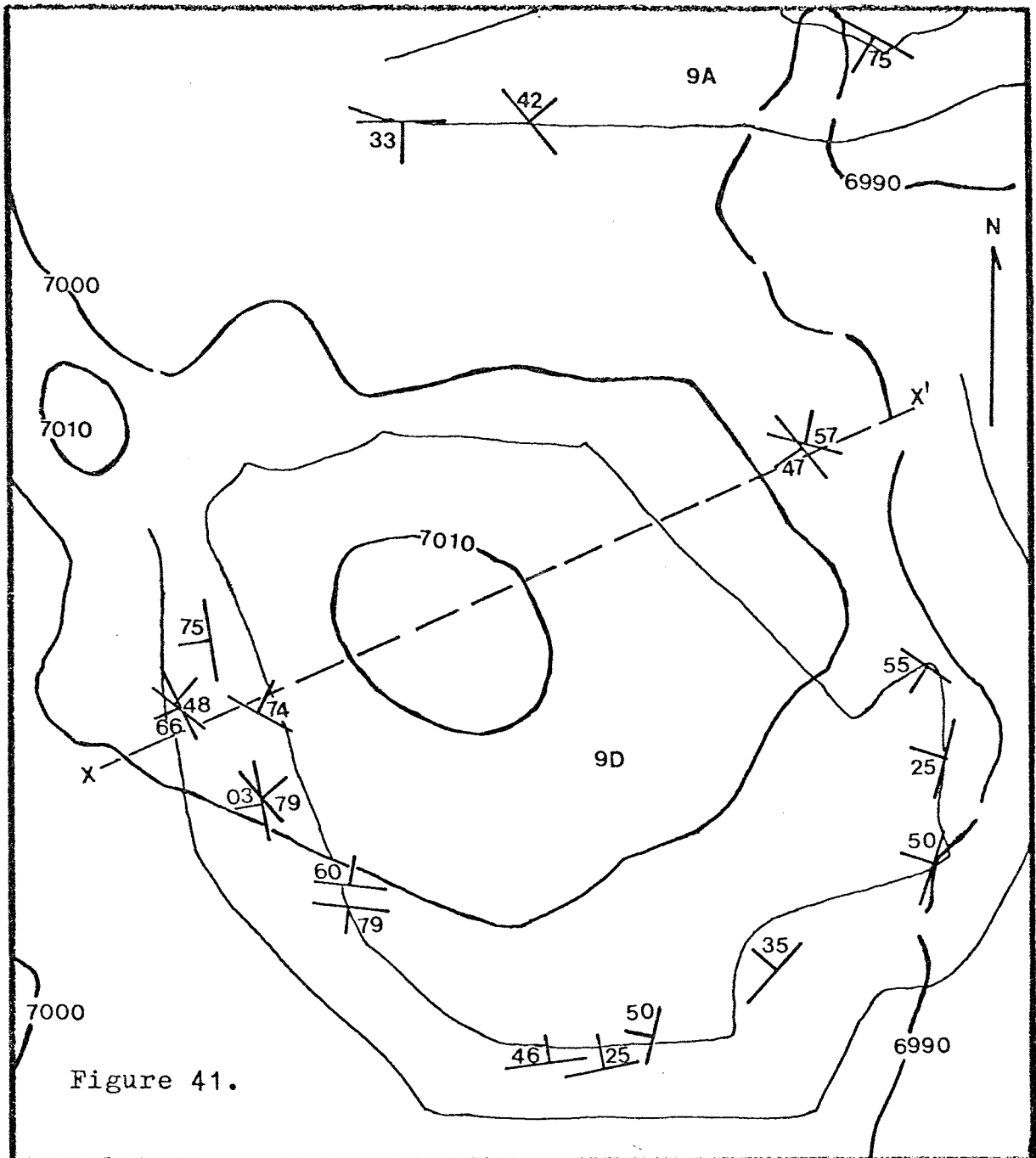


Figure 41.

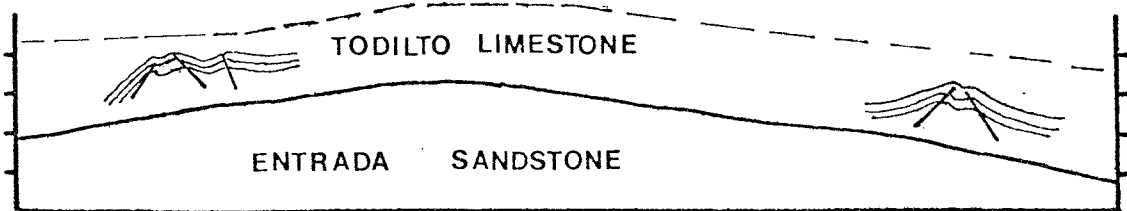


Figure 41A.

Station 9D (Figure 41) exhibits the best correlation of the strike of the axial planes of the intraformational folds to the strike of the flanks of the domes at any locality in the study area. The axial planes of the intraformational folds situated low on the flanks of the domes dip toward the crests of the domes. Conjugate intraformational folds, which occur on the lower flanks of the domes show asymmetry commonly directed away from the domes (see Figure 41A). Thus, the orientation of the single folds and the asymmetry of the conjugate folds both indicate displacement away from the dome.

The intraformational folds near the crests of the domes exposed at other localities exhibit gentle closure with axial planes dipping away from the crests of the domes at a wide range of dip angles.

In the areas of intersection between anticlines of one pre-Dakota fold set and synclines of the other fold set, the intraformational folds exhibit a more complex relationship to the domes and basins, so that the orientations of the axial planes are not parallel to subparallel to either fold trend or structural contour (see geologic station 9M, Plates V and VI). Such intraformational folds also tend to be of smaller half-wavelength and amplitude and they exhibit less closure or limb appression.

At a few locations, the basal units of the Summerville Formation show thickening both in the troughs between intraformational folds and toward the pre-Dakota basins. The bedding within the thickened units is locally indistinct

and therefore it is not known whether the thickening is primary or due to soft sediment flow. An individual unit may thicken from 0.4 to 1.9 feet over twenty feet of lateral distance. These features are rarely well exposed because they occur on the uppermost slopes of the mining excavations and generally are not of a resistant lithology.

GENETIC MODELS OF THE INTRAFORMATIONAL
FOLDS IN THE TODILTO LIMESTONE

Intraformational folding has long been suggested as a controlling feature for the deposition of uranium in the Todilto Limestone. Rapaport (1952) stated that the association of ore with primary folds is not universal. Most folds are unmineralized, and horizontal bedded units contain ore at many places; however, detailed mapping 8 miles east of Haystack Butte showed that five out of seven ore bodies are localized on intraformational folds despite the fact that these folds occupy less than 10 percent of the linear extent of the Todilto rim (Rapaport, 1952, p. 14).

Unfortunately, various terminologies have been used, and there has been a divergence of opinion regarding the age, origin and orientation of the folds and consequently, the relationship between folding and ore deposition. The major opinions have been presented earlier in this study.

Five major genetic models have been selected for discussion; they are the following: 1) soft sediment slumping down the slope of the depositional basin, 2) differential loading and compaction in proximity to bioherms, 3) volumetric changes due to diagenesis, 4) parasitic folding on tectonic features, and 5) soft sediment slump off tectonic features.

Soft Sediment Slumping into the Depositional Basin

Rapaport et al (1952), suggested that the intraformational folds are due to creep of unlithified Todilto

sediments down a gentle slope toward the depositional basin under the weight of an overlying mantle of Summerville sands and silts. The model suggested by Rapaport et al (1952) restricts the development of the intraformational folds to penecontemporaneous deformation during deposition of Summerville sediments in the Late Jurassic. They postulate that the Todilto sediments were in a semi-fluid state because there was no major loss of interstitial waters by excessive loading or desiccation due to subaerial exposure, and because there was no extensive lithification of the Todilto sediments at this early stage.

The effects of slumping vary according to the physical properties of the displaced mass and the mode of origin of the slide. Other features, which could be characteristic of this genetic model include developed slip surfaces, basal breccias along the slip surfaces, and disruption of intraformational folds (Hills, 1963, p. 64).

Given this genetic model, the intraformational folds should exhibit a common orientation of axial planes and inclined, asymmetric, anticlinal profiles across a wide area. If the depositional basin was to the north and northeast, then initially the axial planes should be striking west to northwest and dipping to the south to southwest. The two sets of pre-Dakota folds that constitute the dome and basin system can be theoretically superposed on these inferred south to southwest dipping axial planes using the method outlined by Ramsey (1961, p. 85) to determine the possible reorientations of the intraformational fold set. The

limb-appression is so slight (4° to 10°) in the dome and basin system that only about a 20° change in orientation of the axial planes of the intraformational folds is possible. This is not enough change to produce the distribution of the poles to the axial planes of the intraformational folds occurring in the study area. (See Figure 25.)

Although a few slip-plane surfaces are localized in areas of extreme deformation, there are no slip-plane surfaces greater than 4 feet in length, no basal breccias associated with the slip-planes, nor other evidence to support transport of a sediment mass over a great distance.

Considering the data and evidence presented in this investigation, the soft sediment slumping into the depositional basin model is invalid.

Differential Loading and Compaction in the Proximity of Bioherms

Perry (1963) suggested that the intraformational folds are a result of differential compaction and loading associated with the subsidence of "reef" or biohermal masses into the underlying laminated to thinly bedded and crenulated zones of the Todilto Limestone.

Perry believes that the pseudosparites and intraclastic pseudosparites of the upper zone are in fact "reefs" and associated "fore-reef" talus. Perry (1963, p. 151) believes the "reefs" were of algal origin, although he could not demonstrate this because of the coarse recrystallization.

Perry interprets the intraclastic pseudosparites as two different types of breccia deposits. The first type

is a result of slumpage or caving of an extremely steep "reef" edge and is characterized by large, angular boulders in a silty matrix of the basal Summerville. The second type, produced by gradual erosion of the "reef" edge by wave action, produces breccia fragments which are more rounded and smaller than the slumpage or caving breccias (Perry, 1963, p. 153).

Perry's model of differential loading and compaction in the proximity of bioherms restricts the development of the intraformational fold to be contemporaneous with early diagenesis and produced by the squeezing of the unconsolidated sediments directly beneath the biohermal mass. (See Figures 42 and 43.) The weight of the bioherm was resolved into horizontal forces when acting against the presumably competent underlying Entrada Sandstone. Bioherms that were established and thrived directly upon the Entrada surface exhibit no flexures in the off-bioherm facies, but bioherms that were established on several feet of lime sediments commonly acquired the peripheral flexures in the off-bioherm strata (Perry, 1963, p. 152).

This model restricts the geographic occurrence of the intraformational folds to the biohermal margins or "reef" fronts. Perry indicates that the axial planes should be dipping away from the "reef". (See Figure 43.) He has developed a complex geometry of patch reefs and lagoons (See Figure 44) based on the occurrence of the folds, their axial plane orientation (with the assumption that axial planes dip away from the loading biohermal mass) and the

Figure 42. Stages in the growth of the bioherms or "reefs" and development of the intraformational folds (After Perry, 1963, p. 154).

Figure 43. Section showing a typical "reef" edge and intraformational fold (After Perry, 1963, p. 152).

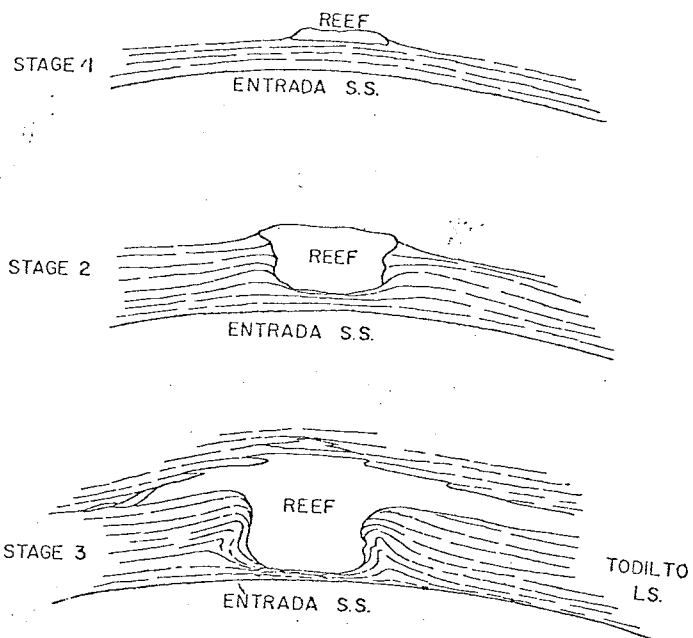


Figure 42.

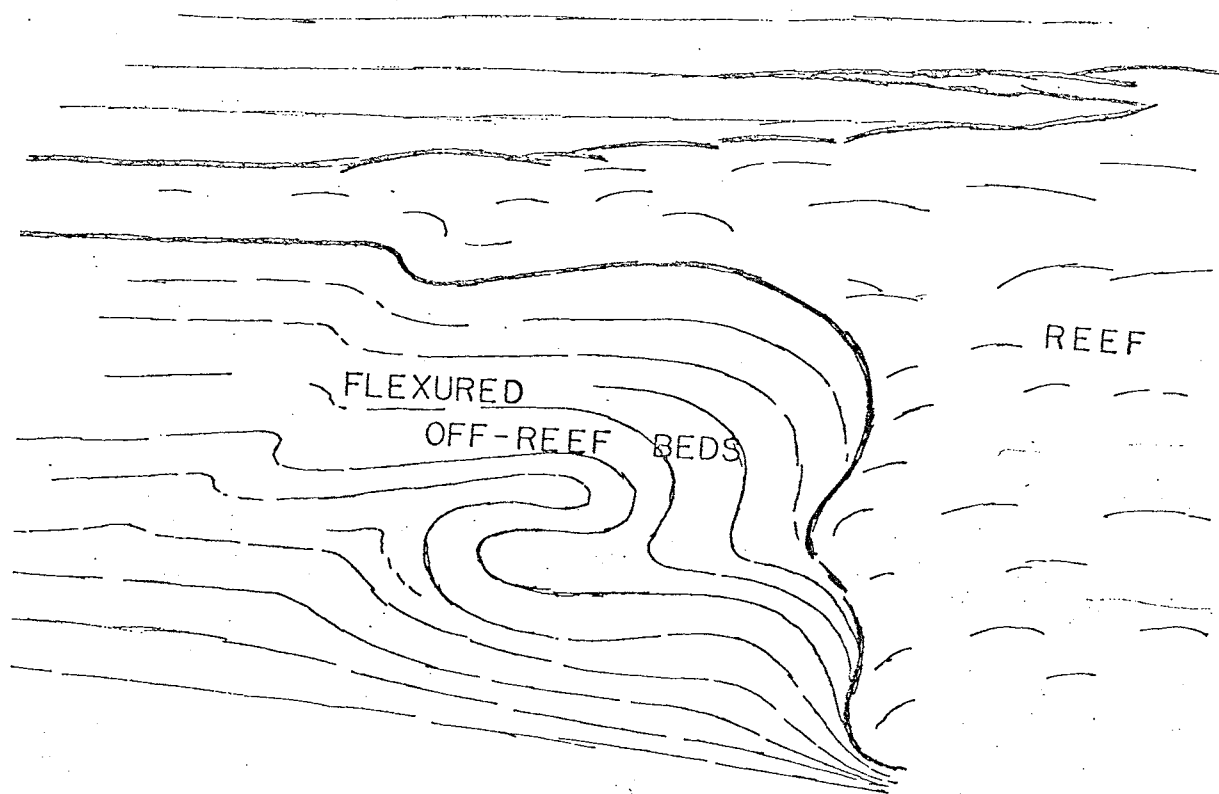


Figure 43.

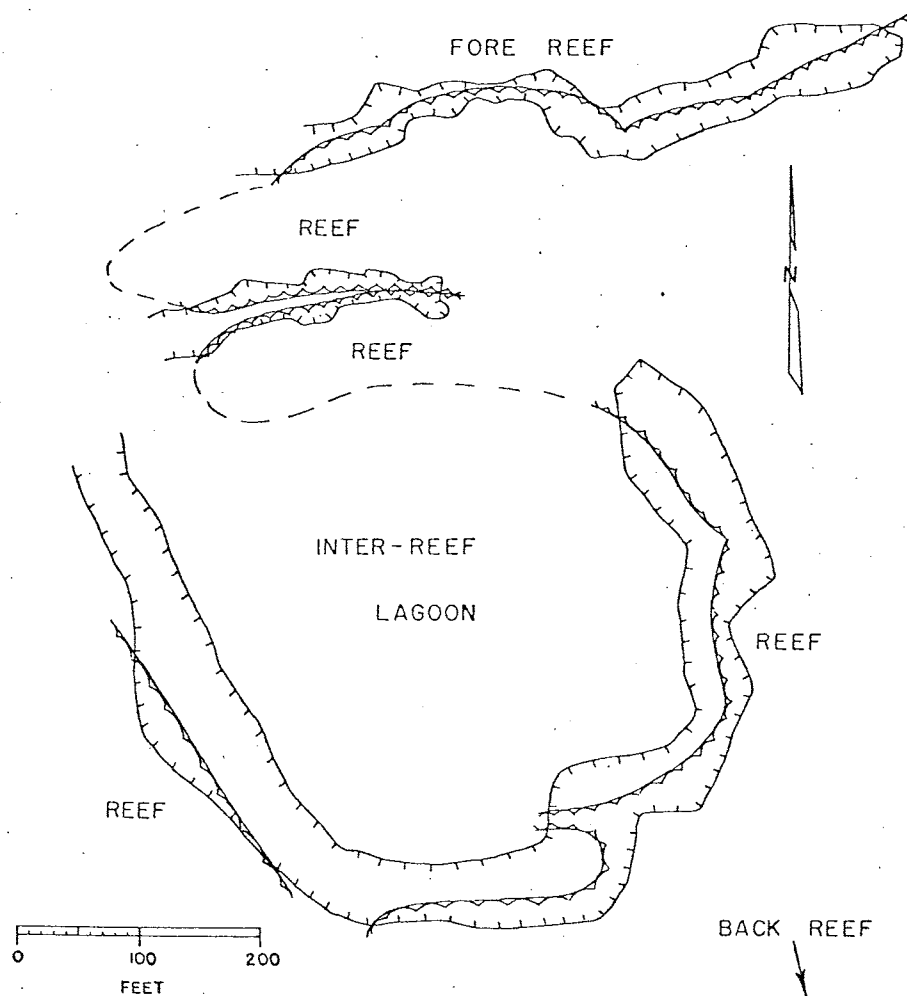


Figure 44. Plan of reef edge around an inter-reef lagoon. The hachured lines indicate outlines of the mining excavations at Stations 9A and 9D, Section 9, T12N, R9W (After Perry, 1963, p.155). Compare with Figure 41.

sedimentary breccia which he interprets as "fore-reef" talus bodies.

The stereographic projections of the axis and axial planes of intraformational folds presented in this investigation exhibit a random distribution of data. The random distribution of structural data would be expected if the folds are directly related to the irregular outlines of the bioherms.

A comparison of Figures 41 and 44 reveals the relationship between the distribution of Perry's bioherms, the intraformational folds and the dome and basin system evident from the structural contours on the Entrada Sandstone-Todilto Limestone contact. Note that in Figure 42 Perry indicates that the bioherms formed on paleotopographic highs, presumably because of shallower water conditions there. If the dome and basin system represents paleotopography, then the bioherms should be found on the domes, but comparison of Figures 41 and 44 shows that the bioherms postulated by Perry occur on the flanks of the domes. If the dome and basin system is the result of tectonic deformation, the structural contours in the vicinity of stations 9A and 9D do not show any evidence of paleotopographic highs coincident with the location of Perry's "reefs". Thus, Perry's sequence of development of the intraformational folds (Figure 42) and his postulated location of "reef" bodies (Figure 44) is inconsistent with the structural contour data.

Perry (1963, p. 150) interprets the "reef" masses as being massive, or locally crudely bedded bodies of equant,

coarsely crystalline limestone. However, close examination of fresh surfaces of the pseudosparites in the features interpreted by Perry as "reef" edges reveals relict crenulations and laminations. (See Figure 43.) Moreover, the relict laminations are folded. The orientation of the relict bedding in the pseudosparites parallels the orientation of the bedding in the intraformational folds adjacent to laminated micrites and crenulated micrites. Where full exposure permits examination of the bedding in the pseudosparites in the "reef" mass, it is vertical and then swings back to the horizontal at the base of the exposure as the folded units in the intraformational fold return to the horizontal.

Evidence in this investigation shows that the "reef" masses are silty pseudosparite units exhibiting relict laminations and crenulations, and at the time of deposition were probably similar to the laminated micrites and crenulated micrites typical of the rest of the Todilto Limestone. The difference in texture is due to the extent of diagenesis (degree of recrystallization probably controlled by position near the top of the Todilto Limestone) rather than a difference in primary facies (reef versus inter-reef deposits). Most importantly, the evidence indicates that the sediments were affected by intraformational folding before they were diagenetically altered to pseudosparites. Thus, there is no evidence to indicate that reefs, or even denser masses of carbonate due to recrystallization, existed before the formation of the

intraformational folds.

The evidence presented in this investigation does not support the basic premises of the model and therefore Perry's differential loading and compaction in proximity to bioherms model is considered invalid.

Volumetric Changes Due to Diagenesis

Bell (1963, p. 14) suggests that the intraformational folds were caused by volumetric changes due to hydration of calcium sulfate which was subsequently leached. He believes that the Grants mining district probably lies along or close to the depositional edge of the upper gypsiferous member of the Todilto Limestone where thin layers of gypsum or anhydrite were formerly interbedded with limestone. Assuming that anhydrite was the primary sulfate mineral, subsequent hydration to gypsum occurred and the attendant volumetric increase produced the crinkly lamination of the upper limestone as well as the intraformational folds (Bell, 1963).

Two types of penecontemporaneous structures are commonly credited to deformation by such volumetric changes; they are enterolithic folds and tepee structures. Enterolithic folds resemble intestinal convolutions and occur as small (generally less than six inches) intraformational contortions, believed to be the result of hydration of anhydrite to gypsum. Enterolithic folds are common in the nodular gypsum units of the coastal sabkha facies (Shearman, 1966). Tepee structures, or megapolygons, are anticlinal features with axial plane fractures which are

often filled with coatings of fibrous carbonate minerals on the fracture wall and vadose sand and silt. (See Figure 45.) Tepees range in size from 10 to 100 feet or more in diameter and may affect as much as 22 feet of the vertical section although they require only about 6 inches of carbonate sediment to start initial growth (Smith, 1974). Lithification of some of the beds appears to have been well advanced during final stages of tepee growth, the beds exhibit flexures of 20° to 30° before rupture and overthrusting occurred. Tepee structures are interpreted (Smith, 1974, p. 68) as fossil pressure ridges which may be superposed on older pressure ridges. (See Figure 46.) The pressure ridges are a result of crystal growth of aragonite or magnesian calcite or possibly evaporite minerals in an intertidal to supratidal flat environment.

The model based on volumetric changes due to diagenesis involves contemporaneous and penecontemporaneous deformation relative to hydration of CaSO_4 , or crystal growth of a diagenetic mineral phase. The irregular, polygonal orientations, vertical axial plane fractures and characteristic tepee profile are diagnostic.

The stereographic projections of poles to axial planes of intraformational folds presented in this investigation exhibit a random distribution which could correspond to orientations presented by the irregular polygonal form. However, the tepee profile does not occur in the study area and most axial planes are inclined. Axial plane fractures do occur; they are sharp planar breaks and

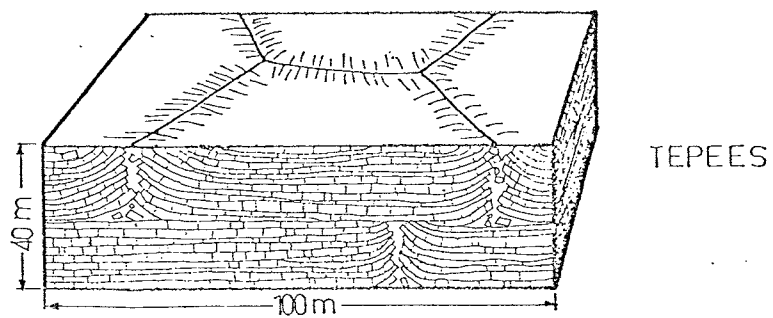


Figure 45. Block diagram showing inter-relationship of tepee structures (After Kendall, 1969, p.2515).

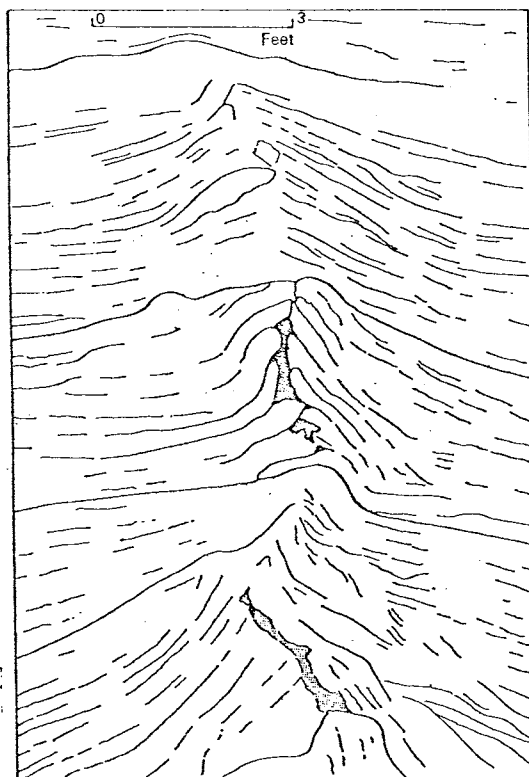


Figure 46. Superposed simple tepees separated by erosion surfaces. Tansill Formation, Guadalupe Mountains, New Mexico (Smith, 1974, p.66).

are always inclined, but are not filled with vadose silt and sand. Many intraformational folds have silty cores, but the silt is laminated and there are thickened portions of silty units which are often continuous for 20 feet or more away from the intraformational folds.

Enterolithic folding is very rare in the study area; Figure 15 illustrates the only possible example which occurs in the crenulated zone. Evidence of possible displacement by crystal growth occurs in only two thin sections in the study area. (See Figures 14 and 16.) The actual extent of displacement in these examples is small (probably less than 1 percent) and limited to the crenulated zone, whereas intraformational folds are not restricted to the crenulated zone and some affect the basal units of the Summerville Formation.

Thus, the absence of large scale structures and the rarity, small extent and restricted stratigraphic occurrence of small scale structures indicative of volumetric expansion during diagenesis suggests that this mechanism may, at best, account for the formation of crenulations, but is unlikely to produce the intraformational folds.

Parasitic or Drag Folding on Tectonic Features

Parasitic folding on tectonic features was introduced for consideration as a genetic model by this investigator. Varying terminologies have led to confusion concerning parasitic and drag folding.

Parasitic folds are small folds on the limbs of larger folds which share the same geometric elements of the larger

folds. The term parasitic fold has been applied by deSitter (1958, p. 280) to drag folds. Billings (1954, p. 82) states that drag folds form when a competent unit slides past an incompetent unit. Such minor folds may form on the limbs of larger anticlines or between thrust sheets but are generally restricted to individual lithologic units. Ramberg (1963, p. 97) says "the component of compressive strain and stress, parallel to layering, causes slack in the competent layer which is accommodated by buckling; whereas the component of shear gives the buckles their tilted monoclinic symmetry which is characteristic to drag folds".

The development of the intraformational folds according to the parasitic or drag fold model is contemporaneous with the development of the dome and basin system. According to Billings (1954), parasitic or drag folds which develop on the limbs of symmetric anticlines that exhibit small to moderate limb appression or closure, have axial planes which dip away from the crests of the anticlines. (See Figure 47.) Parasitic or drag folds which occur on the limbs of asymmetric inclined anticlines with more closure have axial planes that dip toward the crests. (See Figure 48.) The pre-Dakota fold sets comprising the dome and basin system have a fold profile more analogous to the open, symmetrical anticlines in Figure 47.

The axes of drag folds are parallel to those of the major folds. Drag or parasitic folds do not commonly occur near the crests of anticlines as is illustrated in Figures

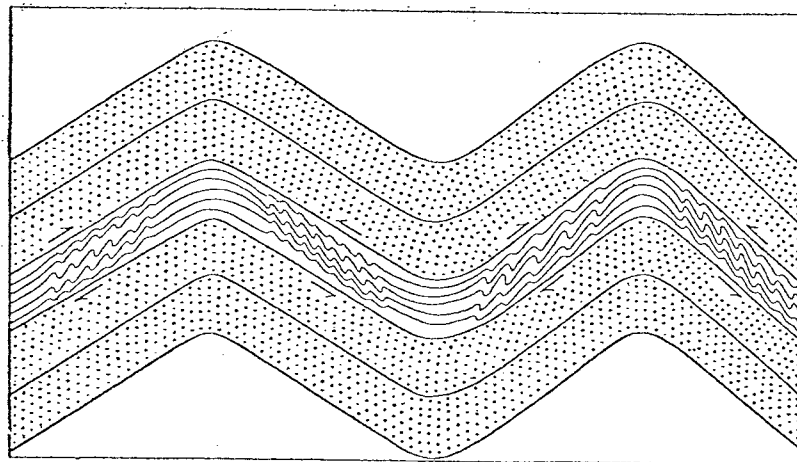


Figure 47. Structural section of symmetrical folds showing relation of drag folds and direction of shearing (After Billings, 1954, p.79).

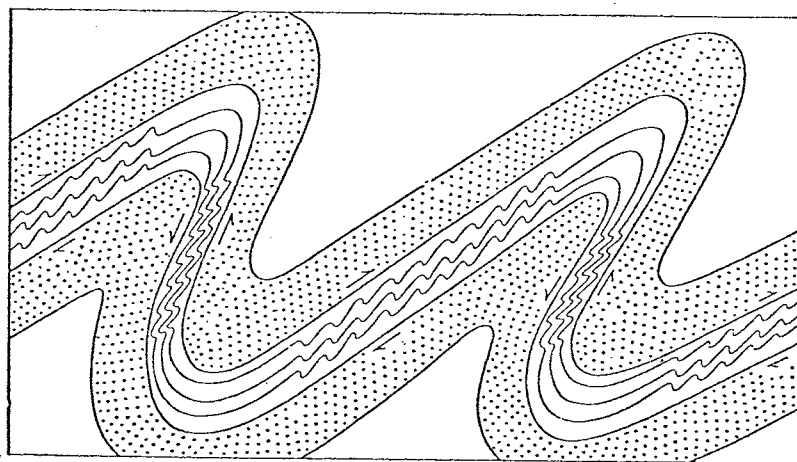


Figure 48. Structural section of asymmetrical inclined folds showing relation of drag folds and direction of shearing (After Billings, 1954, p.79).

47 and 48.

The stereographic projections of axial plane and fold axes of the intraformational folds presented in this investigation exhibit a random distribution of data without a concentration of points which would indicate a set of folds, nor do they reflect the orientation and plunge of the fold axes of the two sets of pre-Dakota folds ($N25^{\circ}W$ and $N85^{\circ}E$) as would be expected with either parasitic or drag folding. The axial planes of the intraformational folds on the flanks of the domes dip toward the crests of the domes (see Figure 41), rather than away from the crests as would drag or parasitic folds because the pre-Dakota domes and basins have symmetric fold profiles with small limb appression (see Figure 47).

The profiles of the intraformational folds do not exhibit a uniform profile at any location in the study area nor are they similar in profile to the two sets of pre-Dakota folds. This supports an origin other than parasitic folding.

A few intraformational folds occur near the crests of the domes, the axial planes of these intraformational folds generally dip away from the domes. These intraformational folds are smaller and exhibit less closure than the intraformational folds that occur lower on the flanks of the anticlines, however their occurrence on the crest of a dome indicates an origin other than drag folding.

The evidence presented in this investigation does not support the model based on parasitic or drag folding on

tectonic features and it is therefore considered invalid.

Soft Sediment Slump or Flow Off Tectonic Features

Hilpert and Moench (1960, p. 441) suggested that the slump or flow of unlithified sediment off tectonic features is responsible for the development of the intraformational folds. This proposal was based on their investigation in the Laguna mining district where they cite the localization of the intraformational folds along the flanks and troughs of larger pre-Dakota folds. They also cite thinning of the Todilto Limestone on the crests and upper flanks of large folds and thickening of the Todilto Limestone in the troughs.

The development of the intraformational folds by the model of soft sediment slump or flow off the pre-Dakota folds is contemporaneous to penecontemporaneous to the development of the pre-Dakota folds. The model suggests that the strike of the axial planes of the intraformational folds should be parallel to subparallel to the strike of the slope down which the sediments have slumped. Because the displacement of bedding is away from crests, the axial planes of the folds should dip toward the higher part of the surface. Units that are affected by flowage folding should exhibit thinning at the crest of the anticlines and thickening at the troughs of the synclines.

The random distribution of the fold axes and axial planes of the intraformational folds on the stereographic projections could represent the various orientations of the surface of the basin and dome system, illustrated in Plate VI, which would be reflected in the strike of the axial

planes of the intraformational folds. Figure 41 presents the relationship between the basin and dome system and the axial planes of the intraformational folds. Folds occurring on the flanks of the domes (intersections of pre-Dakota anticlines) have axial planes that dip toward the crest of the dome and strike parallel to the strike of the contoured surface as expected for this genetic model.

Incomplete exposures in the mining excavations did not permit this investigator to determine if the Todilto Limestone exhibits thinning on the domes and thickening in the basins in the study area.

If this origin of the intraformational folds is correct, then the following constraints on the age of the intraformational folds and the pre-Dakota fold sets can be stated:

- 1) Folding occurred before lithification of the Todilto was completed because the model requires soft sediments.
- 2) Folding occurred before the original sediments underwent neomorphism to pseudosparite because the relict laminations and crenulations are folded.
- 3) Folding occurred after deposition of the basal Summerville units because the basal units of the Summerville are locally folded and the crests of the intraformational folds are not truncated by erosion at the contact with the Summerville Formation.

- 4) Folding occurred after partial lithification of the Todilto because the intraclasts are rounded and show no deformation around other clasts and some folds have brecciated cores.

Thus, the age of intraformational folds and of the pre-Dakota fold sets is contemporaneous with deposition of the basal Summerville.

The model of slump or flowage off tectonic features, which may be superimposed on paleotopography, best accounts for the data, and is believed to be the origin of the intraformational folds in the Todilto Limestone.

SUMMARY AND CONCLUSIONS

Stratigraphy

The Todilto Limestone conformably overlies the transition zone of the Entrada Sandstone in the Grants mining district. The nature of this contact varies from intertonguing to gradational.

The Todilto Limestone ranges from 15 to 28 feet in thickness and can be divided into three lithologic zones: 1) laminated zone, 2) crenulated zone, and 3) recrystallized zone. The three zones are regarded as diagenetic-stratigraphic units.

The occurrence of the laminated zone is common to the Todilto Limestone across the depositional basin. Sparry calcite nodules occur in the crenulated zone and it is felt that the crenulated zone in the Grants mining district correlates to the gypsiferous transition zone between lime and gypsum deposition described in the San Ysidro, New Mexico area by Kirkland (1958). The recrystallized zone rapidly thickens and thins and is irregularly bedded.

The Todilto-Summerville contact is arbitrarily chosen as the upper surface of the topmost continuous bed of limestone. The arbitrary nature of the contact results in the inclusion of several feet of thinly bedded terrigenous clastics in the Todilto Limestone. Definite identification of erosional features has not been made in the study area, however lime intraclasts are present in both the pseudo-sparites of the recrystallized zone of the Todilto Limestone and in the basal units of the Summerville Formation.

The basal units of the Summerville Formation consist of an intraformational conglomerate which grades upward into the quartz-silt arenites and wackes which are characteristic of the Summerville.

Depositional Environment

The paleontologic, petrologic and stratigraphic evidence suggests a complex sequence of environments in the depositional history of the Todilto Limestone. The sandy member of the Entrada Sandstone is an eolian quartz arenite and is overlain by a transition zone which represents inundation by either fluvial or lacustrine waters. The laminated zone of the Todilto Limestone is the result of the gradual enrichment of calcium carbonate in lake waters and then precipitation as the concentration rose. A lake flat-sabkha developed as the lake receded, however the sabkha surface was probably very close to the level of the water table because of the lack of desiccation cracks (this probably marks the beginning of deposition of the bedded gypsum-anhydrite of the gypsum member elsewhere in the basin). Dolomite or skeletal rims of dolomite were not found in the study area. Chemical analyses by previous investigators show 2 percent or less $MgCO_3$. The lack of dolomite in the sabkha environment indicates that the chemical composition of the waters present was not comparable to the composition of marine waters. The upper zone of pseudosparites represents a complex of depositional environments. The relict laminations and relict crenulations in the pseudosparites suggest that the original sediments

represent depositional conditions that were intermittently those of lake and lake flat-sabkha, with open water occurring in ponds and embayments, with lake flat-sabkha developing in the intervening areas, and locally the introduction of terrigenous clastics by fluvial influence. This is supported by the irregular bedding, rapid thickening and thinning of units and the intertonguing nature of the limestone-terrigenous facies change. The Summerville Formation marks the completion of the transition from lacustrine to fluvial environment.

Structural Geology

Intraformational folds occur throughout the Todilto Limestone and extend into the overlying basal units of the Summerville Formation. Most of the intraformational folds are inclined, asymmetric, gentle and open forms.

Stereographic analysis of the orientation data cannot isolate discrete fold sets, nor a sequence of superposed sets, on the basis of geographic domains or fold style. The axial planes have all possible orientations and fold axes are parallel to subparallel to the strike of axial planes and usually plunge 12° or less.

A structural contour map of the contact between the Entrada Sandstone and Todilto Limestone reveals a complex series of domes and basins. There are two major trends of pre-Dakota folds evident on the structural contour map. One set of folds trend $N25^{\circ}W$ with sinuous crestlines and wavelengths of 400 to 575 feet. The other set trends $N85^{\circ}E$ and has wavelengths of 675 to 800 feet.

The strike of the axial planes of the intraformational folds on the flanks of the domes are parallel or subparallel to the strike of the flanks of the domes. The axial planes of the intraformational folds situated on the flanks of the domes dip toward the crests of the domes. The intraformational folds near the crests of the domes exhibit gentle closure with axial planes dipping away from the crest of the domes with a wide range of dip angles.

Five genetic models for the intraformational folds have been examined in this investigation. Soft sediment slump off the domes of the dome and basin system is considered to be the probable cause of the intraformational folding. The formation of the intraformational folds and of the pre-Dakota fold sets is contemporaneous with deposition of the basal Summerville Formation.

Economic Geology

The mining excavations often follow the fold axes and strike of the axial planes of the intraformational folds rather than many of the mineralized areas outlined in early studies based on drill hole data. This indicates that the intraformational folds are a consistent site of uranium deposition.

Future uranium exploration in the Todilto Limestone should focus on the flanks of the domes produced by the two sets of pre-Dakota folds. Shallow seismic investigations, provided that the P-wave velocity of the Todilto Limestone is less than that of the Entrada Sandstone, could save drilling time and expense by first laying out the dome

and basin pattern for an area in order to localize optimum
drill sites.

APPENDICES

APPENDIX I
CLASSIFICATION SYSTEMS

Limestones, Partly Dolomitized Limestones, and Primary Dolomites see Notes				Replacement Dolomites (V)	
>10% Allochems Allochemical Rocks (I and II)		<10% Allochems Microcrystalline Rocks (III)		Undisturbed Bioherm Rocks (IV)	
Sparry Calcite Cement > Micro- crystalline Ooze Matrix		1-10% Allochems		<1% Allochems	
Sparry Allo- chemical Rocks (I)		Microcrystalline Allochemical Rocks (II)		No Allochem Ghosts	
Intrasparudite (Ii:Lr) Intrasparite (Ii:La)		Intramicrorudite* (Ii:Lr) Intramicrocite* (Ii:La)		Allochem Ghosts	
Oisparrudite (Io:Lr) Oisparite (Io:La)		Oimicrorudite* (Io:Lr) Oimicrocite* (Io:La)		Finely Crystalline Intracrystalline Dol- omite (Vi:D3) etc.	
Biosparrudite (Ib:Lr) Biosparite (Ib:La)		Biomicrorudite (Ib:Lr) Biomicrocite (Ib:La)		Coarsely Crystal- line Oolitic Dolomite (Vo:D5) etc.	
Biopelsparite (Ibp:La)		Biopelmicrocite (Ibp:La)		Aphanocrystalline Biogenic Dolomite (Vb:D1) etc.	
Pelsparite (Ip:La)		Pelmicrocite (Ip:La)		Very Finely Crystalline Pellet Dolomite (Vp:D2) etc.	
Intracrasts >25% Oolites >25% Fossils to Pellets Volume Ratio of		Most Abundant Allochem		Evident Allochem	
<25% Intracrasts		Intracrasts: Intracrast- bearing Microcite* (IiLi:Lr or La)		Medium Crys- talline Dolo- mite (V:D4)	
Volumetric Allochem Composition		Oolites: Oolite-bearing Microcite* (IiLo:Lr or La)		Finely Crys- talline Dolo- mite (V:D3)	
Fossils to Pellets		Fossils: Fossiliferous Microcite (IiLb: Lr, La, or Li)		etc.	
3:1-1:3 (bp)		Pellets: Pelletiferous Microcite (IiLp:La)			
<1:3 (p)					

* Designates rare rock types.
 1 Names and symbols in the body of the table refer to limestones. If the rock contains more than 10 per cent replacement dolomite, prefix the term "dolomitized" to the rock name, and use DLr or DLa for the symbol (e.g., dolomitized intrasparite, Li:DLa). If the rock contains more than 10 per cent dolomite of uncertain origin, prefix the term "dolomitic" to the rock name, and use DLr or dLa for the symbol (e.g., dolomitic pelisparite, Ip:dLa). If the rock consists of primary (directly deposited) dolomite, prefix the term "primary dolomite" to the rock name, and use Dr or Da for the symbol (e.g., primary dolomite intramicrocite, Ii:Da). Instead of "primary dolomite microcite" (IiLm:D) the term "dolomicrocite" may be used.
 2 Upper name in each box refers to calcirudites (median allochem size larger than 1.0 mm.); and lower name refers to all rocks with median allochem size smaller than 1.0 mm. Grain size and quantity of ooze matrix, cements or terrigenous grains are ignored.
 3 If the rock contains more than 10 per cent terrigenous material, prefix "sandy," "silty," or "clayey" to the rock name, and "T_s," "T_z," or "T_c" to the symbol depending on which is dominant (e.g., sandy biosparite, IsLb:La, or silty dolomitized pelmicrocite, TzIiLp:DLa). Glauconite, colophane, chert, pyrite, or other modifiers may also be prefixed.

Classification of Carbonate Rocks (after Folk, 1959).

I. Mode of Formation

- P: Passive Precipitation
 P: Normal pore filling
 Ps: Solution-fill
- D: Displacive Precipitation
- N: Neomorphism
 N: as a general term, or where exact process unknown.
 Ni: Inversion from known aragonite.
 Nr: Recrystallization from known calcite.
 Nd: Degrading (also Nid, Nrd).
 Ns: Original fabric strained significantly.
 Ne: Coalescive (as opposed to porphyroid).
 (the above may be combined as Nrds).
- R: Replacement

II. Shape

- E: Equant, axial ratio $1\frac{1}{2}:1$
 B: Bladed, axial ratio $1\frac{1}{2}:1$ to $6:1$
 F: Fibrous, axial ratio $6:1$

III. Crystal Size

Size	Class
-4.0	7
-1.0	6
-0.25	5
-0.062	4
-0.016	3
-0.004	2
-0.001	1

IV. Foundation

- O: Overgrowth, in optical continuity with nucleus.
 O: Ordinary
 Om: Monocrystal
 Ow: Widens outward from nucleus
- C: Crust, physically oriented by nucleant surface.
 C: Ordinary
 Cw: Widens outward from nucleus
- S: Spherulitic with no obvious nucleus (fibrous or bladed calcite only)
- No symbol: randomly oriented, no obvious control by foundation

Summary of code for authigenic calcite (after Folk, 1965).

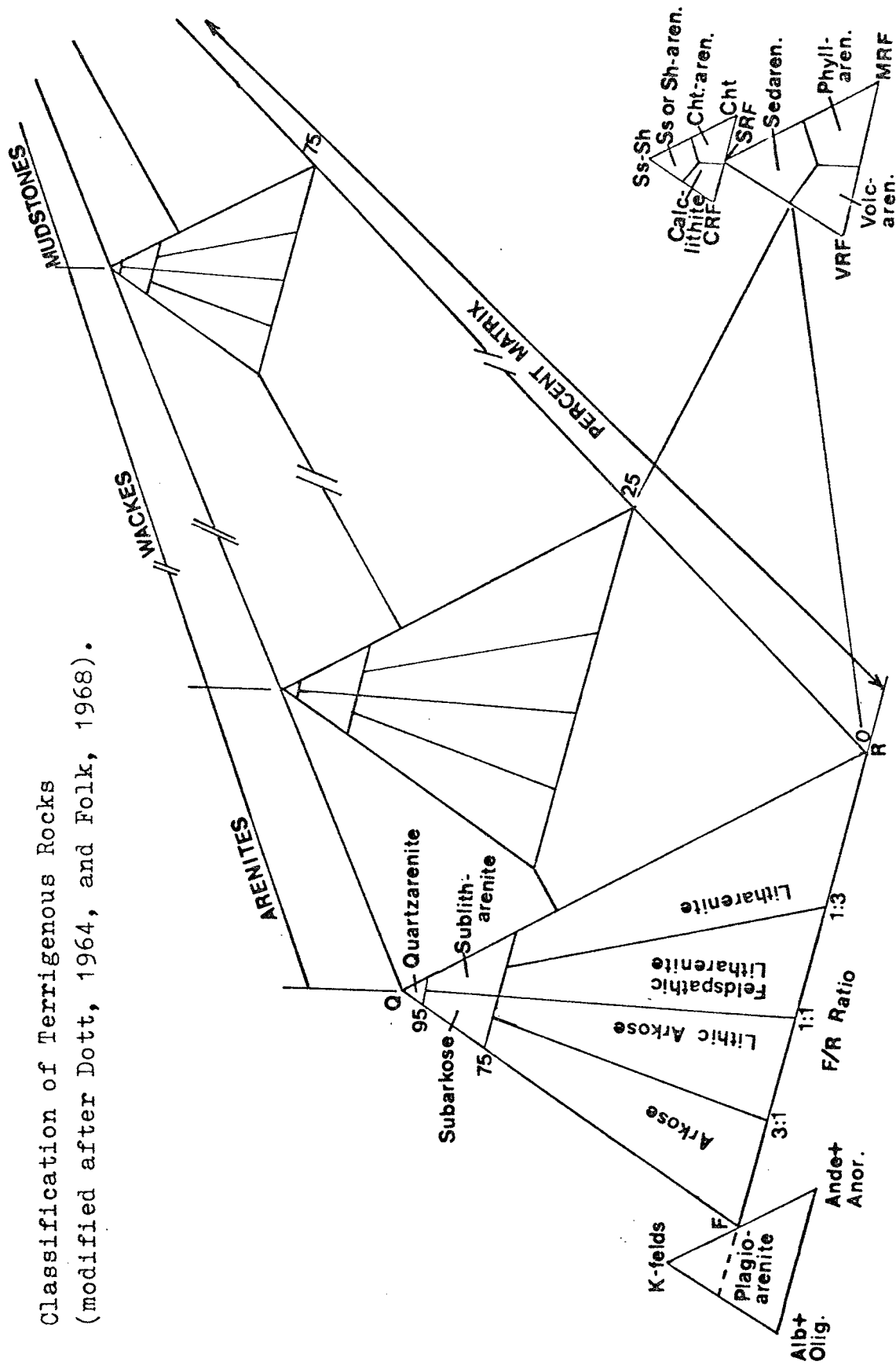
Recognizable Depositional Texture		Depositional Texture is not Recognizable	
Original Components Not Bound During Deposition		Original Components Bound	
Contains Mud		Lacks Mud	
Mud Supported	Grain Supported	GRAINSTONE	
Less than 10% Grains	More than 10% Grains	PACKSTONE	
MUDSTONE	WACKESTONE	BOUNDSTONE	
		CRYSTALLINE CARBONATE	

Classification of Carbonate Rocks (after Dunham, 1962).

Basic Criterion	Subordinate Criteria						
	Character of lower boundary surface of set of cross-strata	Shape of sets of cross-strata	Attitude of axis of set of cross-strata	Symmetry of set of cross-strata	Arching of cross-strata	Dip of cross-strata	Length of cross-strata
Nonerosional surfaces (simple cross-stratification)	Lenticular	Lenticular	Plunging	Symmetric	Concave	High angle (> 20 degrees)	Small scale (< 1 foot)
Planar surfaces of erosion (planar cross-stratification)	Tabular	Tabular	Nonplunging	Asymmetric	Straight	Low angle (< 20 degrees)	Medium scale (1 to 20 feet)
Curved surfaces of erosion (trough cross-stratification)	Wedge-shaped	Wedge-shaped			Convex		Large scale (> 20 feet)

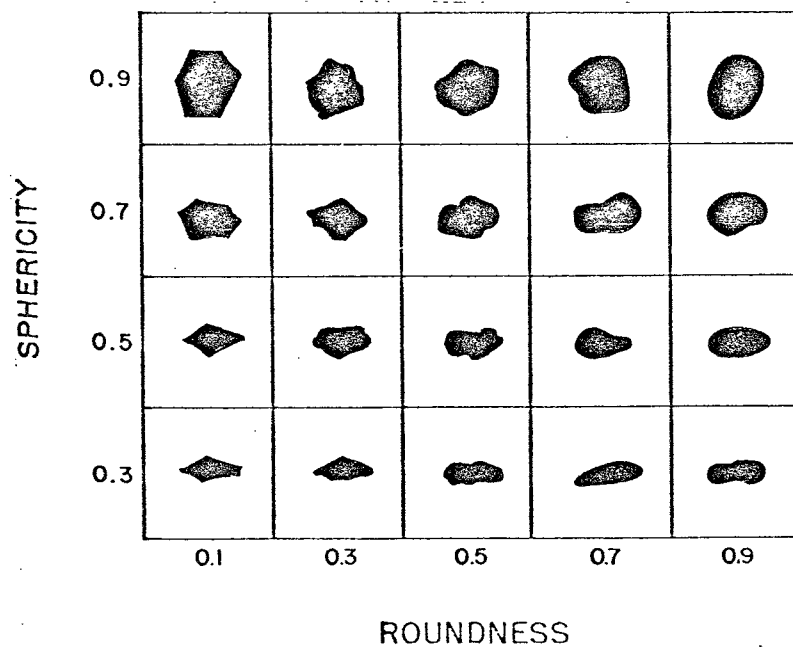
Classification of cross-stratified units (after McKee and Weir, 1953).

Classification of Terrigenous Rocks
 (modified after Dott, 1964, and Folk, 1968).



Thickness of Unit		Terms for Thickness of Stratification Units	Terms for Thickness of Parting Units
Metric System	English System		
-0.3 cm.	$\frac{1}{10}$ in.	Thinly laminated	Super-thinly parted
0.3-1.0	$\frac{1}{10}$ - $\frac{2}{5}$	Thickly laminated	Extra-thinly parted
1-3	$\frac{2}{5}$ -1	Very thinly bedded	Very thinly parted
3-10	1-4	Thinly bedded	Thinly parted
10-30	4-12	Mediumly bedded	Mediumly parted
30-100	1-3 ft.	Thickly bedded	Thickly parted
100-	3-	Very thickly bedded	Very thickly parted

Classification of bedding & parting unit thickness
(after Ingram, 1954).



Classification of sphericity and roundness
(after Krumbein and Sloss, 1963).

Millimeters		Phi (ϕ) units	Wentworth size class
4096		-12	
1024		-10	Boulder
256	256	-8	
64	64	-6	Cobble
16		-4	Pebble
4	4	-2	
3.36		-1.75	
2.83		-1.5	Granule
2.38		-1.25	
2.00	2	-1.0	
1.68		-0.75	
1.41		-0.5	Very coarse sand
1.19		-0.25	
1.00	1	0.0	
0.84		0.25	
0.71		0.5	Coarse sand
0.59		0.75	
0.50	1/2	1.0	
0.42		1.25	
0.35		1.5	Medium sand
0.30		1.75	
0.25	1/4	2.0	
0.210		2.25	
0.177		2.5	Fine sand
0.149		2.75	
0.125	1/8	3.0	
0.105		3.25	
0.088		3.5	Very fine sand
0.074		3.75	
0.0625	1/16	4.0	
0.053		4.25	
0.044		4.5	Coarse silt
0.037		4.75	
0.031	1/32	5.0	
0.0156	1/64	6.0	Medium silt
0.0078	1/128	7.0	Fine silt
0.0039	1/256	8.0	Very fine silt
0.0020		9.0	
0.00098		10.0	Clay
0.00049		11.0	
0.00024		12.0	
0.00012		13.0	
0.00006		14.0	

Terminology and class intervals for grade scales
(From Pettijohn, Potter & Siever, 1972).

APPENDIX II
STRUCTURAL DATA

Table 1.

Data for Intraformational Folds Plotted on Base Maps

Section 9, T12N, R9W

Station	Axial Plane	Fold Axis
9A	N88°E, 38°E	S78°W, 6°
	N35°W, 42°E	N22°W, 8°
	N89°W, 50°E	S87°W, 4°
	N43°W, 47°E	S37°E, 8°
	N61°W, 75°W	S63°E, 1°
	N84°E, 27°W	S80°W, 8°
	N54°E, 70°W	S54°W, 1°
9C	N60°W, 61°W	S58°E, 2°
	N10°E, 73°W	N9°W, 7°
	N12°W, 43°W	S12°E, 1°
9D	N9°W, 75°W	N15°W, 1°
	N57°W, 48°E	S69°E, 38°
	N29°W, 66°W	N30°W, 36°
	N61°W, 74°E	N59°W, 2°
	N15°W, 3°W	N28°W, 5°
	N29°W, 79°E	S14°E, 18°
	N87°W, 60°E	S88°W, 16°
	N86°W, 79°W	S17°W, 16°
	N77°E, 46°W	N70°E, 6°
	N73°E, 25°W	N70°W, 5°
	N10°E, 50°W	N13°E, 7°
	N37°E, 35°W	S40°W, 9°
	N17°E, 84°E	N18°E, 9°
	N5°E, 25°W	S24°W, 11°
	N57°W, 55°W	S16°W, 9°
N40°W, 47°W	S39°E, 2°	
N70°W, 57°E	N70°W, 1°	

Table 1. (continued)

Section 9, T12N, R9W

Station	Axial Plane	Fold Axis
9E	N89°W, 64°E	N78°E, 8°
	N35°E, 6°W	N70°E, 0°
	N36°W, 74°E	S30°E, 6°
	N12°W, 60°E	N2°E, 20°
	N0°E, 70°NE	S7°W, 12°
9F	N47°W, 74°E	N41°W, 33°
	N13°W, 47°W	N16°W, 1°
	N64°E, 53°E	N27°E, 8°
	N52°W, 38°W	N9°W, 9°
	N46°W, 18°E	N88°W, 6°
9G	N8°W, 42°E	N8°W, 1°
	N19°E, 81°E	N22°E, 4°
9H	N12°W, 57°E	N2°W, 10°
	N14°E, 34°E	S10°W, 2°
9I	N52°W, 89°W	S80°E, 7°
	N88°W, 52°W	S88°E, 2°
	N86°W, 32°W	N75°W, 1°
	N82°W, 75°E	N84°W, 2°
	N63°W, 65°W	S67°E, 2°
	N77°W, 43°W	S50°W, 26°
	N87°W, 49°W	N67°W, 12°
N71°E, 11°W	S76°W, 2°	
9J	N5°W, 31°E	N29°W, 1°
	N55°W, 64°E	S41°E, 4°
	N34°W, 36°E	N35°W, 0°

Table 1. (continued)

Section 9, T12N, R9W

Station	Axial Plane	Fold Axis
9K	N47°W, 72°E	S47°E, 22°
	N89°E, 66°E	S86°E, 14°
	N21°E, 24°E	N31°W, 4°
9L	N10°E, 20°W	N13°W, 12°
	N37°E, 60°E	N41°E, 4°
	N33°W, 36°W	N27°W, 9°
	N84°W, 55°E	S57°E, 4°
	N68°E, 58°E	S82°E, 3°
9M	N59°W, 69°W	N54°W, 3°
	N52°E, 55°E	N51°E, 15°
	N70°E, 54°E	N84°W, 5°
	N37°W, 62°W	S38°E, 5°
	N27°W, 66°E	N20°W, 8°
	N51°W, 69°W	N40°W, 8°
	N53°E, 58°E	S56°W, 1°
	N75°E, 68°W	S71°W, 1°
	N20°E, 57°E	N12°E, 3°
	N73°E, 76°E	S72°W, 2°
N71°W, 64°E	S70°E, 1°	
N80°W, 77°W	S70°E, 6°	
9N	N84°E, 33°W	N90°E, 0°
	N62°W, 48°E	N73°W, 6°

Section 15, T12N, R9W

Station	Axial Plane	Fold Axis
15A	N64°E, 82°E	N64°E, 1°
	N33°E, 88°E	S33°W, 1°
	N69°E, 64°E	N68°E, 1°

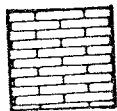
Table 1. (continued)

Section 15, T12N, R9W

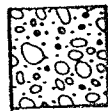
Station	Axial Plane	Fold Axis
15A	N72°E, 59°E	S78°W, 1°
	N66°W, 79°W	N58°W, 4°
15B	N76°W, 23°E	N73°W, 1°
	N72°E, 87°W	S74°W, 4°
	N63°E, 49°W	N80°E, 9°
	N56°W, 62°E	S72°E, 8°
15C	N28°E, 36°E	N21°E, 5°
	N24°E, 55°W	N31°E, 2°
	N60°E, 46°W	S73°W, 2°
	N77°E, 34°E	N75°W, 2°
	N79°E, 29°E	S74°E, 11°

APPENDIX III
SYMBOLS FOR STRATIGRAPHIC SECTIONS

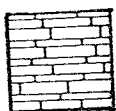
Symbols for Stratigraphic Sections



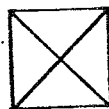
Laminated micrite



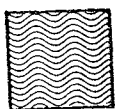
Concretionary Silt arenite



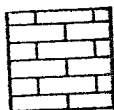
Thinly bedded micrite



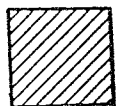
Covered Section



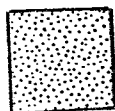
Crenulated micrite



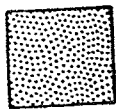
Pseudosparite



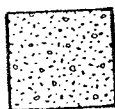
Gypsum



arenite



Cross-bedded arenite



Silt arenite

BIBLIOGRAPHY

- Allen, J.E., and Balk, R., 1954, Mineral resources of Fort Defiance and Tohatchi quadrangles, Arizona and New Mexico: N. Mex. Inst. Min. and Technology, State Bur. Mines and Mineral Res. Bull., v. 36, 192p.
- Anderson, R.Y., and Kirkland, D.W., 1960, Origin, Varves and Cycles of Jurassic Todilto Formation, New Mexico: Am. Assoc. Petroleum Geologists Bull., v. 44, n. 1, pp. 37-52.
- Ash, H.O., 1958, The Jurassic Todilto Formation of New Mexico: Unpublished Master's Thesis, University of New Mexico, 63p.
- Baker, A.A., Dane, C.H., and Reeside, J.B., Jr., 1936, Correlation of the Jurassic Formations of parts of Utah, Arizona, New Mexico and Colorado: U.S. Geol. Survey, Prof. Pap. 183, 66p.
- _____, _____, _____, 1947, Revised Correlation of Jurassic Formations of parts of Utah, Arizona, New Mexico and Colorado: Am. Assoc. Petroleum Geologists Bull., v. 31, n. 9, pp. 1664-1668.
- _____, Dobbin, C.E., Mcknight, E.T., and Reeside, J.B., Jr., 1927, Notes on the Stratigraphy of the Moab Region, Utah: Am. Assoc. Petroleum Geologists Bull., v. 11, n. 8, pp. 785-788.
- Bell, K.G., 1963, Uranium in Carbonate Rocks: U.S. Geol. Survey, Prof. Pap. 474-A, 29p.
- Billings, M.P., 1954, Structural Geology, (2nd Edit.): Prentice-Hall, Inc., Englewood Cliffs, N.M., 514p.
- Bradbury, D., and Kirkland, D.W., 1968, Upper Jurassic Aquatic Hemiptera from the Todilto Formation, Northern New Mexico: Geol. Soc. America, Annual Mtng Abstracts of 1966, S.P. 101, p. 24.
- Butler, G.P., 1969, Modern evaporite deposition and geochemistry of coexisting brines, the sabkha Trucial Coast, Arabian Gulf: Jour. Sedimentary Petrology, v. 39, pp. 70-89.
- Dane, C.H., and Bachman, G.O., 1957, Preliminary Geology Map of the Northwestern Part of New Mexico, U.S. Geol. Survey, Miscellaneous Geologic Investigations Map. I-224.
- Darton, N.H., 1928, Red Beds and Associated Formations in New Mexico: U.S. Geol. Survey Bull. 794. 356p.

- Dott, R.H., Jr., 1964, Wacke, gray wacke and matrix - What approach to immature sandstone classification?:
Jour. Sedimentary Petrology, v. 34, pp. 625-632.
- Dunham, R.J., 1962, Classification of carbonate rocks according to depositional texture: in Classification of Carbonate Rocks, (Ham, W.E., editor) Am. Assoc. Petroleum Geologists Mem. 1, pp. 108-121.
- Dunkle, D.H., 1942, A new fossil fish of the family Leptolepidae: Cleveland Mus. Nat. History, Sci. Pub., v. 8, n. 5, pp. 61-64.
- Dutton, C.E., 1885, Mount Taylor and the Zuni Plateau: In Powell, J.B., Sixth Annual Report of the U.S. Geol. Survey, 1884-1885, pp. 106-198.
- Ellsworth, P.C., and Mirsky, A., 1952, Preliminary Report on Relation of Structure to Uranium Mineralization in the Todilto Limestone, Grants District, New Mexico, U.S. Atomic Energy Commission, RME-4020.
- Eugster, H.P., and Surdam, R.C., 1973, Depositional Environment of the Green River Formation of Wyoming: A Preliminary Report Geol. Soc. America, v. 84, pp. 1115-1120.
- Fleuty, M.J., 1964, The description of folds: Proc. Geol. Association, v. 75, pp. 461-492.
- Folk, R.L., 1959, Practical Petrographic Classification of Limestones, Am. Assoc. Petroleum Geologists Bull., v. 43, pp. 1-38.
- _____, 1965, Some aspects of recrystallization in ancient limestones. In: L.C. Pray and R.C. Murray (Editors), Dolomitization and Limestone Diagenesis: A Symposium-Soc. Econ. Paleontologists and Mineralogists, Spec. Publ. 13, pp. 14-48.
- _____, 1968, Petrology of Sedimentary Rocks: Austin, Texas, Hemphill's Pub., 124p.
- Gableman, J.W., 1956, Uranium deposits in Limestone, U.S. Geol. Survey, Prof. Pap. 300, pp. 386-404.
- Gilluly, J. and Reeside, J.B., Jr., 1928, Sedimentary rocks of the San Rafael Swell and adjacent areas in eastern Utah, U.S. Geol. Survey, Prof. Pap. 150-D, pp. 61-110.
- Glennie, K.W., 1972, Permian Rotliegendes of Northwest Europe, Interpreted in Light of Modern Desert Sedimentation Studies, Am. Assoc. Petroleum Geologists Bull., v. 56, n. 6, pp. 1048-1071.

- Granger, H.C., 1963, Mineralogy, In: Geology and Technology of the Grants Uranium Region, N.Mex. Inst. Min. and Technology, State Bur. Mines and Mineral Res., Mem. 15, pp. 21-37.
- Gregory, H.E., 1917, Geology of the Navajo Country, U.S. Geol. Survey, Prof. Pap. 93, 161p.
- Harshbarger, J.W., Repenning, C.A. and Irwin, J.H., 1957 Stratigraphy of the Uppermost Triassic and Jurassic Rocks of the Navajo Country, U.S. Geol. Survey, Prof. Pap. 291, 74p.
- Hills, E.S., 1963, Elements of Structural Geology: John Wiley and Sons, Inc., New York, 483p.
- Hilpert, L.S., 1963, Regional and Local Stratigraphy of Uranium Bearing Rocks, In: Geology and Technology of the Grants Uranium Region, N.Mex. Inst. Min. and Technology, State Bur. Mines and Mineral Res., Mem. 15, pp. 6-18.
- _____, 1969, Uranium Resources of Northwestern New Mexico, U.S. Geol. Survey, Prof. Pap. 603, 166p.
- _____, and Moench, R.H., 1960, Uranium Deposits of the Southern Part of the San Juan Basin, New Mexico, Econ. Geology, v. 55, n. 3, pp. 429-463.
- Imlay, R.W., 1952, Correlation of the Jurassic Formations of North America, Exclusive of Canada: Geol. Soc. America Bull., v. 63, pp. 953-992.
- Ingram, R.L., 1954, Terminology for the thickness of stratification and parting units in sedimentary rock: Geol. Soc. America Bull., v. 65, pp. 937-938.
- Kelly, V.C., 1963, Tectonic Setting, In: Geology and Technology of the Grants Uranium Region, N.Mex. Inst. Min. and Technology, State Bur. Mines and Mineral Res., Mem. 15, pp. 19-20.
- Kendall, C.G.St.C., 1969, An environmental reinterpretation of the Permian evaporite/carbonate shelf sediments of the Guadalupe Mountains: Geol. Soc. America Bull., v. 80, pp. 2503-2526.
- _____, and Skipwith, P.A., 1969, Holocene shallow-water carbonate and evaporite sediments of Khor al Bazam, Abu Dhabi, southwest Persian Gulf, Bull. Am. Assoc. Petroleum Geologists, v. 53, pp. 841-869.
- Kerr, P.F., 1959, Optical Mineralogy: McGraw-Hill Co., New York, 442p.

- Kirkland, D.W., 1958, The Environment of the Jurassic Todilto Basin, New Mexico: Unpublished Master's Thesis, University of New Mexico, 69p.
- Koerner, H.E., 1930, Jurassic Fishes from New Mexico: Am. Jour. Science, 5th ser., v. 19, p. 463.
- Krumbein, W.S. and Sloss, L.L., 1963, Stratigraphy and Sedimentation, (2nd Edit.): W.H. Freeman and Co., San Francisco, 660p.
- Lookingbill, J.L., 1953, Stratigraphy and structure of the Gallina Uplift, Rio Arriba County, New Mexico: Unpublished Master's Thesis, University of New Mexico, 118p.
- Lucia, F.J., 1972, Recognition of Evaporite-Carbonate Shoreline Sedimentation, in: Recognition of Ancient Sedimentary Environments, Edited by Hamblin & Rigby, S.E.P.M. Mem. 16, pp. 160-191.
- McKee, E.D., et al., 1956, Paleotectonic maps, Jurassic system: U.S. Geol. Survey, Miscellaneous Geologic Investigation Map I-175.
- , and Weir, G.W., 1953, Terminology for Stratification and Cross-stratification in Sedimentary Rocks: Geol. Soc. America Bull., v. 64, pp. 381-390.
- McLaughlin, E.D., Jr., 1963, Uranium Deposits in the Todilto Limestone of the Grants District, In: Geology and Technology of the Grants Uranium Region, N.Mex. Inst. Min. and Technology, State Bur. Mines and Mineral Res., Mem. 15, pp. 136-149.
- National Research Council, 1948, Rock-Color Chart: New York, Geol. Soc. America, Wash. D.C.
- Nevin, C.M., 1942, Principles of Structural Geology, (3rd Edit.): John Wiley and Sons, Inc., New York, 320p.
- Nichols, R.L., 1946, McCarty's Basalt Flow, Valencia County, New Mexico, Geol. Soc. America Bull., v. 57, n. 11, pp. 1049-1086.
- Northrop, S.A., 1950, General Geology of Northern New Mexico, In: Soc. Vertebrate Paleon. Guidebook, Fourth Field Conference, pp. 26-47.
- Perry, B.L., 1963, Limestone Reefs as an Ore Control in the Jurassic Todilto Limestone of the Grants District, In: Geology and Technology of the Grants Uranium Region, N.Mex. Inst. Min. and Technology, State Bur. Mines and Mem. 15, pp. 150-156.

- Pettijohn, F.J., Potter, P.E. and Siever, R., 1972, Sand and Sandstone: Springer-Verlag, New York, 618p.
- Picard, M.D. and High, L.R., 1972, Criteria for Recognizing Lacustrine Rocks, In: Recognition of Ancient Sedimentary Environments, Edited by Hamblin & Rigby, S.E.P.M. Mem. 16, pp. 108-145.
- Ramberg, H., 1963, Evolution of drag folds: Geol. Magazine, v. 100, pp. 97-106.
- Ramsey, J.G., 1961, The Effects of Folding upon the Orientation of Sedimentation Structures: Jour. Geology, v. 69, pp. 84-100.
- Rapaport, I., 1952, Interim report on the ore deposits of the Grants district, New Mexico, U.S. Atomic Energy Commission, RMO-1031.
- _____, Hadfield, J.P. and Olson, R.H., 1952, Jurassic Rocks of the Zuni Uplift, New Mexico, U.S. Atomic Energy Commission, RMO-642, Tech. Inf. Service, Oak Ridge, Tennessee.
- Shearman, D.J., 1966, Origin of marine evaporites by diagenesis: Trans. Inst. Mining and Metallurgy, v. 75, Sec. B, Bull. 717, pp. 208-215.
- Silver, Caswell, 1948, Jurassic Overlap in Western New Mexico, Am. Assoc. Petroleum Geologists Bull., v. 32, n. 1, pp. 68-81.
- Sitter, L.U.de, 1958, Boudin and parasitic folds in relation to cleavage and folding: Geologic Mijnb., v. 20, pp. 277-286.
- Smith, C.T., 1954, Geology of the Thoreau Quadrangle, McKinley and Valencia Counties, New Mexico, N.Mex. Inst. Min. and Technology, State Bur. Mines and Mineral Res., Bull. 31, 30p.
- _____, Budding, A.J. and Pitrat, C.W., 1961, Geology of the Southeastern Part of the Chama Basin: N.Mex. Inst. Min. and Technology, State Bur. Mines and Mineral Res., Bull. 75, 57p.
- Smith, D.B., 1974, Origin of tepees in Upper Permian shelf carbonate rocks of Guadalupe Mountains, New Mexico: Am. Assoc. Petroleum Geologists Bull., v. 58, n. 1, pp. 63-70.
- Swain, F.M., 1946, Middle Mesozoic Nonmarine Ostracoda from Brazil and New Mexico: Jour. Paleontology, v. 20, pp. 543-555.

- Tanner, W.F., 1965, Upper Jurassic Paleogeography of the Four Corners Region: Jour. Sedimentary Petrology, v. 35, n. 3, pp. 564-574.
- Thaden, R.E. and Ostling, E.J., 1967, Geologic Map of the Bluewater Quadrangle, Valencia and McKinley Counties, N.M., U.S. Geol. Survey, Map GQ-679.
- _____, Santos, E.S. and Ostling, E.J., 1967, Geologic Map of the Dos Lomas Quadrangle, Valencia and McKinley Counties, New Mexico: U.S. Geol. Survey, Map GQ-680.
- Truesdell, A.H. and Weeks, A.D., 1960, Paragenesis of Uranium in Todilto Limestone near Grants, New Mexico, U.S. Geol. Survey, Prof. Pap. 400-B, pp. B52-B54.
- Wright, H.E., Jr. and Becker, R.M., 1957, Correlation of Jurassic Formations Along Defiance Monocline, Arizona-New Mexico, Am. Assoc. Petroleum Geologists Bull., v. 35, n. 3, pp. 607-614.
- Wright, J.C. and Dickey, D.D., 1958, Pre-Morrison Jurassic Strata of Southeastern Utah, In: Intermountain Assoc. Petroleum Geologists Guidebook, Ninth Annual Field Conference, Geology of the Paradox Basin, pp. 172-181.

This thesis is accepted on behalf of the faculty of the
Institute by the following committee:

John R. McMillan

Ch. J. Presiding

Robert H. Wain

Date Aug. 26, 1976